Journal of the OPTICAL SOCIETY *of* AMERICA

VOLUME 38
No. 3

MARCH
1948

Loss in Resolving Power Caused by Primary Astigmatism, Coma, and Spherical Aberration in Telescopic Systems . . . . . HOWARD S. COLEMAN AND SAMUEL W. HARDING 217

Calibration Method for Infra-Red Prism Spectrometers . . . . . D. S. MCKINNEY AND R. A. FRIEDEL 222

Fluorescence Efficiency and Hole Migration in Zinc Sulphides . . . . . M. E. WISE AND H. A. KLASENS 226

Quanta Explanation of Vision and the Brightness Impression for Various Times of Observation and Visual Angles . . . . . M. A. BOUMAN AND H. A. VAN DER VELDEN 231

Visibility of Distant Objects . . . . . SEIBERT Q. DUNTLEY 237

Comparison of Computed and Experimental Detection Ranges of Objects Viewed with Telescopic Systems from Aboard Ship . . . . . H. S. COLEMAN AND W. S. VERPLANCK 250

Survey of Near Infra-Red Communication Systems . . W. S. HUXFORD AND JOHN R. PLATT 253

Principles of Optical Communication Systems . . HARTLAND S. SNYDER AND JOHN R. PLATT 269

Some Spectral Characteristics of Mercury Arcs for Use in Study of the Raman Effect . . . . . D. H. RANK AND J. S. MCCARTNEY 279

Determination of the Depolarization Factors of Highly Polarized Raman Lines . . . . . A. E. DOUGLAS AND D. H. RANK 281

Intensity and Polarization of Brillouin Spectra . . . . . D. H. RANK, J. S. MCCARTNEY, AND G. J. SZASZ 287

Table of Planckian Radiation . . . . . PARRY MOON 291

Published monthly
at Prince and Lemon Sts., Lancaster, Pa.
by the
AMERICAN INSTITUTE OF PHYSICS
Incorporated
57 East 55 Street, New York 22, New York
FOR AND UNDER THE EDITORIAL SUPERVISION OF THE
OPTICAL SOCIETY OF AMERICA

THE OPTICAL SOCIETY OF AMERICA

Officers of the Society

RUDOLF KINGSLAKE, *President*
Eastman Kodak Company
Rochester, New York

WILLIAM F. MEGGERS, *Vice President*
National Bureau of Standards
Washington 25, D. C.

ARTHUR C. HARDY, *Secretary*
Massachusetts Institute of Technology
Cambridge 39, Massachusetts

W. W. GRAEPER, *Treasurer*
Bausch & Lomb Optical Company
Rochester 2, New York

The Board of Directors consists of the above officers; the Editor of the Journal; the Past President; and five directors-at-large.

G. R. HARRISON, *Editor and Past President*
Massachusetts Institute of Technology
Cambridge 39, Massachusetts

Directors-at-Large

FRANK BENFORD
General Electric Company
Schenectady, New York

F. M. BISHOP
Eastman Kodak Company
Rochester 4, New York

WALLACE R. BRODE
Ohio State University
Columbus 10, Ohio

A. H. BENNETT
American Optical Company
Buffalo 11, New York

E. H. LAND
Polaroid Corporation
Cambridge, Massachusetts

Local Sections

STANLEY S. BALLARD, *Secretary for Local Sections*

Rochester Section

ARTHUR F. TURNER, *President*
ROBERT N. WOLFE, *Vice President*
PAUL W. STEVENS, *Secretary*
HOMER C. IMES, *Treasurer*

Detroit Section

GERALD M. RASSWEILER, *Chairman*
JOHN SCHUCH, *Vice Chairman*
DANIEL L. HARMON, *Secretary*
HENRY TUTTLE, *Treasurer*

Niagara Frontier Section

ALLEN B. FUHR, *President*
GUY H. FETTERLEY, *Secretary*
HOYT G. THOMPSON, *Treasurer*

Patrons

AMERICAN OPTICAL COMPANY — BAUSCH & LOMB OPTICAL COMPANY
EASTMAN KODAK COMPANY

Corporation Members

ALLIED CHEMICAL AND DYE CORPORATION, NATIONAL ANILINE DIVISION, Buffalo, New York
AMERICAN CYSTOSCOPE MAKERS, INC., New York, New York
AMERICAN OPTICAL COMPANY, Southbridge, Massachusetts
ARGUS, INCORPORATED, Ann Arbor, Michigan
BAUSCH & LOMB OPTICAL COMPANY, Rochester, New York
BELL & HOWELL COMPANY, Chicago, Illinois
BELL TELEPHONE LABORATORIES, INC., New York, New York
CENTURY LIGHTING, INC., New York, New York
CORNING GLASS WORKS, Corning, New York
R. R. DONNELLEY & SONS COMPANY, Chicago, Illinois
E. I. DUPONT DE NEMOURS & COMPANY, INC., Chemical Department, Experimental Station, Wilmington, Delaware
EASTMAN KODAK COMPANY, Rochester, New York
EDMUND SALVAGE COMPANY, Oaklyn-Audubon, New Jersey
FAIRCHILD AVIATION CORPORATION, Jamaica, New York
FARRAND OPTICAL COMPANY, INC., New York, New York
FISH-SCHURMAN CORPORATION, New York, New York
GAERTNER SCIENTIFIC CORPORATION, Chicago, Illinois
W. & L. E. GURLEY, Troy, New York
INTERCHEMICAL CORPORATION, New York, New York
KEUFFEL & ESSER COMPANY, Hoboken, New Jersey
KOLLSMAN INSTRUMENT DIVISION OF SQUARE D COMPANY, Elmhurst, New York
NATIONAL CARBON COMPANY, Cleveland, Ohio
NATIONAL TECHNICAL LABORATORIES, South Pasadena, California
PERKIN-ELMER CORPORATION, Glenbrook, Connecticut
POLAROID CORPORATION, Cambridge, Massachusetts
PORTMAN MACHINE TOOL COMPANY, New Rochelle, New York
SIMPSON OPTICAL MANUFACTURING COMPANY, Chicago, Illinois
SOCONY-VACUUM LABORATORIES, Paulsboro, New Jersey
ARTHUR H. THOMAS COMPANY, Philadelphia, Pennsylvania
UNIVIS LENS COMPANY, Dayton, Ohio
ZENITH OPTICAL COMPANY, Huntington, West Virginia

THE OPTICAL SOCIETY OF AMERICA was organized in 1916 "*to increase and diffuse the knowledge of optics in all its branches, pure and applied, to promote the mutual interests of investigators of optical problems, of designers, manufacturers and users of optical instruments and apparatus of all kinds and to encourage cooperation among them.*" It aims to serve the interests of all who are engaged in any branch of optics from fundamental research to the manufacture of optical goods.

MEMBERSHIP

Regular Members: "Any person who has contributed materially to the advancement of optics is eligible for regular membership."

Associate Members: "Any person who is interested in optics is eligible for associate membership."

Corporate Members: "Any corporation desirous of encouraging the work of the Society is eligible for corporation membership."

Patrons: The payment, within any one year, of $1000 or more toward the expenses of the Society by any corporation or individual entitles such corporation or individual to the rank of patron.

The Society cordially invites to membership all who are interested in any branch of optics, either in research, in instruction, in optical or illuminating engineering, in the manufacture and distribution of optical goods of all kinds, or in physiological and medical optics.

ANNUAL DUES

Regular members, $8.50; Associate members, $6.00; Corporate members, $50.00. These dues include subscription to the Society's official journal, the *Journal of the Optical Society of America.*

CHANGES OF ADDRESS

All changes of address of members of the Optical Society of America should be communicated to the Secretary, Professor Arthur C. Hardy, Massachusetts Institute of Technology, Cambridge 39, Massachusetts.

Journal of the
OPTICAL SOCIETY
of AMERICA

VOLUME 38, NUMBER 3 MARCH, 1948

The Loss in Resolving Power Caused by Primary Astigmatism, Coma, and Spherical Aberration in Telescopic Systems*

HOWARD S. COLEMAN AND SAMUEL W. HARDING
The Optical Inspection Laboratory, The Pennsylvania State College, State College, Pennsylvania
(Received July 24, 1947)

The loss in resolving power caused by mixtures of, and by pure primary astigmatism, coma, and spherical aberration has been studied for telescopic systems. Resolution measurements were made by use of Foucault ["Memoire sur la construction des telescopes en verre argente," Annales de l'observatoire imperial de Paris **5**, 217 (1858)] test objects of various inherent brightness contrasts. Results of these measurements were analyzed in terms of the magnitude of the aberrations expressed in terms of the Rayleigh ["Investigations in optics, with special reference to the spectroscope," Phil. Mag. **8**, 411 (1879)] limit appropriate to the best visual focus for the telescopic systems under consideration. For high contrast test objects the loss in resolution was found to be of the order of five percent per Rayleigh limit and different for each aberration. The loss per Rayleigh limit was found to be greatest for astigmatism and least for coma. On a percentage basis, the loss in resolution caused by a given aberration was found to be greater for test objects of low contrast than for those of high contrast.

INTRODUCTION

METHODS are not available by means of which it is possible to transform the numerical results obtained by conventional ray tracing into estimates of resolving power of optical systems. This is often of particular interest in visual telescopic systems. In order to develop a new telescopic system, the usual procedure is to make the best possible design based on previous experience and then to construct a "pilot model," which can be examined experimentally. This procedure is costly and time consuming. For this reason an effort has been made on the part of the government to develop some method whereby the resolving power of telescopes could be estimated from design constants. In this connection both theoretical and experimental studies were conducted which have resulted in useful information to the designer as to the tolerable amount of aberrations in telescopic systems. It is the purpose of this paper to present some of the experimental data obtained in this study in which the aberrations considered were of the primary order.

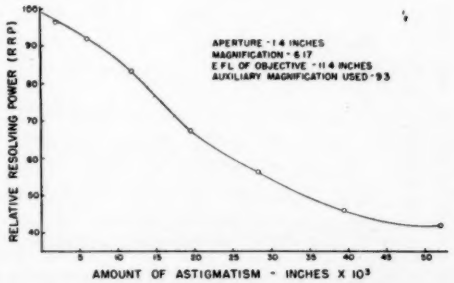

FIG. 1. Relative resolving power *vs.* amount of astigmatism present for astigmatism modifier No. 1. 100 R.R.P. = 55.4 mm-rad. $\times 10^6$. Inherent contrast of Foucault test objects = 96 percent.

This work was performed, in part, under Contract OEMsr 1197 between the Office of Scientific Research and Development and The Pennsylvania State College.

TABLE I. K.D.C. resolution measurements on the astigmatism modifier No. 1, for Focault test objects of various inherent contrast.

Amount of astigmation (inch $\times 10^3$)	Inherent contrast of test objects (percent)	Spacing of test object (lines/inch)	"S" values (inches)	Scale readings (inches)
0	96.0	38.9	16.1	16.0
0	60.0	39.0	16.0	15.4
0	42.0	39.1	16.0	14.8
0	22.0	39.1	16.0	13.8
0	15.0	25.1	24.9	19.2
0	11.6	25.2	24.8	17.1
0	6.0	25.3	24.7	13.0
2.0	96.0	38.9	16.1	15.5
2.0	60.0	39.0	16.0	15.0
2.0	42.0	39.1	16.0	14.3
2.0	22.0	39.1	16.0	13.2
2.0	15.0	25.1	24.9	17.6
2.0	11.6	25.2	24.8	15.9
2.0	6.0	25.3	24.7	11.7
11.8	96.0	38.9	16.1	13.4
11.8	60.0	39.0	16.0	12.3
11.8	42.0	39.1	16.0	10.5
11.8	28.0	25.1	24.9	14.3
11.8	15.0	25.1	24.9	10.5
11.8	15.0	20.0	31.2	13.3
11.8	7.5	19.5	32.0	9.0
28.3	96.0	38.9	16.1	9.1
28.3	69.0	25.1	24.9	13.3
28.3	45.0	25.2	24.8	10.0
28.3	26.0	19.5	32.0	9.9
28.3	17.0	10.0	62.5	14.0
28.3	9.0	9.9	63.2	9.9
52.0	92.0	30.0	20.8	8.9
52.0	71.0	20.0	31.2	12.3
52.0	47.0	19.9	31.4	9.5
52.0	27.0	10.0	62.5	11.9
52.0	17.0	10.0	62.5	7.5

TABLE II. K.D.C. resolution measurements on the coma modifier for Focault test objects of various inherent contrasts.

Amount of coma (inch $\times 10^4$)	Inherent contrast of test objects (percent)	Spacing of test object (lines/inch)	"S" values (inches)	Scale readings (inches)
0	96.0	38.9	16.1	16.1
0	60.0	39.0	16.0	15.5
0	42.0	39.1	16.0	15.1
0	22.0	39.1	16.0	14.0
0	15.0	25.1	24.9	19.9
0	11.6	25.2	24.8	18.8
0	7.4	38.9	16.1	10.8
0	6.0	25.3	24.7	13.6
−6.63	96.0	38.9	16.1	15.4
−6.63	60.0	39.0	16.0	15.1
−6.63	42.0	39.1	16.0	14.6
−6.63	22.0	39.1	16.0	13.1
−6.63	15.0	25.1	24.9	18.8
−6.63	11.6	25.2	24.8	17.7
−6.63	6.0	25.3	24.7	12.6
−13.2	96.0	38.9	16.1	14.6
−13.2	60.0	39.0	16.0	14.1
−13.2	42.0	39.1	16.0	13.1
−13.2	22.0	39.1	16.0	11.6
−13.2	15.0	25.1	24.9	15.2
−13.2	11.6	25.2	24.8	12.9
−13.2	7.5	19.5	32.0	12.1
−19.9	96.0	38.9	16.1	13.6
−19.9	60.0	39.0	16.0	12.5
−19.9	42.0	39.1	16.0	11.8
−19.9	22.0	39.1	16.0	9.6
−19.9	15.0	25.1	24.9	12.0
−19.9	11.6	25.2	24.8	9.9
−19.9	9.0	9.9	63.2	20.0
−26.5	96.0	38.9	16.1	12.0
−26.5	60.0	39.0	16.0	11.2
−26.5	42.0	39.1	16.0	10.2
−26.5	28.0	25.1	24.9	13.4
−26.5	15.0	20.0	31.2	11.0
−26.5	9.0	9.9	53.2	15.3
−33.2	96.0	38.9	16.1	10.4
−33.2	69.0	25.1	24.9	15.0
−33.2	45.0	25.2	24.8	13.2
−33.2	28.0	25.1	24.9	10.9
−33.2	15.0	20.0	31.2	9.8
−33.2	9.0	9.9	63.2	11.7

THE APPARATUS AND PROCEDURE

Resolving-power measurements were made for a number of telescopic systems using the K.D.C. apparatus.[1] In these measurements Foucault test objects of different contrast were used. The telescopic systems studied are referred to as aberration modifiers and have been described in detail in another connection.[2] These modifiers are telescopic systems designed to produce practically pure, or mixtures, of the primary aberrations in any desired amounts and are approximately of the same general characteristics as many military instruments of current design. In this paper, the modifiers are designated as the

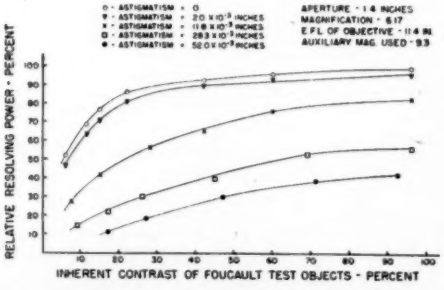
APERTURE - 1.4 INCHES
MAGNIFICATION - 6.17
E.F.L. OF OBJECTIVE - 11.4 IN.
AUXILIARY MAG. USED - 9.3
RELATIVE RESOLVING POWER - PERCENT
INHERENT CONTRAST OF FOUCAULT TEST OBJECTS - PERCENT

FIG. 2. Relative resolving power *vs.* inherent contrast of Foucault test objects for astigmatism modifier No. 1. 100 R.R.P. = 55.4 mm-rad. $\times 10^6$.

[1] H. S. Coleman and S. W. Harding, J. Opt. Soc. Am. **37**, 263 (1947).

[2] H. S. Coleman, D. G. Clark, and M. F. Coleman, "Interferometer studies of telescopic systems," J. Opt. Soc. Am. **37**, 671 (1947).

TABLE III. K.D.C. resolution measurements on the spherical aberration modifier No. 1, for Focault test objects of various inherent contrasts.

Amount of spherical aberration (inch $\times 10^3$)	Inherent contrast of test objects (percent)	Spacing of test objects (lines/inch)	"S" values (inches)	Scale readings (inches)
14.6	96.0	38.9	16.1	13.5
14.6	60.0	39.0	16.0	12.6
14.6	42.0	39.1	16.0	11.8
14.6	22.0	39.1	16.0	10.4
14.6	15.0	25.1	24.9	13.5
14.6	11.6	25.2	24.8	12.1
14.6	7.5	19.5	32.0	11.4
29.2	96.0	38.9	16.1	11.4
29.2	60.0	39.0	16.0	10.5
29.2	42.0	39.1	16.0	9.9
29.2	28.0	25.1	24.9	14.4
29.2	15.0	25.1	24.9	11.6
29.2	11.6	25.2	24.8	10.0
29.2	7.5	19.5	32.0	9.9
43.8	96.0	38.9	16.1	10.0
43.8	69.0	25.1	24.9	14.5
43.8	45.0	25.2	24.8	13.5
43.8	28.0	25.1	24.9	12.5
43.8	15.0	25.1	24.9	10.5
43.8	9.0	9.9	63.2	18.8
58.4	96.0	38.9	16.1	9.0
58.4	69.0	25.1	24.9	13.5
58.4	45.0	25.2	24.8	12.7
58.4	28.0	25.1	24.9	11.7
58.4	15.0	25.1	24.9	9.9
58.4	15.0	20.0	31.2	12.4
58.4	9.0	9.9	63.2	16.0
70.0	92.0	30.0	20.8	10.8
70.0	69.0	25.1	24.9	12.3
70.0	45.0	25.2	24.8	11.4
70.0	28.0	25.1	24.9	10.6
70.0	15.0	20.0	31.2	10.4
70.0	9.0	9.9	63.2	13.5

TABLE IV. K.D.C. resolution measurements on the spherical aberration modifier No. 2, for Foucault test objects of various inherent contrasts.

Aperture of modifier (inches)	Amount of spherical aberration (inch $\times 10^3$)	Inherent contrast of test objects (percent)	Spacing of test objects (lines/inch)	"S" values (inches)	Scale readings (inches)
1	42.8	96.0	38.9	11.7	11.5
1	42.8	60.0	39.0	11.7	10.9
1	42.8	42.0	39.1	11.6	10.4
1	42.8	22.0	39.1	11.6	9.3
1	42.8	15.0	25.1	18.1	13.1
1	42.8	11.6	25.2	18.1	11.9
1	42.8	6.0	25.3	18.0	9.1
1	42.8	4.0	9.9	46.0	16.8
1.25	66.9	96.0	38.9	14.6	12.6
1.25	66.9	60.0	39.0	14.6	11.9
1.25	66.9	42.0	39.1	14.5	11.1
1.25	66.9	22.0	39.1	14.5	9.9
1.25	66.9	15.0	25.1	22.6	13.9
1.25	66.9	11.6	25.2	22.6	12.1
1.25	66.9	6.0	25.3	22.5	9.2
1.25	66.9	4.0	9.9	57.4	17.7
1.5	95.8	96.0	38.9	17.6	11.1
1.5	95.8	60.0	39.0	17.6	10.4
1.5	95.8	42.0	39.1	17.5	9.9
1.5	95.8	22.0	39.1	17.5	9.1
1.5	95.8	15.0	25.1	27.3	12.6
1.5	95.8	11.6	25.2	27.3	11.1
1.5	95.8	7.5	19.5	35.5	10.7
1.5	95.8	4.0	9.9	69.2	12.7
1.75	130.0	96.0	38.9	20.5	10.5
1.75	130.0	60.0	39.0	20.4	10.0
1.75	130.0	42.0	39.1	20.4	9.5
1.75	130.0	22.0	39.1	20.4	8.7
1.75	130.0	15.0	25.1	31.8	11.7
1.75	130.0	11.6	25.2	31.7	10.2
1.75	130.0	7.5	19.5	40.8	9.8
2	170.0	96.0	38.9	23.4	10.6
2	170.0	60.0	39.0	23.3	10.0
2	170.0	42.0	39.1	23.3	9.5
2	170.0	22.0	39.1	23.3	8.8
2	170.0	15.0	25.1	36.4	11.7
2	170.0	11.6	25.2	36.4	10.5
2	170.0	7.5	19.5	46.7	9.5
2.5	264.0	96.0	38.9	29.2	10.6
2.5	264.0	60.0	39.0	29.2	10.0
2.5	264.0	42.0	39.1	29.1	9.6
2.5	264.0	22.0	39.1	29.1	8.8
2.5	264.0	15.0	25.1	45.3	11.8
2.5	264.0	11.6	25.2	45.3	10.2
2.5	264.0	7.5	19.5	58.3	9.1

astigmatism modifier No. 1, the coma modifier, the spherical aberration modifier No. 1, the spherical aberration modifier No. 2, and the $6\times25\times4°$ f:11.5 aberration modifier. All of these modifiers produce practically pure primary aberrations, except the last mentioned, which produces a mixture of primary astigmatism, coma, and spherical aberration.

Consideration was given to the possibility of expressing the magnitude of the aberrations in terms of a generalized coordinate such as the Rayleigh limit. Since visual telescopic systems were involved, this required that the focal position of the eyepiece be determined for the best subjective appearance of the image of the test object. For the magnitude of aberrations present in the optical systems mentioned here, the best visual focus was found to be near the paraxial focus for primary coma and spherical aberration, and half-way between the sagittal and tangential astigmatic surfaces for primary astigmatism. These results and an optical-path difference equation described by Kingslake,[3] may be used to derive expressions by means of which the magnitude of one Rayleigh limit for each of the aberrations mentioned here may be computed. These expressions are somewhat different from

[3] R. Kingslake, "Interferometer patterns due to primary aberrations," Trans. Opt. Soc. **27**, 94 (1926).

TABLE V. K.D.C. resolution measurements on the $6\times25\times4°$ f:11.5 aberration modifier for Focault test objects of various inherent contrasts.

Rotation of objective (degrees)	Amount of aberration (inches $\times10^5$) Astigmatism	Coma	Spherical aberration	Inherent contrast of test objects (percent)	Spacing of test objects (lines/in.)	"S" values (inches)	Scale readings (inches)
0	0	0	57.1	96.0	38.9	11.7	11.1
0	0	0	57.1	60.0	39.0	11.7	10.5
0	0	0	57.1	42.0	39.1	11.6	9.8
0	0	0	57.1	22.0	39.1	11.6	9.3
0	0	0	57.1	15.0	25.1	18.1	13.1
0	0	0	57.1	11.6	25.2	18.1	12.0
0	0	0	57.1	6.0	25.3	18.0	9.5
1	5.5	−1.5	57.1	96.0	38.9	11.7	10.0
1	5.5	−1.5	57.1	60.0	39.0	11.7	9.5
1	5.5	−1.5	57.1	42.0	39.1	11.6	8.8
1	5.5	−1.5	57.1	22.0	39.1	11.6	8.5
1	5.5	−1.5	57.1	15.0	25.1	18.1	12.3
1	5.5	−1.5	57.1	11.6	25.2	18.1	11.1
1	5.5	−1.5	57.1	6.0	25.3	18.0	8.2
2	12.6	−2.72	57.1	96.0	38.9	11.7	9.0
2	12.6	−2.72	57.1	60.0	39.0	11.7	8.4
2	12.6	−2.72	57.1	28.0	25.1	18.1	12.2
2	12.6	−2.72	57.1	15.0	25.1	18.1	10.1
2	12.6	−2.72	57.1	11.6	25.2	18.1	8.8
2	12.6	−2.72	57.1	7.5	19.5	23.3	9.0
3	27.2	−4.34	57.1	93.0	25.2	18.1	12.0
3	27.2	−4.34	57.1	69.0	25.1	18.1	11.5
3	27.2	−4.34	57.1	45.0	25.2	18.1	11.1
3	27.2	−4.34	57.1	28.0	25.1	18.1	10.0
3	27.2	−4.34	57.1	15.0	20.0	22.8	9.1
3	27.2	−4.34	57.1	9.0	9.9	46.0	13.5
4	48.4	−5.66	57.1	93.0	25.2	18.1	10.0
4	48.4	−5.66	57.1	69.0	25.1	18.1	9.5
4	48.4	−5.66	57.1	45.0	25.2	18.1	8.9
4	48.4	−5.66	57.1	26.0	19.5	23.3	9.9
4	48.4	−5.66	57.1	17.0	10.0	45.6	15.0
4	48.4	−5.66	57.1	9.0	9.9	46.0	10.5
5	75.6	−7.64	57.1	94.0	20.0	22.8	10.8
5	75.6	−7.64	57.1	71.0	20.0	22.8	10.4
5	75.6	−7.64	57.1	47.0	19.9	22.9	9.8
5	75.6	−7.64	57.1	27.0	10.0	45.6	15.9
5	75.6	−7.64	57.1	17.0	10.0	45.6	13.0

those in current use given by Conrady,[4] who assumed that the best focal position was mid-way between the paraxial and marginal foci. This assumption is probably valid for aberrations up to one Rayleigh limit but probably could not be tested by visual focusing of a telescope because

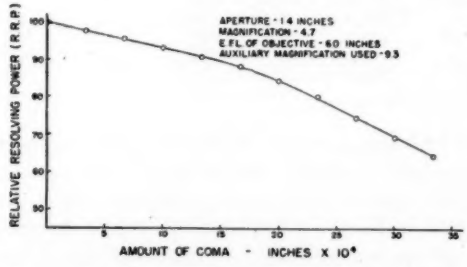
APERTURE - 1·4 INCHES
MAGNIFICATION - 4·7
E.F.L. OF OBJECTIVE - 6·0 INCHES
AUXILIARY MAGNIFICATION USED - 9·3
RELATIVE RESOLVING POWER (R.R.P.)
AMOUNT OF COMA - INCHES X 10⁵

FIG. 3. Relative resolving power *vs.* amount of coma present for the coma modifier. 100 R.R.P. = 55.4 mm-rad. $\times10^5$. Inherent contrast of Foucault test objects = 96 percent.

[4] A. E. Conrady, *Applied Optics and Optical Design* (1943), part one, pp. 434, 393, 137.

of the limitations imposed by the Rayleigh limit itself. The expressions found for the magnitude of one Rayleigh limit for those aberrations considered here are given in the following three equations.

$$\text{astigmatism} = \lambda/\sin^2\theta, \tag{1}$$

$$\text{coma}_T = 3\lambda/4\sin\theta, \tag{2}$$

$$\text{spherical aberration} = \lambda/\sin^2\theta. \tag{3}$$

In the above equations, λ is the effective wavelength of the light from the test object, and θ is

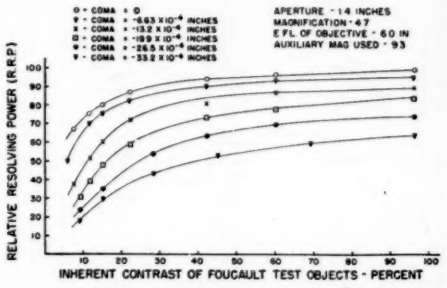
APERTURE - 1·4 INCHES
MAGNIFICATION - 4·7
E.F.L. OF OBJECTIVE - 6·0 IN
AUXILIARY MAG USED - 9·3
RELATIVE RESOLVING POWER (R.R.P.)
INHERENT CONTRAST OF FOUCAULT TEST OBJECTS - PERCENT

FIG. 4. Relative resolving power *vs.* inherent contrast of Foucault test objects for the coma modifier. 100 R.R.P. = 55.4 mm.-rad. $\times10^5$.

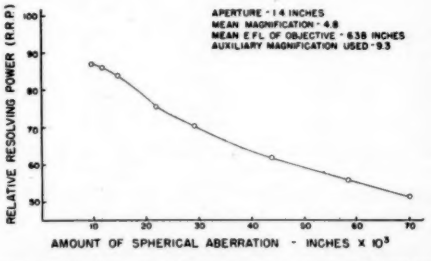
APERTURE - 1·4 INCHES
MEAN MAGNIFICATION - 4·8
MEAN E.F.L. OF OBJECTIVE - 6·38 INCHES
AUXILIARY MAGNIFICATION USED - 9·3
RELATIVE RESOLVING POWER (R.R.P.)
AMOUNT OF SPHERICAL ABERRATION - INCHES X 10⁵

FIG. 5. Relative resolving power *vs.* amount of spherical aberration present for the spherical aberration modifier No. 1. 100 R.R.P. = 55.4 mm-rad. $\times10^5$. Inherent contrast of Foucault test objects = 96 percent.

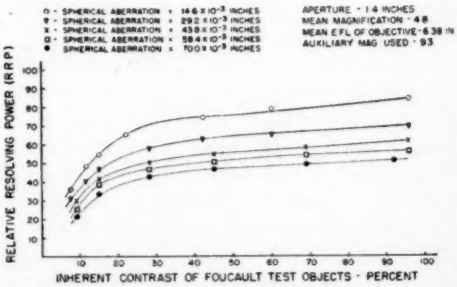
APERTURE - 1·4 INCHES
MEAN MAGNIFICATION - 4·8
MEAN E.F.L. OF OBJECTIVE - 6·38 IN
AUXILIARY MAG USED - 9·3
RELATIVE RESOLVING POWER (R.R.P.)
INHERENT CONTRAST OF FOUCAULT TEST OBJECTS - PERCENT

FIG. 6. Relative resolving power *vs.* inherent contrast of Foucault test objects for spherical aberration modifier No. 1. 100 R.R.P. = 55.4 mm-rad. $\times10^5$.

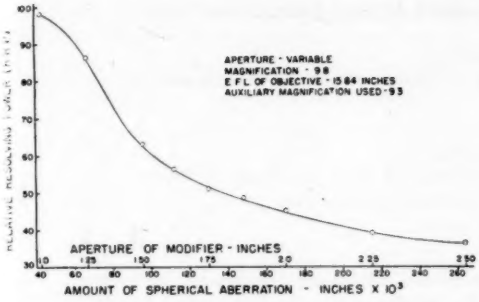
APERTURE - VARIABLE
MAGNIFICATION - 98
E F L OF OBJECTIVE - 1584 INCHES
AUXILIARY MAGNIFICATION USED - 93
APERTURE OF MODIFIER - INCHES
AMOUNT OF SPHERICAL ABERRATION - INCHES X 10³

FIG. 7. Relative resolving power *vs.* amount of spherical aberration present for the spherical aberration modifier No. 2. 100 R.R.P. = 55.4 mm-rad. $\times 10^6$. Inherent contrast of Foucault test objects = 96 percent.

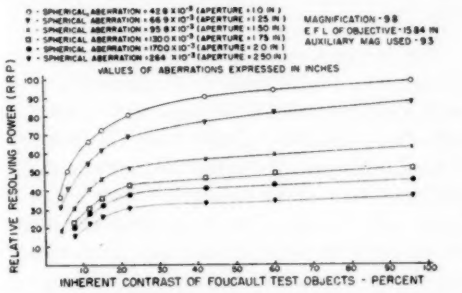
MAGNIFICATION - 98
E F L OF OBJECTIVE - 1584 IN
AUXILIARY MAG USED - 93
VALUES OF ABERRATIONS EXPRESSED IN INCHES
RELATIVE RESOLVING POWER (R R P)
INHERENT CONTRAST OF FOUCAULT TEST OBJECTS - PERCENT

FIG. 8. Relative resolving power *vs.* inherent contrast of Foucault test objects for spherical aberration modifier No. 2. 100 R.R.P. = 55.4 mm-rad. $\times 10^6$.

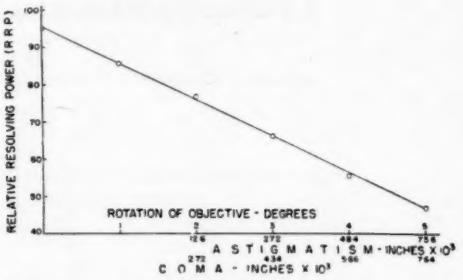

FIG. 9. Relative resolving power *vs.* amount of aberration present for the $6 \times 25 \times 4°$ *f*:11.5 aberration modifier. 100 R.R.P. = 55.4 mm-rad. $\times 10^6$. Inherent contrast of Foucault test objects = 96 percent. Amount of spherical aberration present = 57.1×10^{-3} inches (constant).

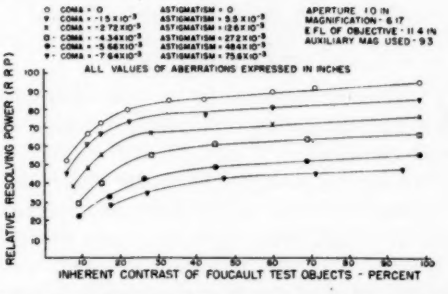
APERTURE 10 IN
MAGNIFICATION - 6 17
E FL OF OBJECTIVE - 11 4 IN
AUXILIARY MAG USED - 93
ALL VALUES OF ABERRATIONS EXPRESSED IN INCHES
RELATIVE RESOLVING POWER (R R P)
INHERENT CONTRAST OF FOUCAULT TEST OBJECTS - PERCENT

FIG. 10. Relative resolving power *vs.* inherent contrast of Foucault test objects for the $6 \times 25 \times 4°$ *f*:11.5 aberration modifier. 100 R.R.P. = 55.4 mm-rad. $\times 10^6$. Amount of spherical aberration present = 57.1×10^{-3} (constant).

the angle the marginal ray through the objective makes with the optical axis of the telescopic systems considered.

THE DATA

The data are presented in tabular and graphic form. Tables I to V, inclusive, show the data obtained in the laboratory measurements. Figures 1 to 10, inclusive, show plots of the relative resolving power of the aberration modifiers either as a function of the magnitude of the aberration present or of the inherent contrast of the target.

DISCUSSION AND CONCLUSIONS

The discussion and conclusions concerning the study of the loss of resolving power caused by the primary aberrations of astigmatism, coma, and spherical aberration are presented in the following statements:

1. It is evident from the preceding data that the loss in resolving power caused by the primary aberrations is considerable even for aberrations of moderate magnitude. These losses may be used as a guide to the designer as to the tolerable amounts of aberrations.

2. An analysis of the data presented shows that the loss in resolution per Rayleigh limit, as defined here, for coma and for spherical aberration is approximately one percent while there is an eight percent loss for astigmatism. This indicates that even a fraction of a Rayleigh limit of astigmatism cannot be tolerated in a telescopic system of the highest quality.

3. It is evident from the preceding data, that on a percentage basis, the loss in resolving power caused by the primary aberrations is greater for test objects of low contrast than for those of high contrast.

ACKNOWLEDGMENT

The authors wish to acknowledge the interest and assistance received from Dr. R. Kingslake of the Eastman Kodak Company, Rochester, New York.

A Calibration Method for Infra-Red Prism Spectrometers[1]

D. S. McKINNEY
Chemistry Department, Carnegie Institute of Technology, Pittsburgh, Pennsylvania

AND

R. A. FRIEDEL[2]
Research and Development Division, Office of Synthetic Fuels, U. S. Bureau of Mines, Central Experiment Station, Pittsburgh, Pennsylvania

(Received July 28, 1947)

A method of high accuracy applicable to various prisms in infra-red spectrometry has been used to calibrate NaCl and KBr prisms. The method requires only a small number of experimental bands, is practically independent of resolving power, provides an extensive wave-length range, and permits a tabulated calibration without the necessity of drawing calibration curves. The procedure is described in detail with an example.

INTRODUCTION

THE principal method used in recent years for calibrating infra-red rocksalt spectrometers between 5 and 15 microns has been that of Oetjen, Kao, and Randall.[3] Their method employs some 150 points from the spectra of NH_3, CO_2, and H_2O vapor measured on both a prism and a grating spectrometer, with the resolving power of the latter adjusted to that of the prism instrument. Under these conditions, wave-lengths of the bands calculated from the grating characteristics are transferable directly to the prism instrument being calibrated.

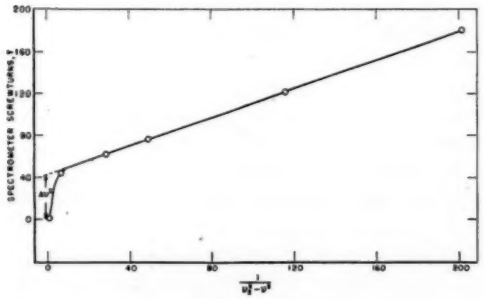

FIG. 1. Relationship between spectrometer screw-turns, T, and $1/(\nu_2^2-\nu^2)$ for research-type NaCl spectrometer from 0.6 to 15.0 microns; C_2H_2, C_2H_4, C_6H_6, and NaD calibration points.

The original calibration of a research spectrometer at the Chemistry Department of Carnegie Institute of Technology was based on 20 points calculated by Cross[4] from the dimensions of his instrument and refractive index values for rocksalt. Precise interpolation between Cross' points was not possible because of doubt as to the proper curvature of the line. Accordingly, it was decided to search for an empirical equation which could be used to carry out this interpolation. The equation found proved to be of sufficient accuracy to describe the whole curve, from the visible region to 15 microns, without relying on refractive index data which might be in error because of impurities in the rocksalt sample used to obtain the data.

EQUATION

The empirical equation is based on the curve (Fig. 1) obtained from six spectral bands by plotting for each band the spectrometer screw-turn value, T, *vs.* $1/(\nu_2^2-\nu^2)$, where ν is the corresponding frequency and ν_2 is a Restrahlen or neighboring frequency of the prism material. The curve is a straight line from about 3.5 to 15 microns. Curvature in the short wave-length region is attributed to absorption of NaCl in the ultraviolet region, for which a correction term has to be applied. The obvious form of the correction would correspond to the above frequency term, namely, $1/(\nu_1^2-\nu^2)$, in which ν_1 would be the frequency of the absorption band

[1] Published by permission of the Director, U. S. Bureau of Mines and presented before the Optical Society of America, fall meeting, 1946.

[2] Initial work on this subject submitted in partial fulfillment of the requirements for the degree of Doctor of Science at Carnegie Institute of Technology.

[3] R. A. Oetjen, Chao-Lau Kao, and H. M. Randall, Rev. Sci. Inst. **13**, 515 (1942).

[4] P. C. Cross, Rev. Sci. Inst. **4**, 197 (1933).

TABLE I. Spectral data for NaCl calibration. ($\nu_2 = 125$ cm^{-1}).

	Compound	Wave-length in microns[a]	Frequency in cm^{-1} [a]	Screw-turn T[b]	$\frac{1}{\nu_2^2-\nu^2}$	$\frac{B}{\nu_2^2-\nu^2}$	$A\nu^2$	T_0
I	Na	0.5890	16,969	2,166.6	$-0.37431\cdot10^{-8}$	−2.222	390.744	−1778.08
II	H_2O	2.673	3,741	1,740.6	$-7.15335\cdot10^{-8}$	−45.774	18.991	−1777.38
III	CO_2	4.225	2,367	1,670.0	$-17.8984\cdot10^{-8}$	−114.532	7.603	−1776.93
IV	H_2O	5.463	1,830	1,590.2	$-30.0005\cdot10^{-8}$	−191.973	4.544	−1777.63
V	H_2O	6.107	1,637	1,541.1	$-37.5355\cdot10^{-8}$	−240.190	3.636	−1777.65
VI	H_2O	6.784	1,474	1,483.9	$-46.3596\cdot10^{-8}$	−296.656	2.948	−1777.61
VII	NH_3	8.490	1,177.9	1,313.1	$-72.8957\cdot10^{-8}$	−466.460	1.883	−1777.68
VIII	NH_3	9.057	1,104.1	1,247.5	$-83.0971\cdot10^{-8}$	−531.739	1.654	−1777.58
IX	NH_3	9.876	1,012.6	1,145.9	$-99.0360\cdot10^{-8}$	−633.733	1.391	−1778.25
X	NH_3	10.540	948.8	1,056	$-113.0459\cdot10^{-8}$	−723.382	1.222	−1778.56
XI	NH_3	11.206	892.4	959.5	$-128.081\cdot10^{-8}$	−819.594	1.081	−1778.01
XII	NH_3	12.075	828.2	823.6	$-149.189\cdot10^{-8}$	−954.663	0.931	−1777.34
XIII[c]	CO_2	13.875	720.7	507.5	$-198.498\cdot10^{-8}$	−1270.191	0.705	−1776.99
XIV	CO_2	14.97	668.0	293.1	$-232.235\cdot10^{-8}$	−1486.074	0.606	−1778.57

[a] Values for points IV and XIII inclusive obtained from R. A. Oetjen, C. L. Kao, and H. M. Randall, Rev. Sci. Inst. 13, 515 (1942).
[b] All screw-turn values corrected for small, uncompensated temperature shifts, etc., using 4.225μ CO_2 band as base point.
[c] The 13.417μ NH_3 band was included formerly, but because of unreproduceability due to broadness it has been omitted.

in the ultraviolet. Since these data could not be found in the literature and since it is desirable not to introduce another parameter into the equation, the first two terms of the expansion are used: $1/(\nu_1^2-\nu^2) = \text{constant} + A\nu^2 + \cdots$. The final form of the equation is

$$T + T_0 = A\nu^2 + B/(\nu_2^2 - \nu^2),$$

where B is the slope of the straight-line portion of T *vs.* $1/(\nu_2^2-\nu^2)$, $A\nu^2$ is the correction term for ultraviolet absorption, and T_0 is a nearly constant term which varies slightly with wave-length. There is notable similarity between this equation and the refractive index equation:

$$n^2 = 1 + (e^2/\pi m)\sum_i N_i/(\nu_i^2 - \nu^2).$$

Calibration involves first the simple evaluation of constants A and B as illustrated below. Then the nearly constant T_0 terms are calculated for each experimentally determined absorption band and the values plotted against corresponding wave-lengths. Lastly, the spectrometer screw-turn value T can be calculated for any chosen frequency and a complete calibration obtained.

The slight variation of T_0 values is attributed to deviation of the apparently straight-line portion of T *vs.* $1/(\nu_2^2-\nu^2)$ from perfect linearity. The original T_0 curve, using five absorption bands and the NaD line, is curve *a* of Fig. 2. In order to minimize errors, the total spread of T_0 values is decreased by using a better method for calculating the constant B and by changing ν_2 from one Restrahlen frequency, 192.5 cm^{-1}, to the principal Restrahlen frequency at 184 cm^{-1}. The resulting curve *b* gives a total spread of T_0 values equivalent to only 0.006 micron at 10 microns. The S-shape of the curve was somewhat dubious but has been verified on another research instrument using the same experimental points, and also on a Perkin-Elmer spectrometer at the Bureau of Mines using 13 selected bands from the spectra of NH_3, CO_2, and H_2O vapor by Oetjen, *et al.*, and the NaD line. The T_0 curve obtained for the latter conditions is shown in Fig. 3. The calibration range in this case has been extended to the 14.97μ CO_2 band with the production of another minimum in the curve. For the Perkin-Elmer instrument 125 cm^{-1} is

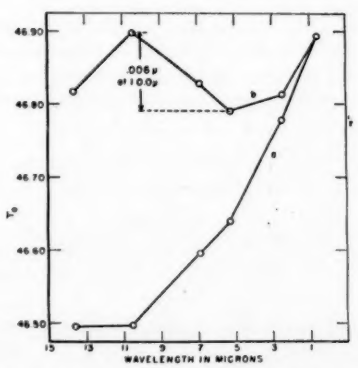

FIG. 2. T_0 curves for research-type NaCl spectrometer; C_2H_2, C_2H_4, C_6H_6, and NaD calibration points. Curve *a*: $\nu_2 = 192.5$ cm^{-1}, B calculated from 10.5 and 13.7μ bands. Curve *b*: $\nu_2 = 184$ cm^{-1}, B calculated from 2.5 and 13.7μ bands.

TABLE II. Spectral bands for KBr calibration.

	Compound	Wave-length in microns	Frequency in cm^{-1}	Screw-turns[a] T
I	CO_2	14.970	668.0	1334.0
II	CO_2	16.181	618.0	1243.7
III	CH_3OH	18.215	549.0	1083.7
IV	H_2O	19.003	526.23	1016.0
V	H_2O	19.902	502.45	935.5
VI	H_2O	21.155	472.68	814.0
VII	H_2O	21.831	458.05	744.5
VIII	H_2O	23.854	419.20	518.5
IX	H_2O	25.137	397.81	363.0
X	H_2O	25.962	385.17	256.0
XI	H_2O	26.628	375.54	170.0
XII	H_2O	27.020	370.09	115.5

[a] 14.970μ CO_2 band used as base point for correction due to temperature shift, etc.

found to be the value of ν_2 most satisfactory for keeping the spread of T_0 values small. The ordinate in Fig. 3 is in terms of small divisions on the wave-length drum; the equivalent in microns is given at various wave-lengths to illustrate the magnitude of the variation.

CALIBRATION PROCEDURE FOR NaCl PRISM

The method of calibrating a Perkin-Elmer spectrometer with NaCl prism follows in detail. Complete sample data using the 14 points referred to above are given in Table I and in the necessary steps of the procedure.

1. *Rough A value:* Plot screw-turns, T, *vs.* $1/(\nu_2^2-\nu^2)$. Extrapolate linear part of curve and measure distance on T axis from the extrapolated portion to the NaD-line value as indicated in Fig. 1 for a research-type instrument. This quantity is the correction term for the NaD-line value, $A\nu_{Na}^2$, from which A is calculated: e.g., $T_{Na}-T_{intercept}=2166.6-1779=387.6=A\nu_{Na}^2$; $\therefore A=387.6\div 287{,}946{,}961=1.345\cdot 10^{-6}$. Calculate $A\nu^2$ for the first three wave-lengths.

2. *Final B value:* Solve simultaneous equations of $T+T_0=A\nu^2+B/(\nu_2^2-\nu^2)$ for B, using data from points III and XIII of the table (T_0 considered constant):

$$\text{e.g., III:}\quad 1670.0+T_0=7.536-B\cdot 17.898\cdot 10^{-8}$$
$$\text{XIII:}\quad 507.5+T_0=0.699-B\cdot 198.498\cdot 10^{-8}$$
$$B=6.3990\cdot 10^{+8}.$$

Calculate $B/(\nu_2^2-\nu^2)$ for all points.

3. *Final A value:* Calculate T_0 from the equation for the first three points and plot T_0 *vs.* wave-length. Adjust A arbitrarily until a smooth curve is obtained. The value of A chosen for the present calibration is $1.357\cdot 10^{-6}$; if the difference between rough and final A values is appreciably greater than found here, it is desirable to recalculate B. Calculate $A\nu^2$ for all points.

4. *T_0 curve:* Calculate T_0 for all points and plot T_0 *vs.* wave-length (Fig. 3).

5. *Tabulated calibration:* Calculate T, screw-turns, for as many wave-lengths as the accuracy requires; get the necessary T_0 values from the T_0 *vs.* wave-length curve. Tabulate the data or draw a calibration curve if desired.

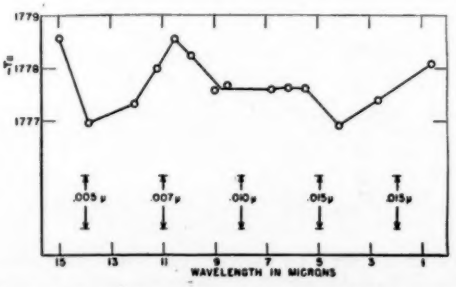

FIG. 3. T_0 curve for NaCl prism, Perkin-Elmer spectrometer; NH_3, H_2O, CO_2, and NaD calibration points. Wave-length equivalents of T_0 variations are indicated.

CALIBRATION OF KBr PRISM

The calibration of a KBr prism is simpler because there is no short wave-length curvature (Fig. 4) and, therefore, no necessity for the $A\nu^2$ correction term. The principal Restrahlen frequency of KBr, 115.2 cm^{-1}, is used for the term, ν_2. Experimental points from the spectra of CO_2, H_2O, and CH_3OH vapor are listed in Table II. Wave-lengths for the H_2O vapor points are obtained from the grating spectrum of Randall, *et al.*[5] The high resolution of this spectrum does not detract appreciably from the accuracy of the calibration since the bands selected are sufficiently symmetrical to obviate the use of

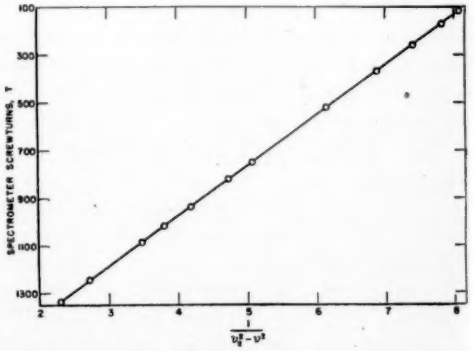

FIG. 4. Relationship between spectrometer screw-turns, T, and $1/(\nu_2^2-\nu^2)$ for KBr prism. Perkin-Elmer spectrometer, from 15 to 27 microns; CO_2, CH_3OH, and H_2O vapor calibration points.

[5] Randall, Dennison, Ginsburg, and Weber, Phys. Rev. **52**, 160 (1937).

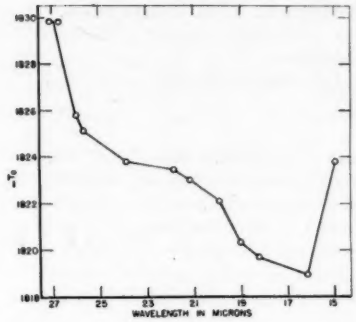

FIG. 5. T_0 curve for KBr prism, Perkin-Elmer spectrometer; CO_2, CH_3OH, and H_2O vapor calibration points.

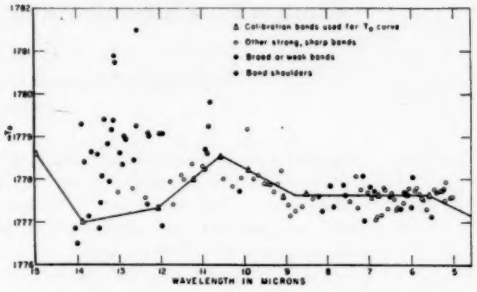

FIG. 6. Comparison of calibration methods: T_0 points, calculated from our spectra for all the NH_3 and H_2O bands used by Oetjen, *et al.*, are plotted together with portion of T_0 curve for the present calibration. Bands are arbitrarily classified according to strength or sharpness.

weighted averages for groups of resolved bands. Data from a spectrum of lower resolution, such as the KBr spectrum of H_2O by Weber and Randall,[6] would be preferable, but the accuracy of their work is insufficient. However, the tracing of the spectrum given in their article is very helpful in identifying the bands obtained on the Perkin-Elmer instrument. The T_0 curve (Fig. 5) follows somewhat the same pattern as the corresponding curve for NaCl.

Bands for H_2O vapor and the one band for CH_3OH vapor are obtained by simply placing a dish of the liquid in the small Perkin-Elmer housing with salt windows removed. Intensities of atmospheric H_2O vapor bands thus increase only slightly, but advantageously.

DISCUSSION

The chief advantages of the method are: (1) the extensive wave-length range, (2) the small number of bands required, (3) practical independence of resolving power since the bands chosen should be sufficiently sharp and symmetrical on most instruments, (4) accurate interpolation between experimental points because any number of points may be calculated, (5) applicability to various prisms, (6) tabulation of data without the necessity of drawing the usual complex calibration curve, and (7) exposure of doubtful points obtained from broad, weak, or unsymmetrical bands. The significance of the last item for a NaCl prism is shown in Fig. 6. The method of Oetjen, *et al.*, is compared with the present calibration by calculating from our spectra T_0 values for all NH_3 and H_2O points used by them. With one notable exception, all values for the bands which are arbitrarily classified as strong or sharp fall closely in line with those of the very sharp bands which determine the T_0 calibration curve. But, bands which are broad or which appear only as shoulders, because of our slightly lower resolving power, produce scattered T_0 values; this is particularly true for the longer wave-length NH_3 bands. Further, the 15μ CO_2 fine structure bands which are included in their calibration method, are detectable on the present instruments but are not reliable. A calibration curve drawn through such scattered points is questionable and not conducive to good accuracy.

Modifications of the method outlined are obviously possible. The T *vs.* $1/(\nu_2^2-\nu^2)$ curve in Fig. 1 is sufficiently linear between about 3.5 and 15 microns to permit an accurate calibration between these limits without dangerous interpolation and without evaluation of constants. Thus $1/(\nu_2^2-\nu^2)$ may be calculated for a whole range of frequencies, the values applied to the straight line, and the screw-turn values read off directly.

We wish to express our thanks to Ruth Borgman and Lois Pierce who carried out most of the measurements and calculations.

[6] L. Weber and H. M. Randall, Phys. Rev. **40**, 835 (1932).

Fluorescence Efficiency and Hole Migration in Zinc Sulphides

M. E. WISE AND H. A. KLASENS
Material Research Laboratory, Philips Lamps, Ltd., London, England

(Received July 29, 1947)

General equations are derived for predicting the change in fluorescent intensity of zinc-sulphide phosphors containing more than one kind of impurity activating center, according to the theory of hole migration. The effect on the blue fluorescence efficiency of exciting intensity, temperature, and one other kind of center is discussed. If this other center is a killer which produces no visible radiation, it is shown that the observed fluorescence of ZnS-Ag-Co quantitatively agrees with the theory if the probability that a particular excited Co center will recombine with an electron in the conduction band in unit time is much larger than the corresponding probability for a silver center.

The influence of independent electron traps on the hole migration is also discussed.

I. INTRODUCTION

THE theory of hole migration[1] explains qualitatively a wide range of results. If one makes any combination of changes in the temperature, the exciting intensity, and the concentration of impurities such as Ni or Co, the Klasens-Schön theory nearly always predicts the observed change in the fluorescence efficiency and the color of the phosphor. The theory also explains some color changes during the afterglow.

However, Klasens' equations are the simplest possible for illustrating the theory. Accurate measurements of the effect of change of exciting intensity have shown, however,[2] that the conditions under which these equations are valid are not always satisfied. We therefore endeavored to find equations which are more generally applicable.

II. MATHEMATICAL FORMULATION

We have decided to use notation consistent with that used by Klasens and Wise[3] for decay equations for zinc sulphides containing traps of one depth. Suffices 1, 2, and 3 indicate impurity centers at increasing distances from the filled band. It is assumed, as in (1), that positive holes leave excited silver centers of concentration n_1, at a rate $\gamma_{1f}n_1$, when an electron in the filled S^{--} band receives sufficient thermal energy to be excited to the level of the center. The holes then move through the filled band and recombine with unexcited centers—with silver centers at a rate $\alpha_{f1}(N_1-n_1)n_f$, where n_f is the concentration of holes in the filled band and N_1-n_1 that of unexcited silver centers—or with green centers, say at a rate $\alpha_{f2}(N_2-n_2)n_f$, etc. Similarly, the holes may leave or recombine with other centers.

For the more familiar luminescence processes, we assume that $\mu_1 J$, $\mu_2 J$ centers of the 1st or 2nd kind are ionized per second when the exciting intensity is J; that electrons from these centers are excited into the conduction band, and that the free electrons in the conduction band, of concentration n, recombine with other centers at rates $\beta_1 n n_1$, $\beta_2 n n_2$, $\beta_3 n n_3$. Then the luminescence intensity in quanta per second at blue centers is

$$I_1=\beta_1 n n_1. \tag{2.1}$$

For the present we shall neglect the effect of electron traps. The number of excited electrons is equal to the number of positive holes. With three kinds of excited centers

$$n=n_1+n_2+n_3+n_f, \tag{2.2}$$

$$\frac{dn}{dt}=(\mu_1+\mu_2+\mu_3)J-n(\beta_1 n_1+\beta_2 n_2+\beta_3 n_3), \tag{2.3}$$

$$\frac{dn_1}{dt}=\mu_1 J-\beta_1 n n_1-\gamma_{1f}n_1+\alpha_{f1}(N_1-n_1)n_f, \tag{2.4}$$

$$\frac{dn_2}{dt}=\mu_2 J-\beta_2 n n_2-\gamma_{2f}n_2+\alpha_{f2}(N_2-n_2)n_f, \tag{2.5}$$

$$\frac{dn_3}{dt}=\mu_3 J-\beta_3 n n_3-\gamma_{3f}n_3+\alpha_{f3}(N_3-n_3)n_f. \tag{2.6}$$

We shall write

$$\Gamma_{f1}=\alpha_{f1}N_1\left(1-\frac{n_1}{N_1}\right), \quad \Gamma_{f2}=\alpha_{f2}N_2\left(1-\frac{n_2}{N_2}\right),$$

[1] H. A. Klasens, Nature **158**, 306 (1946); M. Schön, Zeits. f. Physik **119**, 463 (1942).
[2] H. A. Klasens, W. Ramsden, and Chow Quantie, J. Opt. Soc. Am. **37**, 60 (1947).
[3] H. A. Klasens and M. E. Wise, Nature **158**, 483 (1946).

so that coefficients with two suffixes always indicate the transfer of a positive hole. We shall assume that the number of excited centers is always small compared with the number of unexcited centers, so that Γ_{f1}, Γ_{f2}, Γ_{f3} are independent of n_1, n_2, n_3, respectively.

The equilibrium fluorescence is given by

$$\frac{dn}{dt}=\frac{dn_1}{dt}=\frac{dn_2}{dt}=\frac{dn_3}{dt}=0. \tag{2.7}$$

Eliminating n_1, n_2, n_3, and n_f,

$$\begin{vmatrix} n & 1 & 1 & 1 & 1 \\ \cdot & -\gamma_{1f} & -\gamma_{2f} & -\gamma_{3f} & \Gamma_{f1}+\Gamma_{f2}+\Gamma_{f3} \\ J\mu_1 & \beta_1 n+\gamma_{1f} & \cdot & \cdot & -\Gamma_{f1} \\ J\mu_2 & \cdot & \beta_2 n+\gamma_{2f} & \cdot & -\Gamma_{f2} \\ J\mu_3 & \cdot & \cdot & \beta_3 n+\gamma_{3f} & -\Gamma_{f3} \end{vmatrix}=0. \tag{2.8}$$

Solving (2.3) to (2.7) for n_1, n_2, n_3, and n_f, the blue intensity I_1 is given by

$$\frac{I_1}{\beta_1}=nn_1=\frac{J\begin{vmatrix} \cdot & -\gamma_{2f} & -\gamma_{3f} & -(\Gamma_{f1}+\Gamma_{f2}+\Gamma_{f3}) \\ \mu_1 & \cdot & \cdot & \Gamma_{f1} \\ \mu_2 & \beta_2 n+\gamma_{2f} & \cdot & \Gamma_{f2} \\ \mu_3 & \cdot & \beta_3 n+\gamma_{3f} & \Gamma_{f3} \end{vmatrix}}{\Delta} \tag{2.9}$$

where

$$\Delta=\begin{vmatrix} \beta_1 & \beta_2 & \beta_3 & \cdot \\ \beta_1 n+\gamma_{1f} & \cdot & \cdot & \Gamma_{f1} \\ \cdot & \beta_2 n+\gamma_{2f} & \cdot & \Gamma_{f2} \\ \cdot & \cdot & \beta_3 n+\gamma_{3f} & \Gamma_{f4} \end{vmatrix}. \tag{2.10}$$

The generalizations to any number of centers are obvious.

By expanding (2.8) from the first column we can write the equation for n as

$$J\begin{vmatrix} \cdot & 1 & 1 & 1 & 1 \\ \cdot & -\gamma_{1f} & -\gamma_{2f} & -\gamma_{3f} & \Gamma_{f1}+\Gamma_{f2}+\Gamma_{f3} \\ \mu_1 & \beta_1 n+\gamma_{1f} & \cdot & \cdot & -\Gamma_{f1} \\ \mu_2 & \cdot & \beta_2 n+\gamma_{2f} & 1 & -\Gamma_{f2} \\ \mu_3 & \cdot & \cdot & \beta_3 n+\gamma_{3f} & -\Gamma_{f3} \end{vmatrix}=\Delta n^2. \tag{2.11}$$

From now on we shall consider special cases of these results which can be compared with observations.

III. FLUORESCENCE OF PHOSPHORS WITH BLUE AND GREEN CENTERS ONLY

If there are two centers only, say blue and green, with intensities $I_1=\beta_1 nn_1$, $I_2=\beta_2 nn_2$,

$$\frac{I_2}{I_1}=\frac{\mu_2+\dfrac{(\mu_1+\mu_2)\gamma_{1f}\Gamma_{f2}}{\beta_1 n(\Gamma_{f1}+\Gamma_{f2})}}{\mu_1+\dfrac{(\mu_1+\mu_2)\gamma_{2f}\Gamma_{f1}}{\beta_2 n(\Gamma_{f1}+\Gamma_{f2})}}, \tag{3.1}$$

whilst n satisfies

$$\frac{J}{n^2}=\frac{1+\left(\dfrac{\gamma_{1f}\Gamma_{f2}}{\beta_1}+\dfrac{\gamma_{2f}\Gamma_{f1}}{\beta_2}\right)\dfrac{1}{(\Gamma_{f1}+\Gamma_{f2})n}}{\dfrac{\mu_1}{\beta_1}\left(1+\dfrac{\gamma_{1f}}{\Gamma_{f1}+\Gamma_{f2}}\right)+\dfrac{\mu_2}{\beta_2}\left(1+\dfrac{\gamma_{2f}}{\Gamma_{f1}+\Gamma_{f2}}\right)+\dfrac{\mu_1+\mu_2}{\beta_1\beta_2 n}\left(\dfrac{\gamma_{1f}\Gamma_{f2}+\gamma_{2f}\Gamma_{f1}+\gamma_{1f}\gamma_{2f}}{\Gamma_{f1}+\Gamma_{f2}}\right)}. \tag{3.2}$$

The blue efficiency I_1/J is given by

$$\frac{I_1}{J\mu_1}=\frac{1+\left(1+\frac{\mu_2}{\mu_1}\right)\frac{\gamma_{2f}\Gamma_{f1}}{\beta_2 n(\Gamma_{f1}+\Gamma_{f2})}}{1+\left(\frac{\gamma_{f1}\Gamma_{f2}}{\beta_1}+\frac{\gamma_{2f}\Gamma_{f1}}{\beta_2}\right)\frac{1}{(\Gamma_{f1}+\Gamma_{f2})n}}, \quad (3.3)$$

and $I_2/J\mu_2$, of course, is obtained by interchanging suffixes 1 and 2 in the numerator of (3.3).

Now γ_{1f}, γ_{2f} are of the form $S_1e^{-E_1/kT}$, $S_2e^{-E_2/kT}$ and increase with temperature. The green centers are further from the filled band, so $\gamma_{2f}<\gamma_{1f}$, especially at low temperatures. Neglecting γ_{2f}, we get the formulae corresponding to Klasens' simple formulae—thus increasing n has the same effect as cooling the phosphor, i.e., it lowers I_2 anf raises I_1 as before. The main difference is that n is not exactly proportional to $J^{\frac{1}{2}}$. It would be so if $\beta_1=\beta_2$ and holes spend a negligible time in the filled band (i.e., γ_{1f}, $\gamma_{2f}\ll\Gamma_{f1}$, Γ_{f2}).

At very high intensities

$$\frac{n}{J^{\frac{1}{2}}}\doteqdot\frac{\mu_1}{\beta_1}\left(1+\frac{\gamma_{1f}}{\Gamma_{f1}+\Gamma_{f2}}\right)+\frac{\mu_2}{\beta_2}, \quad (3.4)$$

and at low intensities

$$\frac{n}{J^{\frac{1}{2}}}\doteqdot\frac{\mu_1+\mu_2}{\beta_2}. \quad (3.5)$$

IV. FLUORESCENCE OF ZINC SULPHIDE WITH ONE KIND OF LUMINESCENCE CENTER FROM WHICH HOLES MIGRATE AND ONE KIND OF KILLING CENTER FROM WHICH HOLES DO NOT MIGRATE

If the green centers of paragraph 3 are replaced by killer centers, the effect on the blue intensity should be the same, because the only difference between killer and luminescent centers is that free electrons recombining with holes in killer centers give no visible radiations. It will be assumed that holes do not leave killer centers in the temperature range considered because their energy levels are too far from the filled band.

Then from (3.2) and (3.3), with suffixes 2 for cobalt centers and putting γ_{2f} equal to 0, the blue intensity $I_1=\beta_1 n n_1$ in quanta per second is given by

$$\frac{J\mu_1}{I_1}=1+u,$$

where

$$u=\frac{\gamma_{1f}\Gamma_{f2}}{\beta_1 n(\Gamma_{f1}+\Gamma_{f2})}, \quad (4.1)$$

and u satisfies

$$J=\frac{1+u}{u^2/b_1^2+u^3/b_2^2}, \quad (4.2)$$

where

$$b_1=\frac{\gamma_{1f}\Gamma_{f2}}{\beta_1(\Gamma_{f1}+\Gamma_{f2})}\left\{\frac{\mu_1}{\beta_1}\left(1+\frac{\gamma_{1f}}{\Gamma_{f1}+\Gamma_{f2}}\right)+\frac{\mu_2}{\beta_2}\right\}^{-\frac{1}{2}}, \quad (4.3)$$

$$b_2=\frac{\gamma_{1f}\Gamma_{f2}}{\beta_1(\Gamma_{f1}+\Gamma_{f2})}\left\{\frac{\mu_1+\mu_2}{\beta_2}\right\}^{-\frac{1}{2}}. \quad (4.4)$$

From (4.2) it follows that for small values of u (i.e., high exciting intensities)

$$J=\frac{b_1^2}{u^2},$$

or

$$1+u=1+b_1J^{-\frac{1}{2}}.$$

Thus from (4.1)

$$\frac{\mu_1 J}{I_1}=1+b_1J^{-\frac{1}{2}}. \quad (4.5)$$

In the same way it follows that for large values of u (i.e., small exciting intensities)

$$\frac{\mu_1 J}{I_1}=1+b_2J^{-\frac{1}{2}}. \quad (4.6)$$

In Fig. 1, J/I_1 is plotted as a function of $J^{-\frac{1}{2}}$ for $b_1<b_2$ (A) and $b_1>b_2$, (B). (4.5) is the tangent at $J^{-\frac{1}{2}}=0$, $J/I_1=1/\mu_1$, and (4.6) passes through this point of contact and is an asymptote. The curve lies between these lines so that its curvature must change sign. But this is evident only at very low efficiencies.

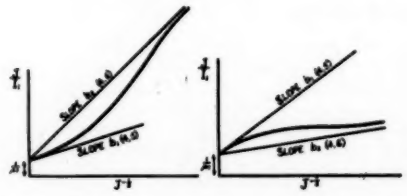

FIG. 1. Form of J/I_1 as a function of $J^{-\frac{1}{2}}$ satisfying $\mu_1J/I_1=1+u$ and $J=\frac{1+u}{u^2/b_1^2+u^3/b_2^2}$; A: $b_1<b_2$; B: $b_2<b_1$.

Klasens, Ramsden, and Chow Quantie have obtained many intensity-dependence curves, and their points appear to be all on the part of the curve near (4.5). Further evidence for this comes from comparing their curves at different temperatures. At low temperatures J/I_1 was nearly constant, so that the value corresponding to infinite exciting intensity could easily be obtained by extrapolation. When the scale factor for J was chosen so that the value of J/I_1 was then equal to 1, the intercepts $(1/\mu_1)$ on the J/I_1 axis at other temperatures were also found to be near 1.*

We next estimated the slopes (b_1) at $J^{-\frac{1}{2}}=0$. In all the curves the slopes increased with $J^{-\frac{1}{2}}$. Thus $b_2>b_1$ and $\beta_2>\beta_1$. There were enough points for testing the full formula (4.2). To do this, values of u were first calculated at various points using (4.1). We found that theoretical and observed values in (4.1) could agree but only if the ratio b_1^2/b_2^2 was very small. When that is so it is seen from (3.2) and (3.3) that with $\beta_2\gg\beta_1$ it is no longer necessary to assume that γ_{2f} is negligible. Also (4.2) and (4.1) simplify to

$$u=b_1\mu_1^{\frac{1}{2}}I_1^{-\frac{1}{2}}. \tag{4.7}$$

So from (4.1)

$$\frac{J}{I_1}=\frac{1}{\mu_1}+\frac{b_1}{(\mu_1 I_1)^{\frac{1}{2}}}. \tag{4.8}$$

If β_2 is very large, (4.3) becomes

$$b_1=\frac{\gamma_{1f}\Gamma_{f2}}{(\Gamma_{f1}+\Gamma_{f2})(\beta_1\mu_1)^{\frac{1}{2}}}\left\{1+\frac{\gamma_{1f}}{\Gamma_{f1}+\Gamma_{f2}}\right\}^{-\frac{1}{2}}. \tag{4.9}$$

We shall now consider this expression in more detail. The factor $[1+\gamma_{1f}/(\Gamma_{f1}+\Gamma_{f2})]^{-\frac{1}{2}}$ gives the effect of the concentration of holes in the filled band. Thus this does not affect the form of the intensity-dependence curves. If n_f is small γ_{1f}/Γ_{f1} is small, b_1 is then of the form

$$b_1=B_1e^{-E_1/kT} \tag{4.10}$$

where B_1 varies with the concentration of the centers but not with intensity or temperature, for it is reasonable to assume that the cross sections for the capture of electrons, holes, and photons do not change markedly with temperature. E_1 can then be deduced from the change of b_1 with temperature for one phosphor. Within the limits of the observed changes of b_1 with temperature (reference 2, Fig. 7) this simplification seemed justified.

* See Fig. 5, reference 2.

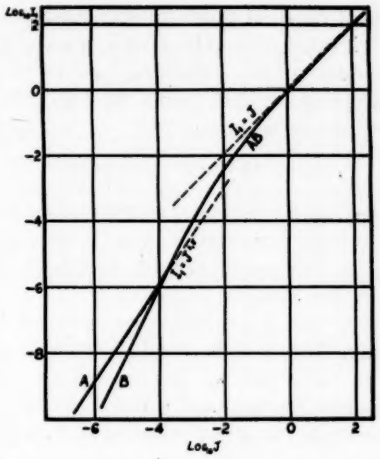

FIG. 2. Theoretical values of $\log_{10} I_1$ *vs.* $\log_{10} J$ when

(A) $(J\mu_1/I_1)=1+u$; $J=\dfrac{1+u}{u^2/b_1^2+u^3/b_2^2}$;

(B) $J/I_1=1/\mu_1+b_1/(\mu_1 I_1)^{\frac{1}{2}}$ with $\mu_1=1$, $b_1=01$, $b_2=1$.

(4.9) and (4.7) now give the very simple result

$$I_1=\beta_1 n^2. \tag{4.11}$$

The physical meaning of (4.10) is that if β_2 is very large the average life of a hole in a killer center is very short. As a result, the concentration of holes in killer centers may still be small, compared with that in silver centers, even when a great percentage of holes migrate from silver centers to killer centers.** Then n is approximately equal to n_1, and (4.11) follows immediately from (2.1). By the use of (4.9) and (4.11) we can rewrite (4.8) as

$$0=\mu_1 J-\beta_1 n^2-\frac{\gamma_{1f}\Gamma_{f2}}{\Gamma_{f1}+\Gamma_{f2}}n. \tag{4.12}$$

(4.12) is identical in form with the equation suggested by Urbach, Urbach, and Schwartz.[4] Their observations in curve III, which covers

** For this reason also probably very few holes leave the killer centers even if their energy levels are nearer the filled band than the silver levels.

[4] F. Urbach, A. Urbach, and M. Schwartz, J. Opt. Soc. Am. **37**, 122 (1947).

the widest range of those for ZnS-Ag-Ni in their Fig. 1, all satisfy this relationship (except for the lowest observation). Assuming $\log J$ to be exact and assuming random errors for $\log I$, the sum of their squares was least for

$$b_1=7.93 \quad \text{and} \quad \mu_1=24.5.$$

We have not observed a power greater than 2, as they obtain in curve IV, Fig. 1, and, as they point out, this could not be explained by an equation like (4.12).

At very low intensities when b_1^2u/b_2^2 is not negligible, J/I_1 will be smaller than its value given by (4.8), but we have not been able to observe this in our experiments. Allowing for their precision, it was estimated that b_2/b_1 was greater than 10 for both ZnS-Ag-Co and ZnS-Ag-Ni.

Figure 2 shows the intensity dependence curve for $b_1=0.1$, $b_2=1$, and $\mu_1=1$ (curve A).

The corresponding curve for b_2 infinite is also plotted (curve B). It will be seen that it nearly coincides with A for efficiencies down to 10 percent, so that I_1, which is proportional to J at high exciting intensities, approaches μ_1J^2/b_1^2 at lower intensities, provided that $I_1^{-\frac{1}{2}}\gg 1/b_1\mu_1^{\frac{1}{2}}$ when $(b_1^2/b_2^2)u\ll 1$. When b_2/b_1 is still larger, the curves A and B will coincide over a wider range. At still lower exciting intensities from (4.6) $I_1=(\mu_1/b_2)J^{\frac{1}{2}}$.

Thus the slope of $\log I_1$ *vs.* $\log J$ changes from 1 to 2 and then falls to $1\frac{1}{2}$. Its change is small over (e.g.) a range of 1 for $\log_{10}I_1$, and if over such a range intensities are measured for various temperatures, amounts of impurities, and wavelengths of exciting radiation (with which μ may vary), each curve may have a different slope depending on which part of a function of the type of A is actually observed. Such an explanation may well apply to some of the intensity dependencies observed by Garlick and Gibson,[5] who questioned whether the simple hole migration theory could explain their results.

It is true that equations such as (4.2) may still oversimplify the physical processes. One can allow, however, for the presence of more than one kind of killing center and of independent electron traps. For example, if there are two kinds of 'killing' impurity centers from which holes do not migrate, with different cross sections of hole capture and different recombination coefficients with free electrons when excited, the form of (4.1) and (4.2) is unchanged.

(4.1)′ becomes

$$u=\frac{\gamma_{1f}(\Gamma_{f2}+\Gamma_{f3})}{\beta_1 n(\Gamma_{f1}+\Gamma_{f2}+\Gamma_{f3})}, \tag{4.13}$$

and

$$b_1=\frac{\gamma_{1f}(\Gamma_{f2}+\Gamma_{f3})}{\beta_1(\Gamma_{f1}+\Gamma_{f2}+\Gamma_{f3})} \times\left\{\frac{\mu_1}{\beta_1}\left(1+\frac{\gamma_{1f}}{\Gamma_{f1}+\Gamma_{f2}+\Gamma_{f3}}\right)+\frac{\mu_2}{\beta_2}+\frac{\mu_3}{\beta_3}\right\}^{-\frac{1}{2}}, \tag{4.14}$$

$$b_2=\frac{\gamma_{1f}(\Gamma_{f2}+\Gamma_{f3})}{\beta_1(\Gamma_{f1}+\Gamma_{f2}+\Gamma_{f3})} \times\left\{\frac{\mu_1}{\Gamma_{f2}+\Gamma_{f3}}\left(\frac{\Gamma_{f2}}{\beta_2}+\frac{\Gamma_{f3}}{\beta_3}\right)+\frac{\mu_2}{\beta_2}+\frac{\mu_3}{\beta_3}\right\}^{-\frac{1}{2}}. \tag{4.15}$$

Thus if β_2 and β_3 are both much greater than β_1, (4.8) is unchanged except that $\Gamma_{f2}+\Gamma_{f3}$ replaces Γ_{f2} everywhere.

V. THE EFFECT OF ELECTRON TRAPS

The effect of electron traps has so far been neglected. It may be important at low temperatures even if the traps are shallow. At liquid-air temperatures it is observed that J/I_1 still varies with $I_1^{-\frac{1}{2}}$ but b_1, although small, is usually larger than the value obtained from (4.10) with the E_1 value deduced from the curves at temperatures between 0 and 100°C.

Now with any one of several hypotheses about the nature of the traps—whether they are associated with excited or unexcited centers or are independent of centers—one of their effects will be to change the apparent value of β_1 with temperature. It is easiest to allow for traps associated with unexcited centers or independent of centers; the number of free electrons becomes (with l trapped electrons)

$$n=n_1+n_2+n_3+n_f-l, \tag{5.1}$$

and with $L-l$ empty traps

$$\frac{dl}{dt}=\alpha n(L-l)-\gamma l. \tag{5.2}$$

[5] G. F. J. Garlick and A. F. Gibson, Nature **158**, 704 (1946), and unpublished correspondence.

The blue luminescence (3.3) in terms of n is unchanged, but n as a function of J has now a more complicated relationship than (3.2); however, J/n^2 remains constant at high but not at low exciting intensities. When $\beta_2 \gg \beta_1$ (4.1) is not changed, but (4.2) becomes

$$J=\frac{b_1^2(1+u)}{u^2}\left\{1+\frac{\alpha L}{\alpha n+\gamma}\right\}, \qquad (5.3)$$

while (4.8) becomes

$$\frac{J}{I_1}=\frac{1}{\mu_1}+\frac{b_1}{(\mu_1 I_1)^{\frac{1}{2}}}\left(1+\frac{\alpha L}{\alpha n+\gamma}\right)^{\frac{1}{2}}. \qquad (5.4)$$

At high temperatures when γ, which is of the form $Se^{-E/kT}$ where E=depth of the electron traps, is very high, the effect of the traps is of course negligible. At low temperatures the value of $(\mu_1 J/I_1-1)$ is too large by a factor

$$[1+\alpha L/(\alpha n+\gamma)]^{\frac{1}{2}},$$

and this may explain an increase in the slope corresponding to b_1.

The results at these temperatures are now being investigated more fully. Meanwhile it is suggested that the physical basis of the equations set up in this paper is the most reasonable one which can include both the simpler results observed so far at higher temperatures and others on phosphors with any number of different kinds of luminescence or killer centers.

We wish to thank Mr. J. A. M. van Moll and the Directors of Philips Lamps, Ltd., for permission to publish this work.

JOURNAL OF THE OPTICAL SOCIETY OF AMERICA VOLUME 38, NUMBER 3 MARCH, 1948

The Quanta Explanation of Vision and the Brightness Impression for Various Times of Observation and Visual Angles

M. A. BOUMAN AND H. A. VAN DER VELDEN
Physical Institute of the University of Utrecht, The Netherlands

(Received July 30, 1947)

In the previous papers (see references 1–3) it was proved that the statistical nature of light and certain properties of the human apparatus for vision determine the threshold values for various times of observation and visual angles (expressed among others by the laws of Ricco, Talbot, and Piper) and the visual acuity. The behavior of these visual functions agreed with the two-quanta case: light is perceived when two quanta are effectively absorbed in the visual purple within an area corresponding to a visual angle of D ($\sim$10′) and within a time τ ($\sim$0.02 sec.). As the chance is negligible that the two quanta are absorbed in one rod, it proved that a rod reacts on the absorption of 1 quantum. The two stimuli will cooperate in the nerve system and give rise to light perception.

From experiments described in the present paper we conclude that after the absorption of a couple of quanta, all quanta absorbed within an area O corresponding with a visual angle o and a time T referred to this first couple of quanta, cause a stimulus which contributes to the brightness impression and the total number of stimuli within an area O and a time T determines the brightness impression.

The experiments mentioned consist in the determination of the dependence of the average numbers of quanta of a flash necessary for a fixed brightness impression on the visual angle and the time of observation.

The area O and the time T are the cause for the existence of the laws of Talbot and Ricco for the brightness impression. As soon as the time of the flash t or the visual angle d exceeds the value T or O, the average number of quanta necessary for a constant brightness impression is proportional to d^2 c.q. t. The area O has the nature of a recipient unit and T of an averaging time.

INTRODUCTION

FROM the explanation presented by the two-quanta hypothesis for the threshold values and visual acuity[1,2,3] for various visual angles and times of observations, several kinds of cooperation are found to exist between the rods activated by the absorption of a quantum: light is perceived when two quanta are effectively absorbed in the visual purple within an area corresponding to a visual angle D ($\sim$10′) and within a time τ ($\sim$0.03 sec.). As the chance that

[1] H. A. v. d. Velden, Physica 9, 179 (1944).
[2] H. A. v. d. Velden, Ophthalmologica 111, 321 (1946).
[3] M. A. Bouman and H. A. v. d. Velden, J. Opt. Soc. Am. 37, 908 (1947).

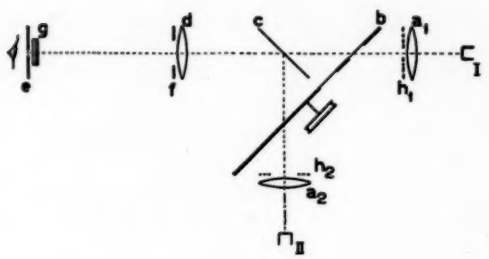

FIG. 1.

the two quanta are absorbed within one rod is negligible, it proves that a rod reacts on the absorption of one quantum. The two stimuli will cooperate somewhere in the nerve system and give rise to a light perception. The presence of activated rods gives rise to a condition of the apparatus for vision so as to decrease the chance for light perception for a certain time and over a certain area of the visual field.

As it can be expected that these effects are important for the brightness impression, we performed experiments suitable for the study of these phenomena concerning brightness impression.

We determine the dependence of the average number of quanta necessary for a certain brightness impression on the visual angle and time of observation for several values of the subjective brightness.

1. THE EXPERIMENTS

For the experiments about the dependence on the time we asked the observer to compare the brightness impressions of two successive flashes of different duration but equal visual angle. The observer had to change the intensity of one of the flashes till he was unable to see any difference in brightness impression of the two flashes.

The tungsten ribbon filament lamps *I* and *II* (Fig. 1) were imaged by the lenses a_1 and a_2 on the screen of the disk *b*, in which two openings were made, so that the light of *I* could only pass through the one, and that of *II* through the other opening. The images of *I* and *II* *via* the mirror *e* are thrown by the lens *d* on the artificial pupil *e*. The size of the openings in the disk and the velocity were such as to make the flash-time for the light of *II* always 0.1 sec. The flash-time for the light of *I* could be regulated between 0.05 sec. and 1 sec. The time between the two flashes was always about 0.5 sec. The screen of the lens *d*, completely filled up by the light of *I* or *II*, is the object for observation. The visual angle is determined by the diaphragm *f*. In front of the pupil *e* a Schott VG_2 filter *g* was placed with a maximum transmission at 5300A. The head of the observer was fixed by means of a mouth-mounting piece. The dark-adapted right eye was used and the spot of the retina on which the flashes were received was situated 7° nasal from the fovea, just like in all our previous experiments.[1–3] The fixation of the right eye was performed by the observation of a red-fixation light with the left eye.*

For several intensities of the test flash of 0.1 sec. of lamp *II* the observer adjusted the currents of lamp *II* to every fixated time of the flash of *II* for which the brightness impression of the two flashes seemed to be equal. Every measurement was repeated several times and the average current value was determined. The experiments were performed for various visual angles by changing the diaphragm *f*.

In Fig. 2a and 2b we give, for some visual angles, the average number of quanta necessary for the same brightness impression as a function of the flash-time.

The same experimental arrangement was adapted to the experiments concerning the dependence on the visual angle.

The diaphragm *f* was removed. The visual angles of the two flashes for which the time was now always equal, were determined by the two diaphragms h_1 and h_2 of the lenses a_1 and a_2. Of the two beams issuing from lens *d* the one due to flash *II* has always the visual angle 30′, as regulated by the diaphragm h_1, while the visual angle of the beam due to flash *I* can be varied from 5′ to 200′ by means of the diaphragm h_1. The condition of the eye and its fixation were

* The intensities were determined according to the lines described in the previous paper (see reference 3): The lamps *I* and *II* were calibrated, so that the average number of quanta of every wave-length incident on the eye could be computed with the aid of the measured properties of the filters, the geometry of the arrangement, and the reflecting and absorbing properties of the lenses and mirror. As we did not use monochromatic light, the number of quanta of every wave-length was given a special weight according the scoptopic luminosity curve, which was given the value one in the optimal value.

quite similar as in the experiments described concerning the dependence on time.

For several intensities of the test flash of 30′ of lamp *II* the observer adjusted the currents of lamp *I* for which the two flashes seemed to be equally bright for every fixated visual angle of the flash of *I*. Again the average of several measurements was determined. The time between the two flashes was again about 0.5 sec. The experiments were performed for several flash-times. In Fig. 3 we give the curves indicating the dependence on visual angle of the average number of quanta of a flash for a certain brightness impression.

2. DISCUSSION

1. The Dependence on Time

When in an area D a very small number of quanta per second is absorbed by statistical fluctuations in the time between two succeeding absorptions, there will be a slight chance that more than one quantum is absorbed in a time τ.[1,2,3] When this happens light is perceived by the cooperation of the nerve stimuli. The duration of this process of an elementary light impression begins at the moment the first quantum is absorbed and ends when the light impression disappears. The brightness-impression and duration will depend on:

a. The accidental number of absorbed quanta and the accidental distribution in time of the absorptions. We know that two absorptions within τ sec. cause light impression, but about the influence of extra absorbed quanta on the brightness impression we know nothing.

b. The way in which the pulses of the activated rods are conducted by the retina, optical nerve, brain center to consciousness. Even if the same rods, as regards time and place, are activated in exactly the same way, it is not sure that the way of conducting is also the same, so that light impressions are not necessarily identical in durations, extension, and brightness.

For very low intensities of the illuminated area of the retina the frequency of the elementary light impression is low. The average time between the beginning of the separate impressions is determined by the chance for the absorption of two quanta within τ.

For increasing intensity this time decreases, and for a sufficient increase it will become smaller than the duration of an elementary light impression. For these intensity values we may expect singularities to occur in the behavior of the

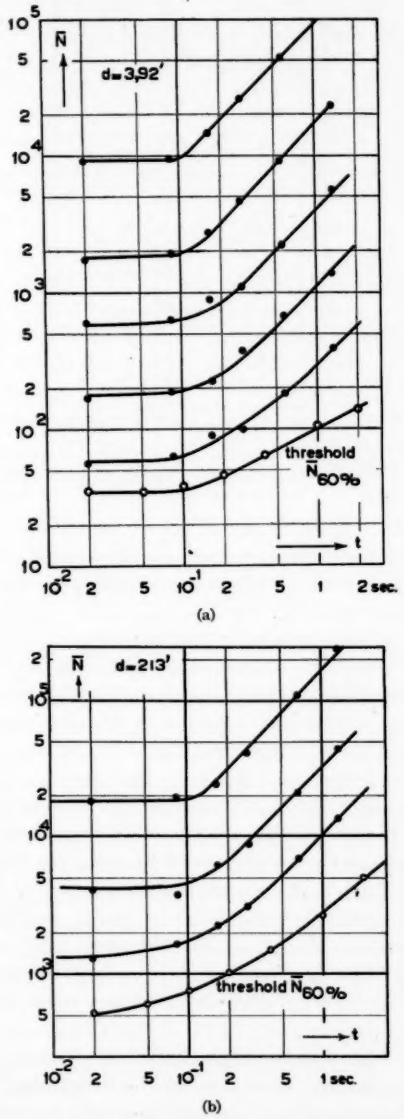

FIG. 2. Curves representing the average number of quanta $\bar{N}$ of a flash necessary for a constant brightness impression as a function of the duration t of the flash. The lowest curve represents the thresholds $\bar{N}_{60\%}$, the average number of quanta for which the chance of observation of the flash is 60 percent.

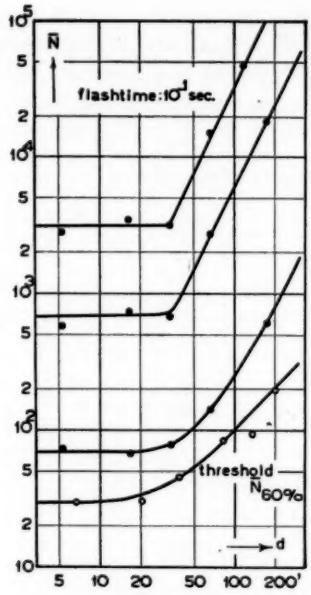

FIG. 3. Curves representing the average number of quanta $\bar{N}$ of a flash necessary for a constant brightness impression as a function of the visual angle of the flash.

brightness impression because the cooperation of the processes of elementary light impressions becomes possible. For the comparison of brightness impressions only the established equal or "just different" values are suitable. For the study of possible singularities one can investigate how a certain brightness impression is obtained for several times of observation. It is not sure that we need the same intensity in order to obtain the same brightness impression for different times.

In Fig. 2a and 2b we show this dependence for two visual angles and several brightness impressions. Each curve represents the average number of quanta necessary for a fixed brightness impression. We give also the threshold curve $\bar{N}_{60\%}$. This is the average number of quanta necessary for a chance of observation of 60 percent.

For increasing flash-times the number of quanta per sec. decreases for the threshold $\bar{N}_{60\%}$. The average time between the two absorptions which give rise to the light impression increases, and the chance for extra absorptions within a certain time of the absorption of the two quanta decreases.

In the lowest curve for a constant brightness impression of Fig. 2a the chance of observation of the flash is still <1 for t values <1 sec. The frequency of the elementary light impressions is small and they will be seen separately. The moments for the perception of light are completely determined by the chance for the absorption of two quanta within τ sec. The shape of the curve deviates from the curve $\bar{N}_{60\%}$ when $t>0.1$ sec. We can conclude that for a certain brightness impression of the visual process of an elementary light impression the average number of quanta per sec. may not decrease below a definite value, as the deviations are such that for values of t, for which $\bar{N}_{60\%}$ is still proportional to $\sqrt{t}$, the number of quanta for the constant brightness impression becomes proportional to t.

It can be concluded from the curves for higher values of the brightness impression where continuous light is perceived, that for a certain brightness impression the average number of absorbed quanta per 0.11 sec. (or *ca.* 3τ) must be constant.

2. The Dependence on the Visual Angle

For the elementary light impression discussed under 1. the points *a* and *b* will also be important for the extension of the impression.

When a flash of very low intensity is given having duration $t \leqq \tau$, and visual angle which is large compared with D, there will be a chance for the absorption of more than one quantum by the statistical fluctuations in an area D.[1,2,3] When this occurs, the stimuli will produce an elementary light impression. The average distance of these impressions is determined by the chance just mentioned. With increasing intensity this chance increases, so that the average distance between the elementary light impressions decreases. An increasing part of the illuminated area will seem to be filled with light. The possibility of cooperation of the elementary impressions increases. It is now important to know the average number of quanta as a function of the visual angle for a constant brightness impression.

The data concerning this dependence are given in Fig. 3. In a way quite analogous to the time-dependence, we can conclude that the average number of quanta per cm² may not be smaller than a definite value, so that the effective

absorption of more quanta, within a certain area of the place of absorption of the two quanta responsible for the occurrence of the light impression, is important for the brightness impression. It can further be concluded that for a constant brightness impression the average number of absorbed quanta per area O with a visual angle o of about 25′ ($\sim 2D$) must be constant.

3. CONCLUSION

In the previous paragraph it was proved that for a certain brightness impression the average number of effective absorptions per 0.11 sec. per area 25′ must be constant for all combinations of time and visual angle of the test flash. The behavior of threshold values $\bar{N}_{60\%}$ for various visual angles flash-times, and visual acuity must be described with the aid of the statistical fluctuations in time and place of the absorptions of the quanta in the separate rods: the two-quanta explanation. The nature of the chemical reactions of the photo-chemical material turned out to be unimportant for these intensities. For the measurements of Figs. 2 and 3, especially for those brightness impressions for which the conditions for the light impression are slightly more than satisfied, and for which the nature of the brightness impression determines the shape of the curve, the intensities are equal or only a little higher than those occurring in the threshold measurements and visual acuity. The chemical properties of the visual purple will here be unimportant also.

In our opinion, the hypothesis of the laws of Talbot and Ricco, for the origin of brightness impression, being of a physiological or psychological nature, must be considered to be correct.

From the conditions for the occurrence of a light impression, it appeared that two stimuli, of two different rods within a time τ and a visual angle D, cooperate and result in a light impression, and the effective absorption of one quantum in a rod causes a stimulus.

It is now quite sure that stimuli can cooperate within an area D' and time τ. From the experiments described in the present article we can conclude that the number of stimuli within an area $o \sim 2D$ and a time $T \sim 3\tau$, caused by the same number of quanta, cooperate to create the brightness impression. As the first absorbed quantum does not give rise to a stimulus from which a light impression results, one may doubt, the two-quanta condition once being satisfied, whether every extra quantum causes a stimulus which increases the brightness impression. As it appeared from the data of Polyak that all recipient elements (rods and cones) can influence each other by the nerve system, it seems to be very probable that every extra stimulus in an area in which already two quanta are absorbed increases the brightness impression. In a subsequent paper it will be proved that this assumption is confirmed by the behavior of the contrast sensitivity.

The behavior of the threshold values did not enable us to decide whether the two quanta must be absorbed within an area D' of the retina or within a distance D of each other. At present we cannot ascertain from the experiments of the brightness impression whether the distance o is the maximum distance within which stimuli can cooperate, or whether there is an area of diameter o in the retina within which cooperation is possible.

By the slight difference in the size of D and o it is, moreover, difficult to insure that the cooperation of all stimuli is already complete when 2 quanta, corresponding to the two-quanta-explanation, are absorbed within a distance D, situated within O. Especially when D' and O are sharply bordered areas of the retina, it might be possible that complete cooperation of all stimuli within O is only possible when all areas D' belonging to O have absorbed two quanta. As for larger visual angles the two-quanta shape in the curves of the brightness impression disappears for lower intensities compared with smaller visual angles it seemed probable that one couple of quanta within D is sufficient for the complete cooperation of all stimuli within O.

4. REMARKS

It appeared that the simultaneous occurrence of large visual angles and long flash-times in the experiments of the threshold values causes deviations from the two-quanta explanation. The chance for a light impression is decreased by the absorption of quanta after 0.1 sec. from the beginning of the flash and over an area O.

The behavior of the visual acuity as a function

of the intensity depended on the shape of the test object that had to be recognized.[3] When the illuminated areas were surrounded completely by dark areas the behavior agreed with the dependence predicted by the threshold values for circular spots. When the illuminated areas adjoined an illuminated periphery the visual acuity was proportional to the intensity, in accordance with the two-quanta explanation. The diminution just mentioned appeared to be less important. This phenomenon is now clear from the facts found by the experiments of the present paper. The quanta absorbed in the surroundings adjoining the test-figure facilitate the brightness impression of the boundary of the illuminated areas of the test figure.

The area O has the nature of a recipient unit as the observer has always the same brightness impression when the total average number of quanta in this area is the same, regardless of the distribution of the places of absorption. Moreover, it is impossible to recognize a figure of which the details are smaller than the area O.

The size of the recipient unit found by ten Doescate[4] on this spot of the retina is smaller. The visual acuity, of which the upper limit is determined by the area O, was the basis for his computation. He used the experiments of Wertheim who did not apply the same test figure. Moreover, the area may differ for different persons.

The area O was till now assumed to be well defined. The quanta absorbed near the border of the area can increases the brightness impression or size of the light impression. As the curves of Fig. 3 show rather sharp bends, it is probable that the border of the area is rather well defined.

The time T has the nature of an averaging time; the observer gets always the same brightness impression when the total average number of quanta within this time is the same, regardless of the distribution in time of the separate absorptions.

In our opinion the critical frequency, which is for the dark-adapted eye and high intensities in the periphery almost independent of the intensity and is about 10, is determined by the time T.

The time T, within which stimuli of the rods can cooperate, may not be sharply defined. The quanta absorbed at the end of a time T can increase the brightness impression or increase the time of the light impression. As the curves of Fig. 2 are rather well-defined it seemed again to be probable that the time T is also rather well defined.

[4] J. ten Doescate, Ophthalmologica **112**, 1 (1946).

The Visibility of Distant Objects

SEIBERT Q. DUNTLEY*
Massachusetts Institute of Technology, Cambridge, Massachusetts
(Received August 12, 1947)

For thousands of years, thousands of mariners have sighted thousands of ships, and have made appropriate entries in their logs. Even so, this mass of miscellaneous information is of little use in predicting the range at which a specified object will be just visible under a new set of circumstances. The purpose of this paper is to identify the principal factors involved in the visibility of an object, to indicate how each factor affects the range of visibility, and to supply charts which, by combining these factors, enable the limiting range to be found under any set of prevailing conditions. (This paragraph has been lifted, almost verbatim, from some material prepared during the war by Professor Arthur C. Hardy, then Chief of the Camouflage Section (16.3) of the NDRC.)

1. INTRODUCTION

DURING the recent war the Camouflage Section (16.3) of the National Defense Research Committee undertook an extensive study of the visibility of distant objects.[1] One result of this research was the construction of nomographic (alignment) charts by means of which laboratory data concerning contrast thresholds for the human eye can be combined with data describing the physical stimulus reaching the observer to predict the limiting range at which a given object will be visually detectable. It is the purpose of this paper to present these charts and to illustrate the manner of their use in predicting the limiting range of visibility for uniform circular objects.** The development of the visibility charts was by no means the sole work of the author; rather, it stems from the combined efforts of many of the personnel of NDRC Section 16.3, its contractors, its liason officers, and its friends. In accordance with the wishes of these contributors the author has prepared this paper.

The visibility of a uniformly luminous object depends upon the apparent contrast between the object and its background, the angular size of the object, its shape, the contrast threshold of the observer at the level of luminance to which his eyes are adapted, and the conditions and technique of observing. Throughout the researches in visibility conducted under the supervision of the NDRC Camouflage Section it was the basic plan to investigate the various factors controlling the apparent contrast of objects, to ascertain from laboratory experiments the contrast thresholds of the human observer, and to devise means for combining this knowledge in such a manner that the limiting range at which an object is visually detectable can be readily predicted. The apparent contrast of distant objects has been discussed by the author,[2–4] contrast thresholds have been reported by Blackwell,[5] and the nomographic visibility charts presented in this paper combine these results in convenient form.[6]

2. THE NATURE OF THE PROBLEM

Both the apparent contrast and the angular size of an object depend upon the distance of the observer, but in accordance with different laws. For example, at a distance of R yards, a circular object of area A square feet subtends an angle α given by:

$$\alpha = 1293A^{\frac{1}{2}}/R \text{ minutes of arc.} \qquad (1)$$

The apparent contrast C_R of any object at a

* Formerly Technical Aide, NDRC Section 16.3.

[1] Summary Technical Report of NDRC Division 16, Volume 2.

** The nomographic visibility charts were prepared by the staff of the Louis Comfort Tiffany Foundation under contract OEMsr 597 with the Office of Scientific Research and Development. The directions for their use, the illustrative examples, and many of the paragraphs of discussion have been taken from the writings of the author in Volume 2 of the Summary Technical Report of NDRC Division 16. Oral presentations have included the formal opening of the Boston University Optical Research Laboratory, December 13, 1946.

[2] S. Q. Duntley, J. Opt. Soc. Am. **36**, 359(A) (1946).
[3] S. Q. Duntley, J. Opt. Soc. Am. **36**, 713(A) (1946).
[4] S. Q. Duntley, J. Opt. Soc. Am. **38**, 179 (1948).
[5] H. R. Blackwell, J. Opt. Soc. Am. **36**, 624 (1946).
[6] S. Q. Duntley, J. Opt. Soc. Am. **36**, 359(A) (1946).

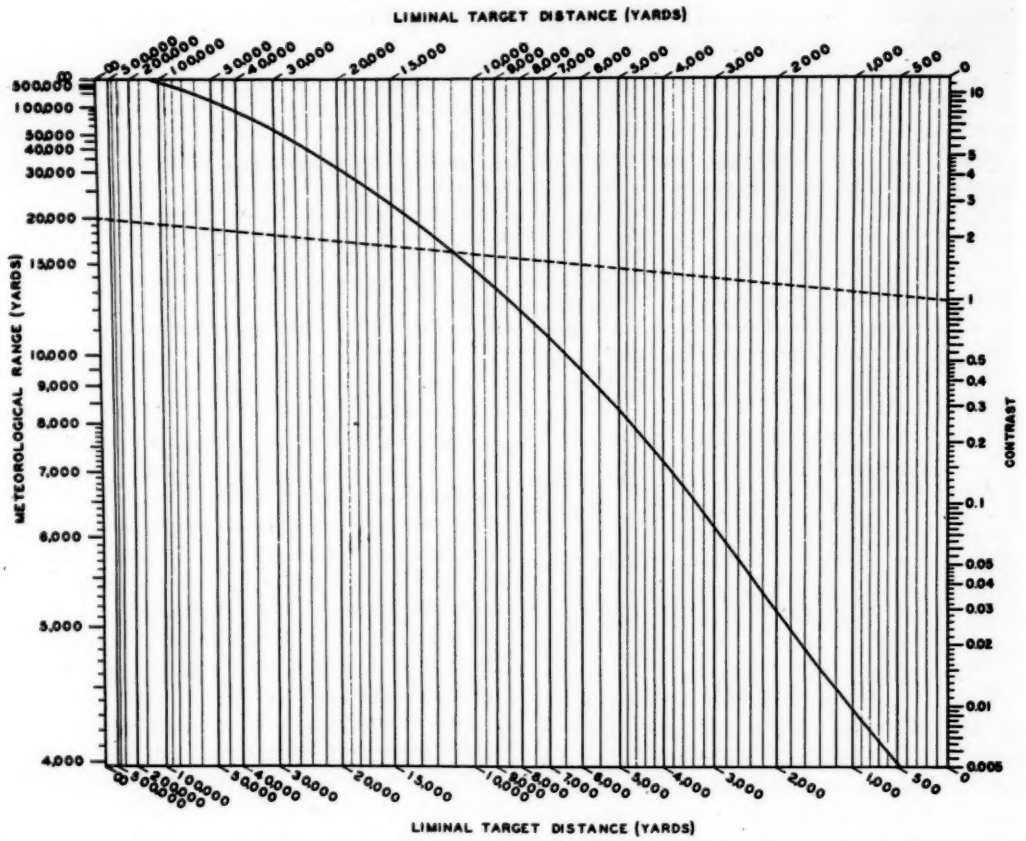

FIG. 1. Nomographic visibility chart. The curve represents visibility data for a uniform, circular object 100 square feet in area when $B_H = 1000$ footlamberts.

distance R has been shown[4] to be related to its inherent contrast C_O by the relation:

$$C_R = (B_O/B_R) C_O e^{-3.912\bar{R}/v}, \qquad (2)$$

where B_O is the inherent luminance of the background, B_R is the apparent luminance of the background, $\bar{R}$ is the optical slant range,[4] and v is the meteorological range. The latter is defined as that distance for which the contrast transmittance[4] of the atmosphere is two percent.

In the special case of an object seen against a background of horizon sky, $B_O = B_R$, and Eq. (2) reduces to:

$$C_R = C_O e^{-3.912R/v}. \qquad (3)$$

Since the contrast threshold of the human observer depends simultaneously upon α and C_R in the manner shown by Fig. 16 of the recent paper by Blackwell,[5] any calculation intended to determine the range at which an object is just detectable must consist of a series of successive approximations. The following example illustrates such a calculation.

Illustrative Example. Let it be required to find the distance at which a uniform circular object, having a projected area of 100 square feet and a luminance of 10 footlamberts, will be liminally visible*** on a day when the meteorological range is 20,000 yards, assuming the object to be viewed along a homogeneous, horizontal path of sight**** against a uniform background of

*** See Section 8 for a definition of liminal object distance.

**** A homogeneous, horizontal path of sight is one for which the luminous density q, the attenuation coefficient β, and the scattering-rate coefficient σ are the same at all points. (Reference 4.)

horizon sky, the luminance of which is 1000 footlamberts. The inherent contrast of the object is:

$$C_O = 10 - 1000/1000 = -0.990.$$

This value indicates that, to a nearby observer, the object appears as a nearly black silhouette. Negative contrast signifies an object darker than its background; positive contrast denotes an object more luminous than its background. It will be noted that negative contrast can never exceed unity ($C_O = -1.00$), whereas there is no upper limit to positive contrast. An important conclusion from the results reported by Blackwell[6] of the Tiffany Foundation is that, for practical purposes, objects darker than the background are as visible as congruent objects lighter than the background when their respective contrasts are numerically equal.†

Since the meterological range is 20,000 yards, it may be assumed that a very large black object would be liminally visible at approximately that range. However, at 20,000 yards the angle subtended by the target is shown by Eq. (1) to be only 0.646 minute. The Tiffany data[5] show the liminal contrast for an object of this angular size to be -0.355. From the definition of meteorological range, however, the apparent contrast of the object is -0.020. Hence, the object is invisible at 20,000 yards.

Although the liminal object distance is now known to be less than 20,000 yards, its actual value must be found by trial: Assume the object

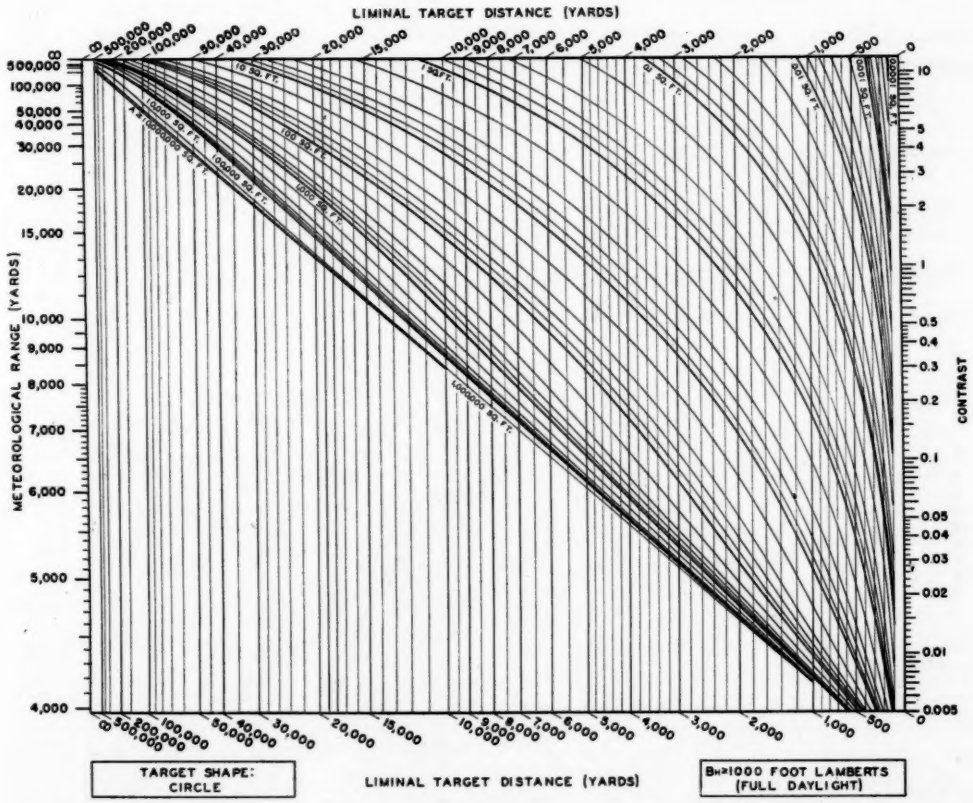

FIG. 2.

† The Tiffany results show a minor exception to this rule for values of adaptation luminance below 10^{-3} footlambert. At these night-time levels large objects darker than their backgrounds are slightly more visible than corresponding objects of numerically equal positive contrast. (Reference 5.)

to be at 10,000 yards. At this distance it subtends an angle of 1.292 minutes, and its apparent contrast is shown by Eq. (3) to be −0.145. From the Tiffany data, the liminal contrast for an object of this angular size is −0.0966. Therefore the object can be seen at 10,000 yards and beyond.

It is evident that the distance at which the object is liminally visible has been "bracketed." If the bracketing process is continued, the answer finally attained is 11,000 yards. It should be evident, however, that such calculations are cumbersome, time consuming, and invite mistakes. Fortunately, they can be avoided completely by the use of nomographic (alignment) charts.

3. THE NOMOGRAPHIC METHOD

Figure 1 shows a nomographic chart capable of making simultaneous allowances for all of the variables. The curved line which crosses the center of the figure represents Tiffany data[5] for the contrast thresholds of a typical observer when his eyes are adapted to full daytime sky brightness, and when the object is uniformly luminous, circular, and 100 square feet in area. An object of any other area could be represented by a different curve, and subsequent nomographic charts in this paper contain a family of curves corresponding to a billion-fold range of areas.

To solve the illustrative example of the preceding section by means of Fig. 1, simply lay a straightedge across the chart in such a manner that it connects 20,000 yards on the scale of meteorological range with 0.99 on the scale of contrast. The position of the straightedge is indicated on Fig. 1 by the dashed line. From the point where the curve is intersected by the straightedge move straight up or straight down

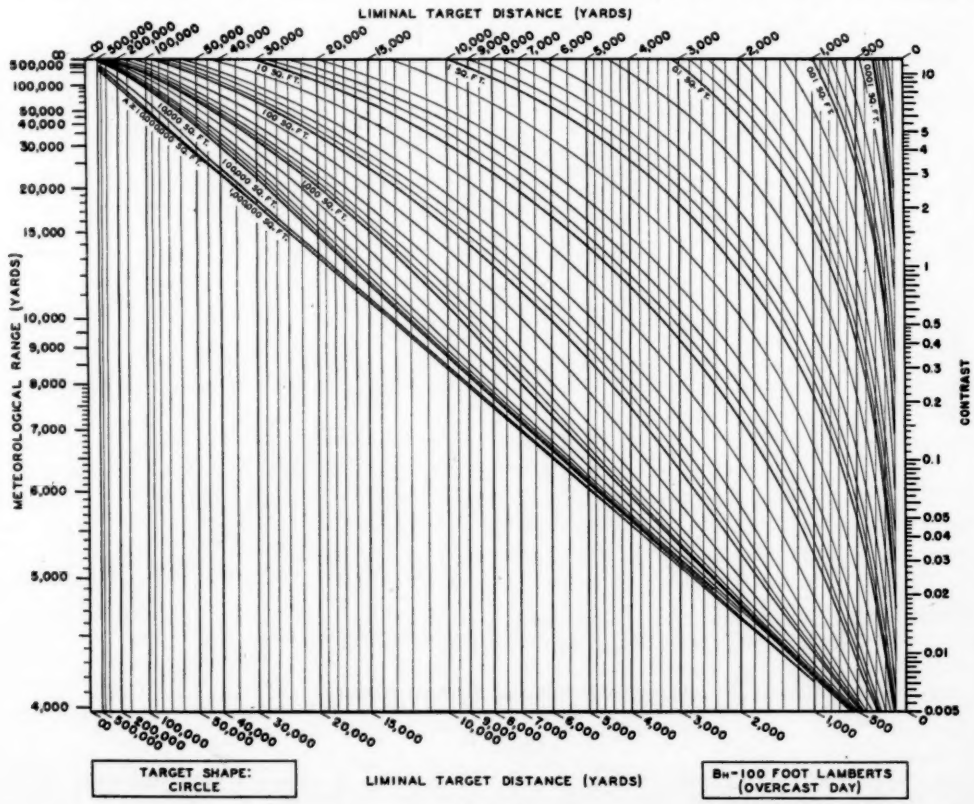

FIG. 3.

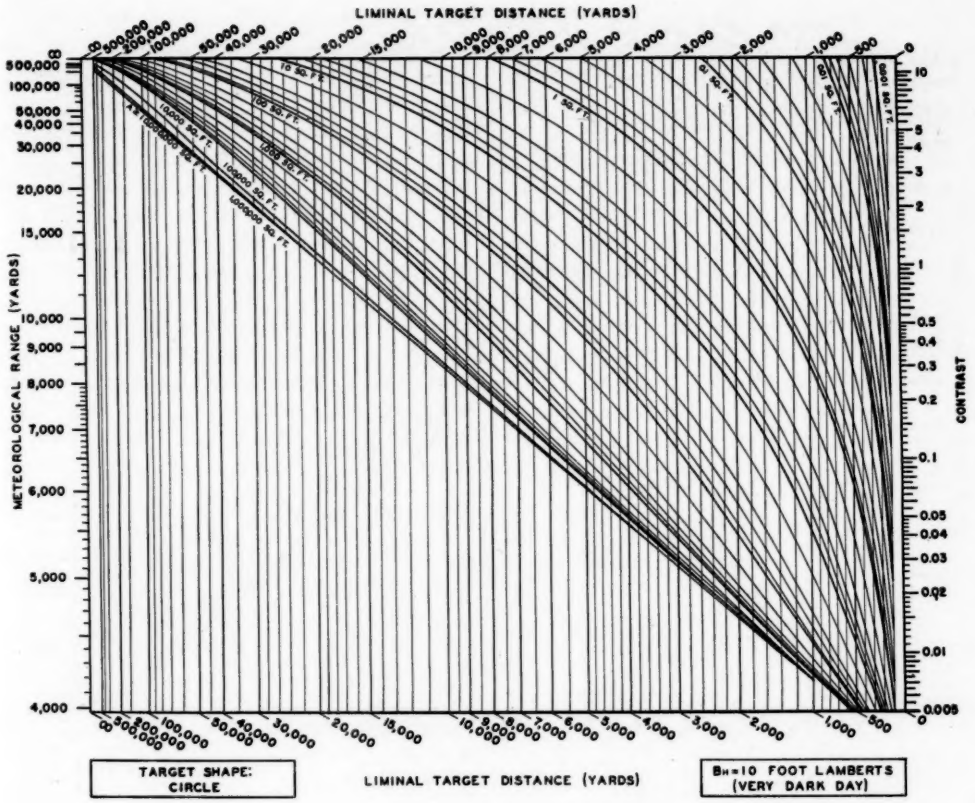

FIG. 4.

to the scale of "liminal target distance."†† The answer, 11,000 yards, read from this scale agrees with the liminal object distance previously obtained by bracketing.

Special Cases

The scales of meteorological range and liminal target distance in Fig. 1 may be multiplied by any factor, provided the value of area assigned to the curved line is multiplied by the square of the factor. This convenient property of the nomographic visibility charts enables them to be used over very wide ranges of their variables. For example, let the scales of meteorological range and liminal target distance be multiplied by $\frac{1}{10}$. The former then applies to fogs in which the meteorological range is as short as 400 yards, and the numbered divisions of the latter begin with 50 yards. The curved line, however, now applies to objects 1 square foot in area. Obviously, if Fig. 1 bore a curve corresponding to an object 10,000 square feet in area on the basis of the scales as originally numbered, the curve would apply to an object 100 square feet in area when the chart is used in the manner just described.

In dealing with objects of very large area, visible at very long distances, the scales of the visibility charts may advantageously be multiplied by 10. The curved line in Fig. 1 then applies to circular objects 10,000 square feet in area, and the dashed line indicates that such an object will be liminally visible at 110,000 yards on a day when the meteorological range is 200,000 yards, provided the inherent contrast of the object is ± 0.99.

†† Synonymous with "liminal object distance."

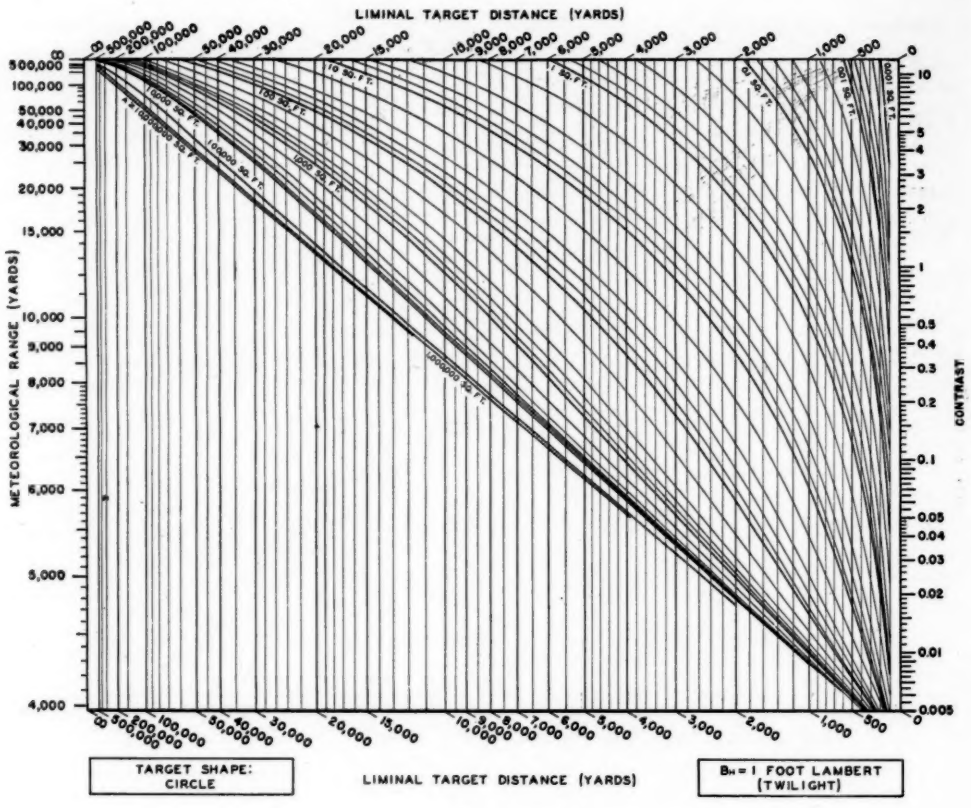

FIG. 5.

Exact Values of Object Area

Since the factor by which the scales are multiplied may have *any* value, the curved line in Fig. 1 can be made to apply to *any* area. For example, let it be required to find the liminal object distance for an object whose area is 64 square feet, assuming other conditions as before. Since the area represented by the curve must be multiplied by 0.64, the scales must be multiplied by 0.80. This means that a meteorological range of 20,000 yards will be represented by the division numbered "25,000" on the chart. If this point is connected by a straightedge (not shown) to 0.99 on the contrast scale, the intersection of the curved line and the straightedge indicates 12,400 on the scale of liminal target distance. After multiplying by the scale factor, 0.80, the liminal object distance is found to be 9920 yards.

The family of curves, each representing a target of different area, which appear on all of the subsequent nomographic visibility charts, is intended to make unnecessary the type of calculation just described. However, for the construction of tables, or for special computations requiring great precision, the method described above should be used.

Other Uses of the Nomograph

The nomographic visibility chart may be considered as a special plot of the Tiffany data[5] on contrast thresholds for the human observer. For example, let it be required to find the liminal apparent contrast of a target 100 square feet in area and 10,000 yards from the observer. Place a straightedge across Fig. 1 in such a manner that it connects the infinity point at the top of the meteorological range scale with the intersection of the curve and the vertical line repre-

senting 10,000 yards. The straightedge then intersects the contrast scale at ±0.097, the value of liminal contrast for this angular subtense.†††

The nomographic visibility chart can be used to solve Eq. (3). For example, let it be required to find the apparent contrast of an object of inherent contrast ±0.99 when it is 10,000 yards from the observer on a day when the meteorological range is 20,000 yards. Place a straightedge across Fig. 1 in the position shown by the dashed line. Place the point of a pencil at the intersection of the straightedge with the vertical target-distance line for 10,000 yards. Rotate the straightedge until it passes through the infinity point at the top of the meteorological range scale. The straightedge now intersects the contrast scale at ±0.145, the apparent contrast of the object. Obviously, this technique can be employed to solve for any of the four quantities in Eq. (3).

4. NOMOGRAPHIC VISIBILITY CHARTS

More than two million observations of uniform circular visual targets were made by a homogeneous group of observers at the Tiffany Foundation under its OSRD contract, and a statistical summary of 450,000 of these observations has been reported by Blackwell.[5] No visibility experiment of comparable magnitude or thoroughness is known to have been reported. The Tiffany data are believed to be by far the most reliable existing information on the contrast thresholds of unrestricted binocular human vision. It is appropriate, therefore, to present these

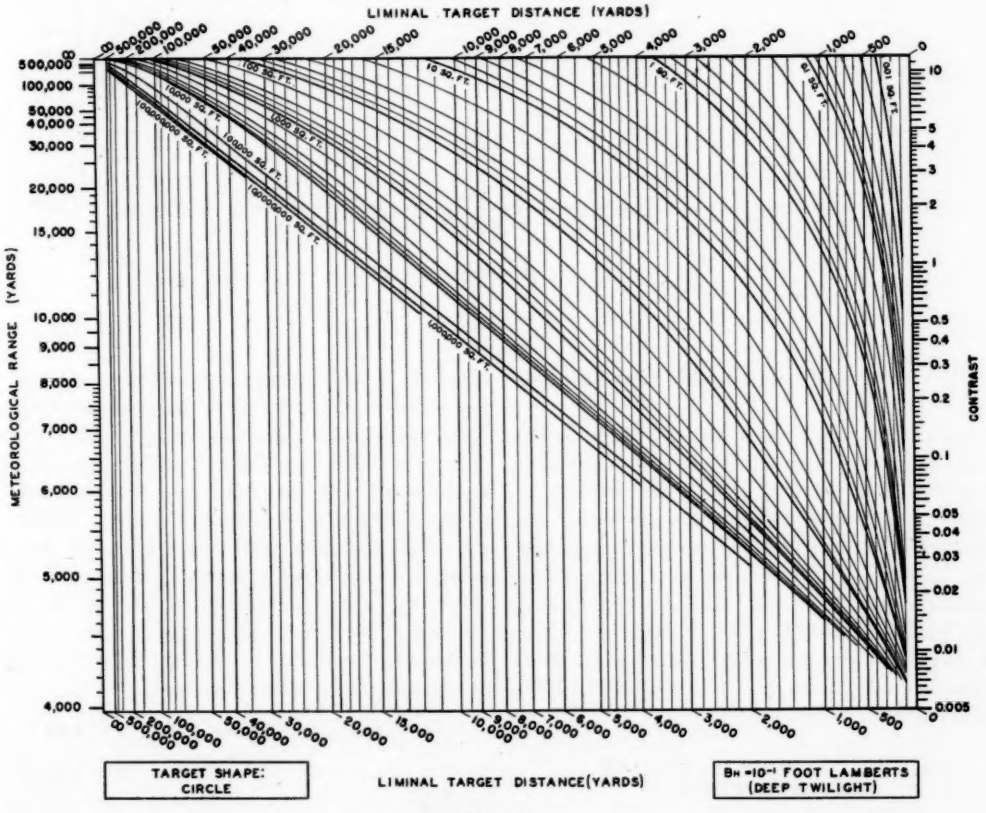

FIG. 6.

††† It will be noted that the locus of liminally visible circular targets subtending the same angle at the eye of the observer is a straight line connecting the infinity point on the meteorological range scale with the point on the contrast scale representing the liminal apparent contrast.

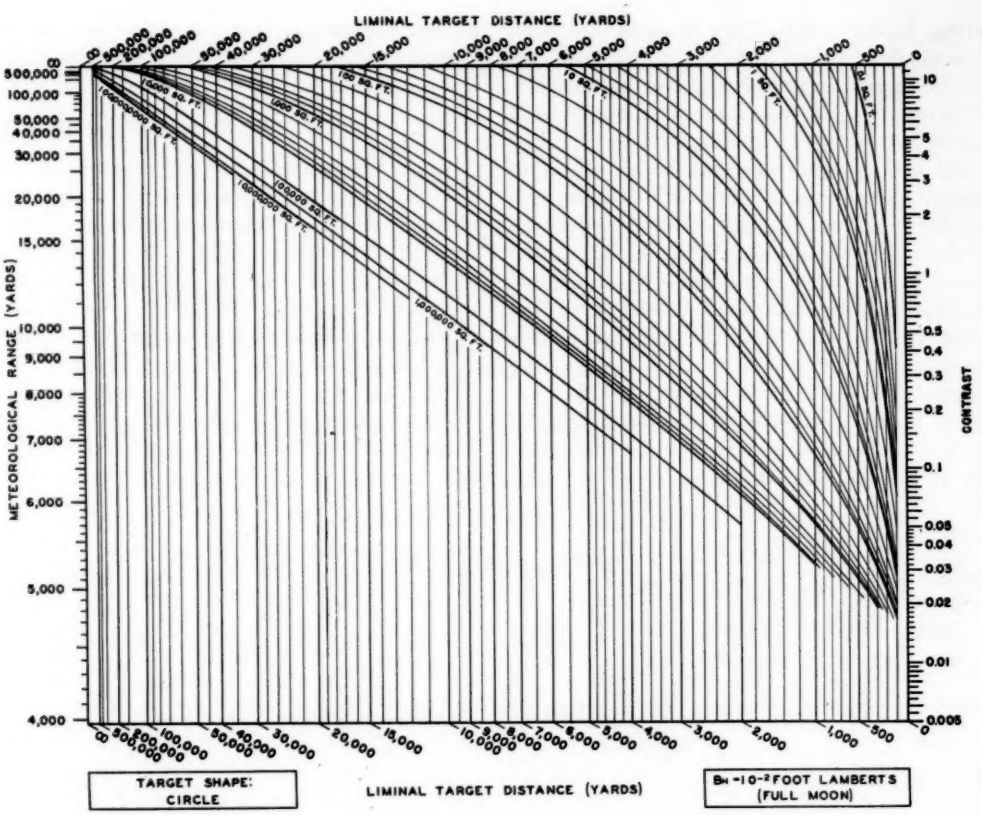

FIG. 7.

data in the form of nomographic charts similar to Fig. 1.

Each of the nine figures (Figs. 2 through 10) is a nomographic visibility chart for uniform circular objects seen against a uniform background of horizon sky having the luminance B_H indicated in the lower right corner of the diagram. Descriptive phrases, such as *overcast day* or *quarter-moon*, have been added to serve as a rough guide in selecting the proper chart for use in a given problem. The charts cover adaptation luminances (B_H) from 10^{-5} footlambert to 1000 footlamberts in decimal steps.

5. VISIBILITY OF NON-CIRCULAR UNIFORM OBJECTS

One of the first experiments performed by the Tiffany Foundation compared the visibility of the silhouette of a ship with that of a uniform circular object having the same area. This experiment suggested that uniform objects of equal area and equal apparent contrast are equally visible regardless of their shape. Later experiments showed, however, that in certain extreme cases correction for object shape is required. Although such corrections will not be treated in this paper, it is important to note that when the time for search is unrestricted no uniform object, regardless of its shape, is more visible than a uniform circular object of equal area and equal inherent contrast.

6. VISIBILITY THROUGH BINOCULARS

The distance at which a specified object is liminally visible through perfect binoculars can be found from the nomographic visibility charts by multiplying the area of the object by the square of the magnifying power of the binoculars

before entering the data on the chart. For example, suppose a perfect 7-power binocular is used by the observer in the illustrative example of Section 3. Since the area of the object is 100 square feet, the area used in entering the chart (Fig. 2) is 4900 square feet and the resulting liminal object distance is 22,500 yards. Recalling that the liminal object distance for the unaided eye is 11,000 yards in this example, it will be noted that the 7-power glasses increased the liminal object distance by a factor of approximately two. Only when the meteorological range is infinite do perfect binoculars having a magnifying power M permit objects to be seen M times as far as they can be seen by the naked eye.

The limiting performance of perfect telescopic systems under optimum conditions has been discussed by Hardy,[7] who showed that binoculars are most effective in increasing the limiting range of detection when the object is small. It should be noted that Hardy's treatment applies only to optimum conditions, while the nomographic visibility charts enable the performance of perfect binoculars to be predicted under virtually any conditions.

The foregoing discussion applies to *perfect* binoculars, by which is meant an instrument whose only effect is to increase the apparent angular size of the object. Actually, even the best binoculars fall somewhat short of the ideal, so that, unless data concerning the contrast rendition[8] of the instrument are used, the liminal object distance predicted by means of the nomographic visibility charts represents a limiting value, never exceeded but sometimes approached by observers using real binoculars.

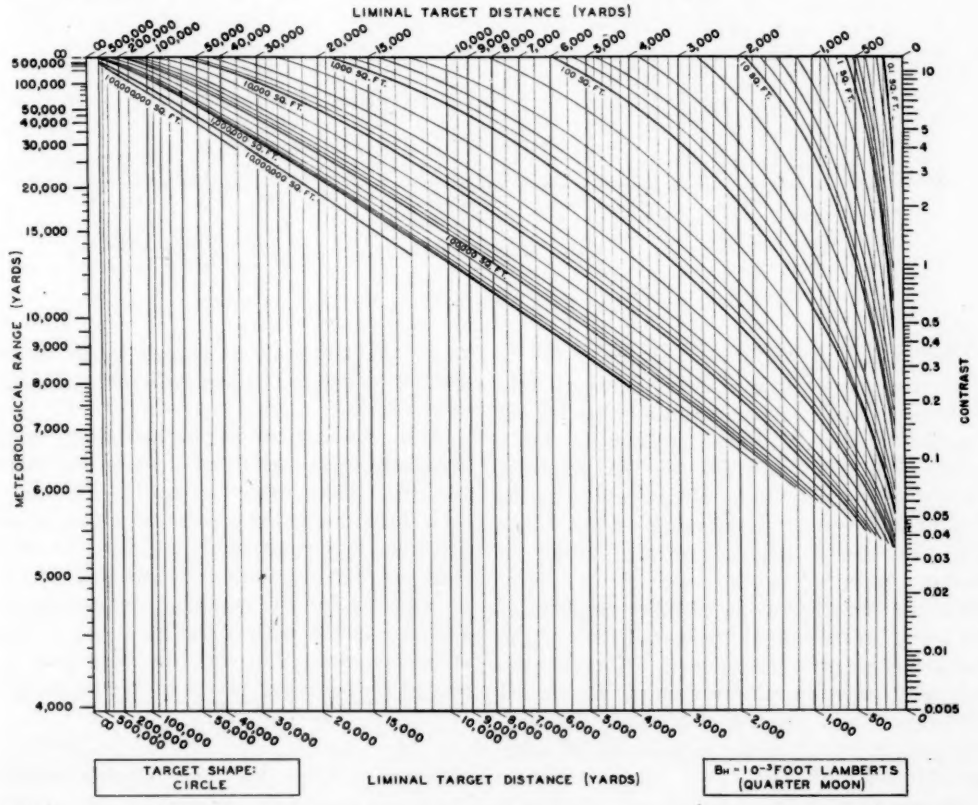

FIG. 8.

[7] A. C. Hardy, J. Opt. Soc. Am. **36**, 283 (1946).
[8] H. S. Coleman, J. Opt. Soc. Am. **37**, 434 (1947).

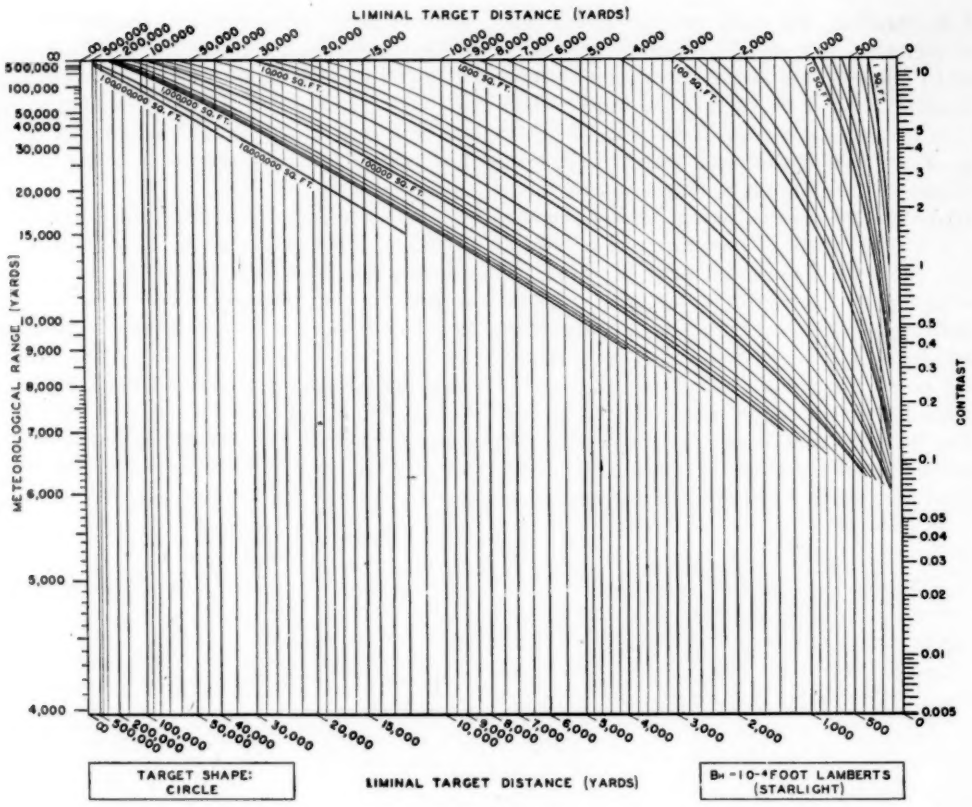

FIG. 9.

7. VISIBILITY ALONG INCLINED PATHS OF SIGHT

The preceding sections have discussed only the special visual task of sighting an object along a horizontal path with the horizon sky for a background. The reduction of the apparent contrast of distant objects along inclined paths of sight and against backgrounds of any luminance has been discussed by the author in another paper.[4] The nomographic visibility charts are useful in solving visibility problems of this type, provided that the parameters of the charts are properly interpreted. Of these, the scale of meteorological range needs no special discussion. The scales of liminal target distance, area, and contrast, however, require the following special interpretation:

Liminal target distance. If the path of sight is other than horizontal the reduction in apparent contrast is dependent upon the optical slant range[4] $\bar{R}$. The scale of liminal target distance should, therefore, be regarded as applying to values of $\bar{R}$.

Area. Because the atmosphere becomes progressively more rarified as altitude is increased, the true slant range ordinarily exceeds the optical slant range. Therefore, the object actually subtends a smaller angle at the eye of the observer than if it were at distance $\bar{R}$. This may be allowed for by entering the nomographic visibility charts with a *reduced* value of object area. The reduced or *effective object area* $\bar{A}$ is related to the object area A by the expression:

$$\bar{A} = (\bar{R}/R)^2 A. \tag{4}$$

Contrast. Since the nomographic visibility charts are constructed around Eq. (3), their use in problems involving Eq. (2) requires that the scale of contrast be identified with the quantity

($B_O C_O / B_R$). This is not, however, a convenient parameter for use in visibility problems. More usable variables occur in a modified form[4] of Eq. (2):

$$C_R = C_O[1-(B_H/B_O)(1-e^{3.912\overline{R}/v})]^{-1}, \quad (5)$$

where B_O is the inherent luminance of the background, and B_H is the equilibrium luminance along the path of sight. The quantity B_H/B_O is referred to as the *sky-ground ratio.*[4]

A modified form of the nomographic visibility charts is shown in Fig. 11. This chart, based on Eq. (5), differs from the preceding nomographs only by the addition of a scale of sky-ground ratio along the inside left margin and by a new scale of inherent contrast which is located near the center of the figure. The manner of using this chart will be illustrated by re-solving the example of Section 3 for the case of the target viewed against a background having a luminance of 200 footlamberts. Since the luminance of the horizon sky was assumed to be 1000 footlamberts, the sky-ground ratio is 5.0. The inherent contrast of the object against its background is:

$$C_O = 10 - 200/200 = -0.95.$$

Place a straightedge across Fig. 11 in such a manner that it connects 5.0 on the sky-ground ratio scale with 0.95 on the contrast scale. Place the point of a pencil at the intersection of the straightedge with the right-hand vertical boundary of the chart, and rotate the straightedge until it connects this point with 20,000 yards (11.4 miles) on the meteorological range scale. From the intersection of the straightedge and the curve for a target area of 100 square feet, proceed vertically to a reading of 6900 yards on

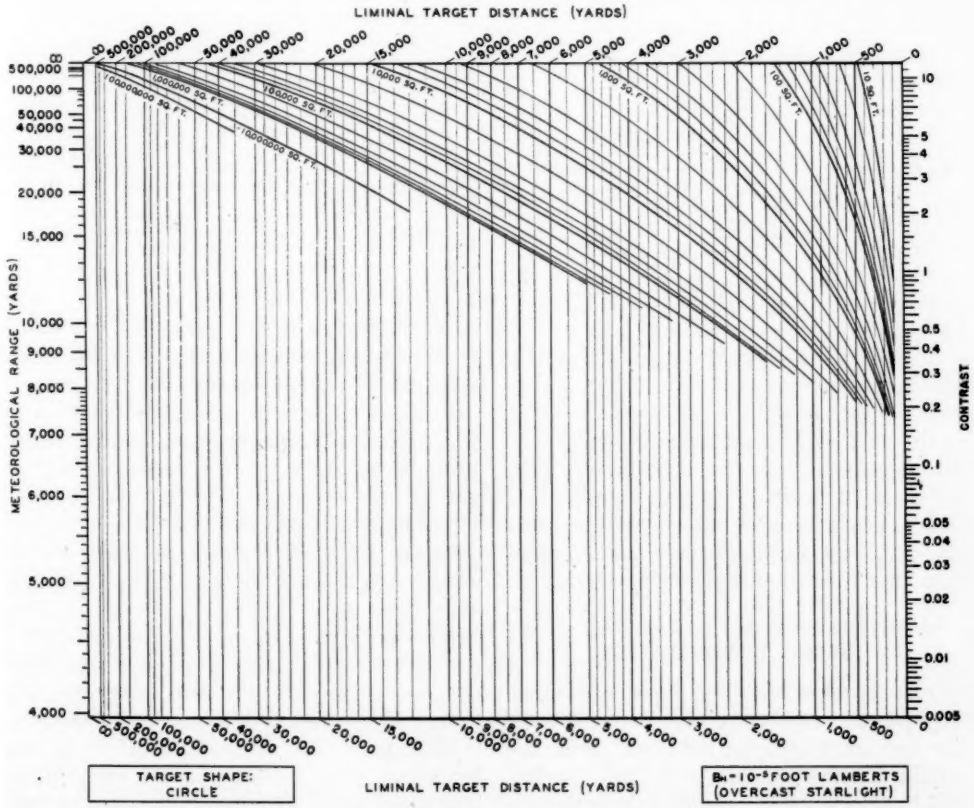

FIG. 10.

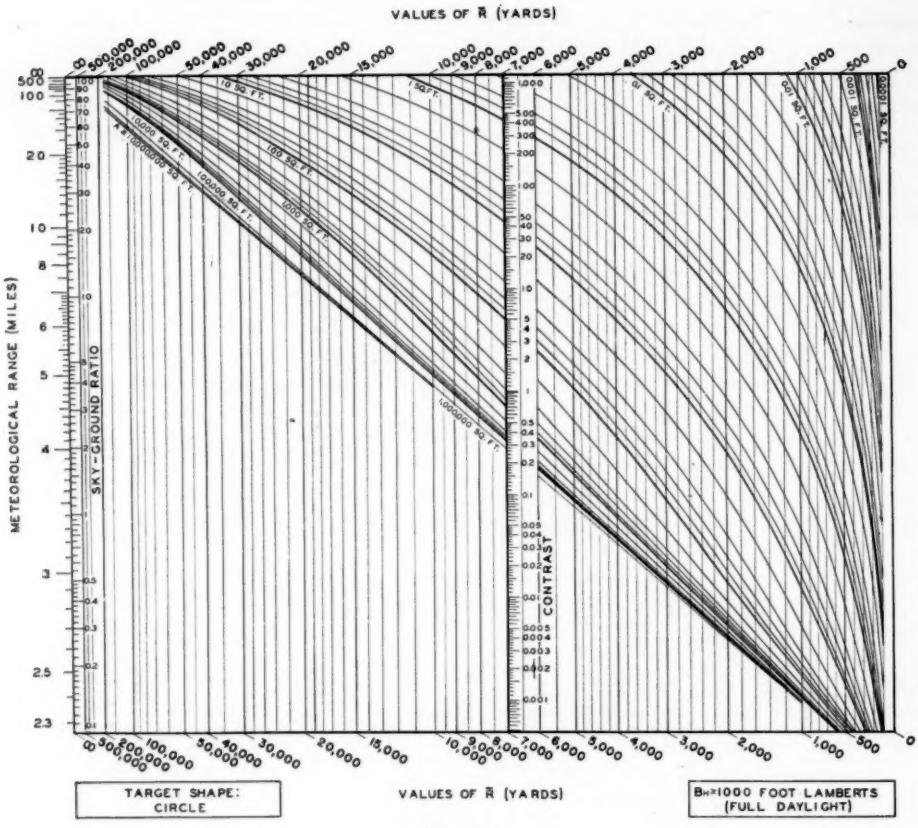

FIG. 11.

the scale marked "*Values of* $\bar{R}$." Along horizontal paths of sight $\bar{R}=R$. Hence, the liminal object distance is 6900 yards.

When the path of sight is not horizontal, it is ordinarily impossible to solve directly for the liminal object distance, since $\bar{R}\neq R$. In such cases, values of liminal inherent contrast for assumed values of slant range R can be determined from Fig. 11, and the liminal object distance can then be found by interpolation.

8. INTERPRETATION OF LIMINAL OBJECT DISTANCE

The nomographic visibility charts presented in this paper are based upon the contrast thresholds for the human observer published by Blackwell of the Tiffany Foundation.[5] The criterion adopted by Blackwell in reporting these thresholds is such that an object is liminally visible when an observer who is *forced* to judge whether the object is present or absent is as likely to be right in his judgment as he is likely to be wrong, due allowance having been made for chance. This criterion, commonly used in psychometric work, is well suited to the needs of the nomographic visibility charts because it has precise physical significance, and because liminal object distance, when so defined, is unlikely to be exceeded in practice when conditions correspond with those upon which the charts are based. It should be borne in mind, however, that the nomographs are based upon data representing the performance of excellent observers under nearly ideal observing conditions. Because of fatigue, discomfort, distraction, and the necessity for search it is to be expected that, in most instances, actual sightings will occur at ranges somewhat less than those indicated by the

charts. On the other hand, the atmosphere is sometimes so inhomogeneous that the actual sighting range may exceed the range indicated by the nomographs. Experience in their use is the best guide to the allowances that should be made for departures from the conditions upon which the charts are based.

Threshold of Confidence

Blackwell[5] has pointed out that the observer of a liminally visible object is quite unaware that half of his forced responses are correct; he has no confidence that he has seen the object. When the contrast of the object is doubled, however, the average observer experiences a threshold of confidence, and will voluntarily report having seen the object.‡ Therefore, at some range, less than the liminal object distance, the observer becomes aware of seeing the object. This has been called the *sighting range.*

The sighting range can be predicted from the nomographic visibility charts by dividing the inherent contrast of the object by 2 before entering the data on the chart. Thus, in the illustrative example discussed in Sections 2 and 3, if the straightedge connects 20,000 yards on the meteorological range scale of Fig. 1 with 0.50 on the contrast scale, an object distance of 9260 yards is indicated. At approximately this distance the object should be seen with threshold confidence. The nomographic visibility charts have been constructed to indicate the liminal target distance rather than the sighting range, because the former quantity has a precise physical significance not shared by the latter.

9. SUMMARY

The limiting range at which a uniformly luminous object can be detected by unaided vision or with perfect binoculars can be predicted from laboratory data on the contrast thresholds of the human observer, and photometric data concerning the luminance of the object, its background, and the optical state of the atmosphere. Nomographic (alignment) charts are presented which eliminate laborious successive approximations and permit the visibility of objects along either horizontal or inclined paths of sight to be predicted.

‡ According to Blackwell (reference 5), the threshold of confidence corresponds approximately with a 90 percent probability of making a correct forced response.

10. ACKNOWLEDGMENT

As stated in the Introduction, the author was but one of a number of contributors to the development of the nomographic visibility charts. Early in the war, at the suggestion of Professor Arthur C. Hardy, then Chief of NDRC Section 16.3, the author began the construction of alignment diagrams for use in visibility problems. These charts were demonstrated to numerous persons, and many contributed suggestions. The first nomograph which successfully eliminated successive approximations was constructed by Dr. George Kimball. This was such an important advance that the Tiffany Foundation was asked to engage Professor Raymond D. Douglass of the Massachusetts Institute of Technology to construct a series of such nomographs. Because these charts suffered from a complex cycle of operations and from precision difficulties in certain ranges of their variables, much effort was expended by all concerned to develop a simpler, more effective type of nomograph. Special mention should be made of the many contributions by Professor Hardy to this development. The stimulating interest of Commander Dayton R. E. Brown during this phase of the work is gratefully acknowledged. The resulting nomographic visibility charts, presented in this paper, were constructed by Professor Douglass.

A Comparison of Computed and Experimental Detection Ranges of Objects Viewed with Telescopic Systems from Aboard Ship*

H. S. COLEMAN
The Optical Inspection Laboratory, The Pennsylvania State College, State College, Pennsylvania

AND

W. S. VERPLANCK
Department of Psychology, Indiana University, Bloomington, Indiana

(Received August 13, 1947)

The relative range performance of approximately 80 telescopic systems of 18 different designs has been determined by statistical methods based on the results of a field test conducted from shipboard. The range at which objects are detectable from aboard ship is compared with the range computed from laboratory measurements of light transmission, magnification, exit pupil, and contrast rendition, using a method described by Hardy and the data of Duntley and Blackwell on the characteristics of the atmosphere and the human eye. The agreement between the results of the field tests and the computations is extraordinary. This is interpreted to mean that the most important factors were taken into account in both the statistical and computational procedures. This implies that if a visibility field test is properly conducted, the results can be expected to agree with those of simulated laboratory tests, and conversely, that properly constructed laboratory tests will yield data which predict accurately the performance of instruments in the field.

INTRODUCTION

IN a field test conducted from aboard ship to study the performance of a number of optical instruments of different designs, the range at which objects are detectable has been determined. In this test a criterion of performance was established. This criterion was taken to be the maximum range at which an object can be detected by means of an optical instrument. In connection with a laboratory study being conducted by the Bureau of Ordnance of the Navy Department in the Optical Inspection Laboratory of The Pennsylvania State College, methods have been developed for computing the range at which objects are detectable by using telescopic systems. These methods are based on a procedure described by Hardy,[1] the data on the reduction in contrast of objects by the atmosphere described by Duntley[2,3] and the contrast discrimination of objects by the human eye described by Blackwell.[4] By means of the methods, it is possible to compute the performance of optical systems from the laboratory measurements of light transmission, magnification, exit pupil, and contrast rendition. Such computations have been made for the instruments used in the field tests. It is the purpose of this paper to present a comparison of the computed and experimental performance values.

TABLE I. Laboratory data for instruments used in field tests.

Instrument	Contrast rendition Day	Night	Exit pupil Day	Night	Transmission	Magnification
4×28×10°	95	85	2.5 mm	7 mm	0.61	4
6×30×8.5°	98	96	2.5 mm	5 mm	0.47	6
6×33×8°	91	75	2.5 mm	5.5 mm	0.45	6
6×42×12°	96	82	2.5 mm	7 mm	0.66	6
6×50×7°	97	90	2.5 mm	—	0.66	6
7×50×7.1°	97	92	2.5 mm	7 mm	0.70	7
7×50×10°	97	87	2.5 mm	7 mm	0.70	7
8×60×8°	97	92	2.5 mm	7.5 mm	0.65	8
9×63×5.7°	96	94	2.5 mm	7 mm	0.72	9
10×50×7°	98	91	2.5 mm	5 mm	0.76	10
10×70×7°	90	82	2.5 mm	7 mm	0.66	10
10×80×7°	88	86	2.5 mm	8 mm	0.48	10
20×120×3°	96	94	2.5 mm	6 mm	0.61	20
21×76×2.8°	96	94	2.5 mm	3.5 mm	0.50	21
25×100×3.6°	94	92	2.5 mm	4 mm	0.65	25
7×50×7.1°	96	93	2.5 mm	7 mm	0.70	7
7×50×7.1°	96	91	2.5 mm	7 mm	0.70	7
10×70×7°	93	75	2.5 mm	7 mm	0.40	10
7×50×7.1°	95	92	2.5 mm	7 mm	0.66	7

THE PROCEDURE

The procedures used in the field test and the laboratory measurements are to be described in

* This paper was prepared in connection with Task C of Contrast NOrd-7958 between the Bureau of Ordnance and The Pennsylvania State College.

[1] A. C. Hardy, J. Opt. Soc. Am. **36**, 283 (1946).
[2] S. Q. Duntley, J. Opt. Soc. Am. **36**, 359 (1946).
[3] S. Q. Duntley, J. Opt. Soc. Am. **36**, 713 (A) (1946).
[4] H. Richard Blackwell, J. Opt. Soc. Am. **36**, 624 (1946).

TABLE II. Computed *vs.* field performance (relative to mounted 7×50×7.1° binoculars) of mounted binoculars at night.*

Description of instrument	Computed performance	Field performance
6×33×7°	76%	73%
6×42×7°	88	76
6×50×7°	102	80
10×70×7°	116	104
7×50×7.1°	100	100
10×50×7°	106	106
10×80×7°	118	115
25×100×3.6°	159	156
20×120×3°	163	163

* Field test range for mounted 7×50×7.1° binoculars—2630 yds. Computed liminal range for 7×50×7.1° binocular—2180 yds.

detail in separate reports and therefore will be mentioned only briefly here.

The procedure for conducting the field test was to approach a group of distant targets in a destroyer escort using the instruments to be tested and recording the ranges at which each of the targets could be first glimpsed, then seen continuously, and finally identified. Observations were made by teams of six men on the signal deck and three man teams on the gun and lower decks. Tests were run in blocks of six runs during which six instruments were rotated among six men so that each man used a different instrument on each run. This rotation was designed to control the variation resulting from differences in the abilities of the observers and conditions during the run. In all runs, at least one of the six instruments was a standard 7×50×7° binocular. This binocular was hand-held and was adopted as a standard against which all other instruments were compared. The ranges obtained by this instrument were taken to be one hundred percent and the ranges for the other instruments were

TABLE III. Computed *vs.* field performance of hand-held binoculars at night.*

Description of instruments	Computed performance	Field performance Based on 7×50×7.1° binoculars	
		Hand-held	Mounted
6×42×12°	83%	95%	82%
7×50×10°	95	103	89
8×60×7°	113	104	90
9×63×5.7°	119	112	97
10×50×7°	106	117	101

* Field test range for hand-held 7×50×7.1° binoculars—2270 yds. Field test range for mounted 7×50×7.1° binoculars—2630 yds. Computed liminal range for 7×50×7.1° binocular—2180 yds.

TABLE IV. Computed *vs.* field performance (relative to mounted 7×50×7.1° binocular) of mounted monoculars at night.*

Description of instrument	Computed performance	Field performance
4×28×10°	59%	46%
6×30×8.5°	70	46
6×33×8°	62	56
21×76×2.8°	140	69

* Field test range for mounted 7×50×7.1° binocular—2630 yds. Computed liminal range for 7×50×7.1° binocular—2180 yds.

expressed in terms of this 7×50×7° range. A total of 190 successive runs were made in a three and a half month period. Of these, 177 were at night and 13 in the daytime. Tests were made on instruments of 18 different designs.

The procedures for making laboratory measurements of light transmission, magnification, and exit pupil have been described in standard textbooks and therefore will not be redescribed here. The methods of making Contrast Rendition measurements have been described in a previous paper.[5]

The procedure for computing the range at which objects are detectable through visual telescopic systems requires a knowledge of the contrast threshold of the human eye under the brightness conditions to which it may be adapted in situations of interest. Such thresholds have been presented by Blackwell. In addition the influence of the atmosphere on the apparent contrast of a target at various distances from the observer must be known. The contrast thresholds and the influence of atmosphere have been incorporated into a set of visibility charts. These charts apply to the unaided eye and are to be described in detail by S. Q. Duntley.[6] For this reason only the

TABLE V. Computed *vs.* field performance for hand-held and mounted instruments at night.*

Description of instrument	Computed performance	Field performance
7×50×7.1° (H. H.)	100%	100%
7×50×7.1° (H. H.)	100	91
10×70×7° (Mtd.)	96	92
7×50×7.1° (Mtd.)	98	115

* Computed liminal range for a 7×50×7.1° binocular—2180 yds.

[5] H. S. Coleman, J. Opt. Soc. Am. **37**, 434 (1947).

[6] S. Q. Duntley, "The visibility of distant objects." To be published in the November 1947 issue of the J. Opt. Soc. Am.

TABLE VI. Computed *vs.* field performance (relative to hand-held 7×50×7.1° binoculars) for hand-held or mounted instruments in daylight.†

Description of instrument	Computed performance	Field performance
7×50×7.1° (H. H.)	100%	100%
7×50×7.1° (H. H.)	100	——
10×70×7° (Mtd.)	110	——
7×50×7.1° (Mtd.)	100	115

† Computed liminal range for a 7×50×7.1° binocular—16,400 yds.

procedures for using these charts in connection with telescopic systems will be presented here. The charts make it possible to predict the liminal detection range for the unaided eye provided the following quantities are known:

1. The inherent target area (A_0);
2. The inherent target contrast (C_0);
3. The brightness level to which the eye is adapted (B_0);
4. The meteorological range (R_m);
5. The shape of the target.

In using the visibility charts to compute the range at which objects are detectable through a visual telescopic system, allowances must be made for any apparent changes in the above five quantities resulting from the use of the system. It is evident that the first three quantities may be affected. The magnification, M, of the optical aid could appear to increase the inherent area by M^2. Stray light in the optical system could reduce the contrast of the retinal image. This would be equivalent to a reduction in inherent contrast of the target by a factor equal to the Contrast Rendition of the optical system. The light transmission and the size of the exit pupil, as compared with the natural pupil of the eye, could control the brightness of the field presented to the eye and hence the brightness level to which it is adapted. The correction in apparent brightness level may be made by computing an apparent light transmission factor by combining the light transmission factor, T_0, the exit pupil size, XP, and the natural pupil size, P, as shown in the following equation:

$$T_a = T_0[(XP)^2/(P)^2].$$

TABLE VII. Computed *vs.* field performance (relative to hand-held 7×50×7.1° binoculars) of hand-held binoculars in daylight.†

Description of instrument	Computed performance	Field performance
10×50×7.1°	110%	100%
7×50×7.1°	100	99
6×42×12°	97	100
7×50×10°	100	102

† Computed liminal range for a 7×50×7.1° binocular—16,400 yds.

TABLE VIII. Computed *vs.* field performance (relative to mounted 7×50×7.1° binoculars) of mounted binoculars in daylight.†

Description of instrument	Computed performance	Field performance
7×50×7.1°	100%	100%
10×80×7°	109	102
10×50×7°	111	105
25×100×3.6°	122	153
20×120×3°	120	173

† Computed liminal range for a 7×50×7.1° binocular—16,400 yds.

THE DATA

The laboratory data obtained for the light transmission, magnification, exit pupil, and contrast rendition of the instruments used in the field tests are presented in Table I. The comparison of the experimental and computed range-performance values for the instruments used in the field tests are presented in Tables II to IX, inclusive, for a variety of conditions considered.

DISCUSSION AND CONCLUSIONS

It is evident that there is a remarkable agreement between the computed and experimental range performance of the optical instruments mentioned in this paper. The general conditions existing and the difficulties encountered in the conducting of a field test, such as mentioned in this paper, would not be expected ordinarily to yield particularly reliable results as far as the grading of a number of optical systems of dif-

TABLE IX. Computed *vs.* field performance (relative to mounted 7×50×7.1° binoculars) of mounted monoculars in daylight.‡

Description of instrument	Computed performance	Field performance
6×33×7°	96%	84%
4×28×10°	84	87
6×33×8°	95	90

‡ Computed liminal range for a 7×50×7.1° binocular—16,400 yds.

ferent designs is concerned. In fact, field tests of this type are generally frowned upon because they frequently are in conflict with the results of laboratory measurements in which the conditions are controlled and can be specified beyond reasonable doubt. The results of the statistical analysis of the data obtained in the field test mentioned here, however, do not support this generally accepted point of view. In fact, the results clearly indicate that if a visibility field test is properly conducted and if the data are properly treated by statistical methods, the results can be expected to be nearly as precise as laboratory measurements. Those discrepancies which do appear seem to be related to such subjective factors in instrument use which relate to the ease of handling of the instrument. In this connection the statistical data indicate a systematic difference between the performance of instruments when mounted and hand-held. This is likely caused by differences in vibration between the instrument and the observer's eyes. This is not taken into account in the computed range values.

The extraordinary agreement between the results of the field test and the computations based on physical measurements of an objective nature indicates that for the detection of objects, it is possible to predict the ranges at which objects are visible with optical systems. There is however, a clear indication that a considerable amount of additional research would be required to extend the type of results presented here to the problem of recognition.

JOURNAL OF THE OPTICAL SOCIETY OF AMERICA VOLUME 38, NUMBER 3 MARCH, 1948

Survey of Near Infra-Red Communication Systems

W. S. HUXFORD
Northwestern University, Evanston, Illinois

AND

JOHN R. PLATT
University of Chicago, Chicago, Illinois

(Received September 22, 1947)

The development of methods of communication by means of light beams is reviewed from the early work of A. G. Bell in 1880 to the termination, in 1945, of the activities carried out under the auspices of the Office of Scientific Research and Development. The review is limited to voice and code systems, and includes a discussion of methods of producing modulated beams of radiation, use of filters to provide security in military applications, and a summary of the various types of photo-sensitive receiving elements used. An attempt is made to correlate the factors responsible for the trend of developments during each period and to evaluate the relative merits of the several types of systems which have been studied. Descriptions of several types of foreign light-beam communication equipments are included. An extensive bibliography has been compiled.

THE successful development of near infra-red optical communication apparatus under NDRC for the Armed Services during the war is the culmination of more than 60 years of sporadic work on such systems in several countries, including a German development program, the magnitude of which must have been comparable to that of the NDRC program. So many of these "photo-phones," "Lichtsprechers," "optical telephones," and the like, for code and voice signaling, have now been produced, that it seems appropriate to present a brief historical review of these systems. The specific equipments described here are necessarily limited to enemy systems and to such American systems or components as have already been reported in the open literature.

I. INTRODUCTION

A. Advantages of the Near Infra-Red

In principle, radiation of any wave-length throughout the electromagnetic spectrum can be used for conveying energy in communication. Radio wave-lengths are excellent for most uses, but for some military purposes they may have a dangerously great communication range, and are subject to skip-distance phenomena, and reception out of line of sight even when ultra high frequencies are used in directed beams. For increased secrecy in combat communication it becomes desirable to go to still shorter wave-lengths for which the beam can be sharply defined and the range definitely limited by the horizon or by atmospheric attenuation.†[1,2]

At wave-lengths shorter than the radar microwave region, radiation is not detected by tuned receivers, but by thermoelectric elements in the region of long heat waves, and photoelectric detectors in the shorter infra-red. Only photoelectric devices have response times short enough to be used for receiving the audiofrequency variations in voice communication, and such communication is therefore limited at present to wave-lengths below 6 microns.

Optical communication systems require much higher powered transmitters than radio systems, to obtain the same range and beam spread, even when atmospheric attenuation is neglected. This is partly because the effective "antenna" areas of practical photo-detector optical systems are much smaller than for radio, and partly because, even for equal received energy, photo-detectors are less sensitive. A narrow-angle optical system may, however, compare in range with a non-directional radio system of the same power.

Sensitive photo-detectors for the region which we shall call the intermediate infra-red (IIR), from 6.0 to 1.4 microns, have been developed only quite recently, most work up to the present time having been done in the very near infra-red (NIR) region, from 1.4 to 0.8 micron. The most serious drawback to systems operating in these regions is their loss of range in daylight. For wave-lengths between 0.8 micron and 0.35 micron, optical systems are limited to daylight use, where a flash of light will not appreciably violate security. Even in the ultraviolet below 0.35 micron, night use is risky because, although the ultraviolet light itself cannot be seen at night, it will produce a strong and very visible fluorescence in the eyes of observers. In addition, atmospheric attenuation becomes very serious in the ultraviolet.

B. Types of Systems

A beam of light or radiation has three properties: intensity, wave-length distribution, and polarization; the variation of any one of these by suitable modulation may be employed as the basis of a communication system. In a rough way, variation of intensity corresponds to amplitude-modulation (a-m) in radio, and variation of wave-length distribution to frequency-modulation (f-m), although the analogies are not exact since the receiver is not tuned to the "optical" frequency.

The desired property of the radiation is modulated at audio- or radiofrequencies. Simple audiofrequency modulation involves amplitude-modulation in the modulating and receiving circuits; this does not mean that the property of the radiation beam which is modulated is necessarily the optical amplitude. If sources and photodetectors with very short response times are used, an r-f carrier wave may also be used in the circuits, with an a-m or f-m audio signal superimposed.

The modulation may be accomplished either by electrically modulating the radiation source, or by using a constant-intensity source and modulating the outgoing beam. In the first case, electrical modulation of the current through a filament lamp or through an arc or gas discharge is now used, though some earlier studies involved sound-pressure modulation of a manometric acetylene flame. For modulating the outgoing beam, most military systems use mechanical modulation, with vibrating mirrors and beam-chopping devices in audiofrequency systems. Supersonic standing-wave grating devices in r-f systems have also been utilized.

It is evident that the modulation technique may determine the size, power, efficiency, and security of the source, and in some cases the design of the receiver. Intensity-modulated audio-

† References may be found in the Bibliography at the end of the article.

frequency systems have been the most common type to date, since they are the simplest in design and construction and most of their components are commercially available. Mechanically modulated systems are the lightest in weight, but electrically modulated ones can attain the highest efficiency of light utilization.

C. Components of Systems

The operation of all these systems may be readily understood by referring to the schematic diagram in Fig. 1. Electrical impulses from the microphone receiving speech at the transmitter are fed into the audio amplifier (and r-f amplifier, if used). This must have an output power capable of modulating the transmitter source or the external modulating device, as the case may be. The intensity, polarization, or wave-length distribution of the radiation leaving the transmitter is thus made to vary in proportion to the modulated voice current. The reflector shown in Fig. 1 represents a general transmitter optical system producing and limiting the emergent beam. The radiation is directed toward the distant receiver through an infra-red filter designed to eliminate the visible portion of the spectrum.

The small amount of infra-red radiation reaching the receiver is concentrated by a mirror or lens upon the detector, which is generally a photo-conductive or photo-emissive cell. If the modulation is in the wave-length distribution or in the polarization of the beam, it must be converted to an intensity variation by a suitable device. The photo-cell current, varying with the intensity of the received radiation, is passed through a load resistor and the varying voltage produced is amplified and fed to headphones or a loudspeaker. Thus, with a series of conversions of energy, highly intelligible conversations can be carried on over a distance of several miles.

D. Security

The military security of an optical communication system depends on two things: first, its range of possible detection; and second, the probability of enemy detection or of message reception within this range. Security with respect to detection is called "system security;" and to reception, "message security." With sufficiently low beam intensity the limit of detection by an enemy equipped with sensitive receivers can be made less than the distance to the horizon. Of course, in such a case the friendly communication range is also limited.

Within receiving range the probability of detection depends on transmitter beam width. It increases about in proportion to this width, or even somewhat faster, since enemy detectors are more likely to be at large angles from a direction known to be friendly, than at smaller ones. The German and Japanese light beam field telephones had beam widths of a few minutes of arc. The maximum linear beam widths at their limiting ranges did not exceed a few dozen feet. It is almost impossible to locate enemy transmitters of this kind except by daylight observation or capture. However, the narrow beam also makes an initial friendly contact quite difficult to establish and maintain.

Within the range and within the beam, the probability of detection depends on the types of enemy receivers. The maximum night visual range (NVR) at which a transmitter can be detected by a dark-adapted eye[4,5] is controlled by the type of filter used.[56,57] Values of NVR for a tungsten beacon and certain plastic filters have been given by Shenk and co-workers.[57]

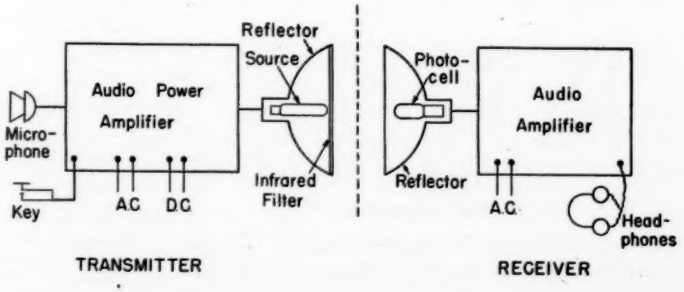

FIG. 1. Essential elements in a complete communication system.

Next to the eye the detectors most dangerous to system security are "image tubes," such as the electron telescopes and phosphor-button receivers discussed by Fluke and Porter.[6] These devices convert an infra-red field of view into a visible field. The German Navy Seehund[31] and the widely publicized American Army "Sniperscopes" and "Snooperscopes" are in this class.[7] They can detect optical transmitters easily if the emergent wave-lengths from the filtered transmitter beam fall within the sensitive wave-length range of the image tube. However, they cannot receive any voice or modulated carrier-wave message.

The devices dangerous to message security are communication receivers themselves and search receivers. The commonest types are designed for intercepting audio intensity-modulated beams, as noted above. If conventional warfare continues, the risk of interception by skillfully designed search receivers will undoubtedly evoke a series of more and more elaborate source types and modulation methods aimed at preserving the security of the transmitter.

II. EARLY SYSTEMS

The success of optical voice communication systems has been dependent on the sources and sensitive detector cells available at any given time. As for sources, Bell and Tainter in 1880 had devised upwards of fifty forms of apparatus for varying a beam of light. Later workers before 1900 used principally voice modulation of carbon arcs, manometric flames, and probably filament lamps. Vibrating mirror and vibrating ribbon-shutter systems for speech frequencies were especially studied in sound motion picture research during the 1920's. Efficient gaseous discharge sources of infra-red radiation capable of a high degree of modulation became available only in the last decade.

Selenium photo-conductive cells were discovered in 1873. They were the only infra-red audio detectors available until the appearance of the Case Thalofide cell in 1917. Cesium-surface photo-tubes were first produced commercially in the late 1920's. Lead sulfide cells for detection in the IIR were developed during the last ten years.

A. Bell's System

Bell and Tainter in America made a photophone in 1880,[8] within four years after the invention of the telephone. They credit A. C. Brown of London with a similar system devised two years earlier. It is interesting to note that this optical wireless voice transmission preceded by several decades any wireless communication by radio. This is about the same interval of time as that which separated the optical semaphore and the telegraph.*

Much of the subsequent work in optical communication is anticipated in Bell's paper. He says

> (1) The source of light may be controlled, or (2) a steady beam may be modified at any point in its path.
>
> In illustration of the first method we have devised several forms of apparatus founded upon Koenig's manometric capsule, operating to cause variations in the pressure of gas supplied to a burner, so that the light can be vibrated by the voice.
>
> In illustration of the second method, I have already shown one form of apparatus by which the light is obstructed in a greater or less degree, in its passage through perforated plates. But the beam may be controlled in many other ways. For instance, it may be polarized, and then affected by electrical or magnetical influences in the manner discovered by Faraday and Dr. Ker. (*sic!*) . . . .
>
> Another method of affecting a beam of light is to pass it through a lens of variable focus formed of two sheets of thin glass or mica containing between them a transparent liquid or gas. The vibrations of the voice are communicated to the gas or liquid, thus causing a vibratory change in the convexity of the glass surfaces and a corresponding change in the intensity of the light received upon the sensitive selenium. We have found that the simplest form of apparatus for producing the effect consists of a *plane mirror of flexible material*, such as silvered *mica or microscope glass*, against the back of which the speaker's voice is directed. (Italics A.G.B.) Under the action of the voice the mirror becomes alternately convex and concave, and thus alternately scatters and condenses the light.

With this latter transmitter Bell and Tainter achieved a voice range of 213 meters using the sun as a source.[9] In a later test they reached 1¼ miles with a code tone. Diagrams of the equipment[10] indicate the use of a deep parabolic mirror about 3 ft. in diameter, on the axis of which was mounted a cylindrical selenium cell 2 in. in diameter and 2½ in. long, with grid spacings about 1/15 in. The receiving angle was apparently about 10° and the transmitter angle, as determined by the solar diameter, about 0.5°.

In looking for better receivers, Bell found a

* A cartoon of the time, in Punch, reprinted in reference 9, depicts courtship by photo-phone across the English channel.

further entertaining phenomenon: that periodic interruption of sunlight on a thin diaphragm or on a powder of almost any substance would produce a musical tone as a result of thermal expansion and contraction.[8,11] A lampblack receiver based on this principle with direct sonic response was successfully used on the photo-phone in place of the electrical selenium receiver. The principle has been used a number of times since in other detectors,[12] though commonly with electrical rather than acoustical detection of the expansion. Bell proposed the use of an acoustic spectrometer or "spectrophone" for exploring infra-red absorption spectra by means of this effect.

B. Early German Work

A bibliography and discussion of some early German optical voice communication systems have been given by Thirring.[13] In 1901 Simon in Göttingen obtained ranges up to 1 km with a 3-foot searchlight having a voice-modulated carbon arc, and much greater ranges were claimed by Rühmer in 1904. The first successful systems from a military point of view were developed by Simon (Germany) and Thirring (Austria) working in cooperation with the Siemens-Halske Company, in 1917.

The Thirring system was put into production but did not reach the front before the first World War was over. The usual source was a 14-inch searchlight, with the arc modulated by inductive coupling between its circuit and the circuit of a carbon microphone. Glow discharge lamps, 5-watt "Nachtlampen," and others were also used successfully in such a reflector, but gave shorter ranges. The receiver employed a selenium photoconductive cell having a sensitive area of about 1 mm². The cell was set at the focus of a 22-cm diameter, 30-cm focal length lens. It was connected to headphones through a four-stage triode amplifier. The receiver sensitivity was limited only by cell noise, which was high; the variation of cell noise with cell area is discussed in Thirring's paper.

The system is reported to have had an average clear weather (ACW) voice range of nearly 8 km and a much longer range with a buzzer code tone which was used for a call signal. The optical angles were probably about 1° for the transmitter beam and ¼° for the receiver directivity pattern. The system apparently was designed to be portable by two men and to operate from a gasoline generator. No filter is mentioned in the account. Perhaps the beam was narrow enough for security without it. A weak infra-red filter could have been used, as selenium cells can be constructed to respond to nearly 1 micron.

Several ingenious German visual blinker code devices of higher security were evolved during the first war which were based on polarization modulation and spectral modulation of the light beam.[14] One of these may have reached the production stage.

An interest in very narrow beams (under 1° of arc) characterized the early German developments. This, together with the static character of World War I which made possible prepared and stationary positions for installing and aligning the equipment, apparently guided subsequent work there and elsewhere almost exclusively into narrow-beam systems. A narrow beam makes for great security, but precision alignment of the units is constantly required in the field. Such systems are quite unsuited to mobile warfare unless automatic guiding is provided.

C. British Admiralty Voice Systems

In 1916 equipment for the transmission of speech by means of light beams was developed under the sponsorship of the British Admiralty Board of Research and Invention. The program was started at the suggestion of Professor W. H. Bragg who proposed the use of a method of modulation in which the image of one grid is caused to move over a second grid. It is of interest to note that Bell had suggested the use of two grids, one fixed in position and the other moved in a direction perpendicular to the grid strips, although he had never actually devised such a system.

An account of the work in England was published by Dr. A. O. Rankine[15] after the termination of World War I. He found that the percent of modulated light obtained from the current-modulated carbon arc was very small and concluded that this method was impractical. The scheme adopted was that of grid modulation of a beam of radiation from a point source.

The optical arrangement first employed is

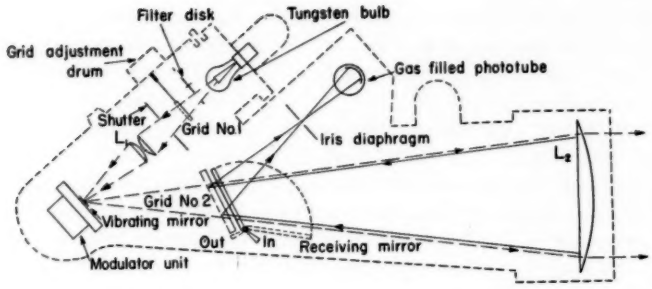

FIG. 2. Vertical section, transceiver head of Japanese photophone.

identical with that later used in the Japanese photo-phone which is illustrated in the diagram of Fig. 2. In the British system the mirror used to impart voice-modulated impulses to the beam was attached by means of a lever to the diaphragm of a gramophone recorder. Angular oscillations of this mirror due to sound waves impinging upon the diaphragm caused the dark images of the first set of grid lines to move over the openings of a second grid, thus producing the desired fluctuations in beam intensity. An alternative arrangement employed a telephone receiver earpiece to drive a reed which carried the small mirror.

The detectors were selenium cells made by Dr. Fournier D'Albe having small sensitive areas and resistances of the order of 10^5 ohms. These cells deteriorated when exposed to daylight, were quite unstable, and their response to pulsating light decreased with increasing frequency in the audible range. It was found that the noise level in these cells was so high that amplification using triode valves was not feasible. The author ascribes most of this noise to the graphite backing used in forming the selenium cells. He suggested that a great increase in range should be possible if cells with improved noise characteristics could be developed.

Despite the simplicity of the components used and the absence of electronic amplifiers in these systems, fair communication ranges were attained. Using a carbon arc and 20-inch projectors of poor quality, a range of $1\frac{1}{2}$ miles with voice was possible, with transmitter and receiver angles of about 0.6°. When the sun was used as a source this range was extended to several miles. Considerable space in the article is devoted to the technique of grid construction and to optical arrangements. The main paper is followed by a lengthy discussion in which at one point Professor W. H. Eccles remarks that a carbon arc system had purportedly been used on ships of the German Navy at sea over a distance of 7 miles.

D. American Systems in the First World War

Invisible ultraviolet and infra-red blinker systems saw field use in World War I in guiding airplanes to landing fields and in keeping convoys together.[17] The ultraviolet sources were observed with telescopes having a fluorescent screen in the focal plane. The infra-red sources in the convoy system were detected by a receiver using the Case Thalofide cell, described below. Receivers converting the infra-red for visual blinker observations were, of course, not possible until after the development of infra-red phosphors and photoemissive tubes and after great advances in electron optics.

Case Code System. An infra-red code system apparently similar to the convoy system was demonstrated by the Case Research Laboratory in October 1917 to representatives of the Army and Navy.[18] In this demonstration, a Case Thalofide cell was mounted in a 24-inch reflector and was part of a triode oscillator circuit connected to earphones.

The Thalofide cell was an oxidized thallous sulfide photo-conductive cell invented by T. W. Case in 1917 which was marketed commercially for a number of years.[19] The sulfide layer, several square centimeters in area, was smeared on a quartz disk. Two interlocking coarse grids of lead were then sprayed on through a stencil to form the electrodes. Cell resistances in the dark were from 100 to 500 megohms. They would decrease by a factor of from 2 to 8 on exposure to $\frac{1}{4}$ foot-candle illumination from a tungsten lamp. The

cells were unfortunately not very stable, especially under strong illumination, and were sealed in a red glass envelope to protect them from ultraviolet light.

In the Case code system, reception of a signal by the Thalofide cell produced a change in pitch of an audible note in the phones. The source was a 60-inch Sperry searchlight covered by a shutter and filter. The filter was made by combining Wratten filters 91, 45, and 53 into a single unit called Wratten 740, which was sealed at the edges against moisture. The filter has a cut-off near 0.8 micron and transmits 50 percent at 1 micron.

With this system infra-red blinker signals over a range of 18 miles, from Fort Hancock to the Woolworth building, caused very distinct changes of pitch in average weather. Further tests were carried out in February 1918 with the Coast Artillery at Fort Monroe, Virginia. At the end of the war smaller versions of this system had been built for two-way communication. In these units the receiver and transmitter both had 8-inch mirrors and were incorporated into a single transceiver head. The source was an 8-volt signal lamp and the beam was modulated by a butterfly shutter. The system operated from a storage battery and could be carried by two men. It had a range of 4 miles.

Case Voice System. Two voice systems were also constructed. In these the source was an acetylene flame, modulated by speaking into a horn connected to the base of the burner. This source was about $\frac{1}{4}$ in.^{2} in area and had an intensity of about 150 cp. The receiver was the Thalofide cell, feeding into a three-stage amplifier.

When the source and cell were each used in 24-inch mirrors, the range was five miles on a clear night. Beam angles were probably of the order of 4° for both transmitter and receiver. With 12-inch mirrors, a 2-mile range was obtained, probably with beam angles of about 8°. This development was not carried further after the conclusion of the war.

Coblentz Signal System. During the first World War, W. W. Coblentz of the U. S. Bureau of Standards studied methods of detecting invisible objects by the radiations they emit and he also developed thermal radiophonic signaling devices.[16] He found that molybdenite was superior to selenium for detecting a beam of radiation modulated at audiofrequencies. One of the molybdenite samples was found to be from 150 to 250 times as sensitive as the gold-leaf radiophone for detecting audio signals.

Field tests were conducted over a 3-mile range using a 250-watt tungsten lamp placed in a 28-cm searchlight reflector. A concave silver-on-glass mirror, 16 cm in diameter, 50-cm focal length, was used to concentrate the radiations upon the molybdenite receiver. The beam was interrupted by means of a sectored disk placed in front of the molybdenite crystal. The current pulses set up in the detector were fed through a three-stage audio amplifier to a telephone head set. The signals transmitted by infra-red radiation (using absorbing screens of unspecified materials) were loud and clear over the 3-mile range for a light pulse having a period of 1/500 of a second.** He also experimented with a change-in-pitch method of signaling which was most effective when a gas-filled potassium hydride photo-tube was employed as receiver.

E. Later Work

In the years between the two world wars some developments occurred which were of importance in providing new sources of modulated radiation. Voice modulation of carbon arcs and glow discharges was studied, but apparently without results of industrial or military value. Studies of optical modulation of the beam emitted by a steady source were more fruitful, however, in suggesting techniques which were tried later in military communication systems.

The most notable industrial advance occurred in the development of sound motion pictures. The units employed have all the elements of an optical communication system plus a troublesome intermediate stage of recording on film. Much study was devoted to sources, methods of modulation, and detectors, with the emphasis on ultraviolet rather than infra-red radiation. Descriptions of this research may be found in the technical journals of the period, such as the publications of the Society of Motion Picture

** Radiation from the full moon received by the system through the infra-red filter caused a loud sound in the telephone receiver, although the intensity was only 3×10^{-7} gram calorie per second.

Engineers. Some of the elements produced in this work were used from time to time in short-range demonstration exhibits to amaze the curious by "talking on a beam of light." Similar short-range communication systems have been presented as novelties in radio magazines such as QST, but appear not to have been intensively developed further in this country for military purposes until the start of World War II.

III. FOREIGN DEVELOPMENTS DURING WORLD WAR II

At the time NDRC began work on optical communication systems in 1941, the equipments now known to have been in military use in enemy countries were the German and Japanese vibrating-mirror units and an Italian system using a modulated filament lamp. The German units employed thallous sulfide and lead sulfide cell receivers, these materials having replaced the selenium receivers of earlier systems following Case's discovery of the thallous sulfide cell. The other systems employed photo-tubes.

A. Italian Photo-Phone

Two Italian voice systems, the type F.F. 115 photo-phone and another similar system using concave mirrors instead of lenses in the optical system, made use of modulated tungsten filaments of about 2-watt rating.[20] The beam angles were about $\frac{1}{2}°$.

The advantage of modulated filament systems is that the source arrangements are small and uncomplicated; like modulated arc lamps, they have no moving parts, and they are readily manufactured by mass production methods. The disadvantage is that the ratio of percentage light modulation to percentage current modulation (modulation ratio) depends on the heating and cooling time of the filaments. For voice modulation, they must therefore be made of very fine wire; but even when the filaments are so fine as to be fragile, the modulation ratio is not very large at speech frequencies above 1000 c.p.s. which are important for intelligibility. Another disadvantage for voice use is that the light output is a very non-linear function of either current or voltage. For code operation, at low frequencies, modulated tungsten lamps are very good IIR sources and give good communication ranges.

B. Japanese Light-Beam Telephone

The simplest method of mechanical modulation of a light beam is the use of a rotating "chopping disk," but this provides a limited kind of code communication. Voice-modulation devices include the vibrating ribbon-shutter, used extensively in sound motion-pictures, and the vibrating mirror or audiofrequency galvanometer.

One system employing a vibrating mirror is the Japanese photo-phone or light-beam telephone. A unique feature of this unit is the incorporation of the projector and receiver optics into a single transceiver head. The optical arrangement has been described by Huxford,[21] and further details of its operational characteristics appear in OSRD Report No. 5763.[23]

Figure 2 shows a vertical section of the transceiver head. Light leaving the lamp filament is broken up into horizontal segments by a metallic grid (grid 1), is reflected by the vibrating mirror, and the image of the bright segments focused in the plane of the second grid. Thus, when amplified voice currents are fed into the galvanometer and cause the mirror to vibrate, the bright images are displaced in proportion to the amplitude of the impressed audio signal, with a consequent variation in the amount of light flux which passes through grid No. 2. At best only 50 percent of the light flux passes both grids. Lens L_2 projects the modulated beam to a distant receiver.

During reception the incoming modulated light is focused by lens L_2 (after reflection from the back of grid 2) upon the cathode of a gas filled Cs-Ag-O photo-tube whose output is amplified to a sufficient level to operate a head set. The intensity of the received signal may be increased by rotating a receiving mirror into the position shown; this mirror must be retracted when the unit is used for transmitting. A set of filters is provided so that white, yellow, red, or infra-red radiation may be used. The angle of spread of the transmitted beam is 0.1° and the receiver angle is about 1°, but the latter can be reduced in daylight by an iris diaphragm to exclude objectionable background light. These sets are compact, having a net weight (exclusive of power source) of 110 pounds, so that one unit may be transported by two men. The night infra-red ACW range is about 1.5 miles.

C. German Lichtsprechers

Three types of German vibrating-mirror systems were in field use in World War II. They are the Lichtsprecher ("Li") series whose model numbers indicate the transmitter/receiver aperture in mm: Li 50/60, Li 80 and Li 250/130. The field equipments weigh 30, 54, and 140 pounds, respectively. All have narrow transmitter and receiver angles (~0.25°), and the ACW day or night range varies from about 2 miles for Li 50/60 to nearly 9 miles for the largest model. The small effect of daylight and the very great ranges attained are largely a result of the insensitivity to background light of the lead sulfide receiver cells, of the small size of these cells (about 1 mm in diameter), and of the extension of the spectral range into the IIR where atmospheric attenuation is less serious.[24, 52]

These three systems are marked by great elegance of design and by optical precision and sturdiness of construction. Apparently all of the Lichtsprecher units were made by Carl Zeiss. References are made to available literature in the following brief account of the transmitter principles applied in these units.

Lichtsprecher 80. Several Li 80 units were captured during the African campaign in 1942, and it is now known that this equipment had been in use in the German Army since 1935.[22] The transmitter and receiver optical systems are in separate tubes, the appearance of the unit being that of oversized binoculars mounted on a tripod. Detailed studies of the transmitter and receiver systems have been made by Kent and Hole,[25] and by the Camp Coles Signal Laboratory[26] and others.[27, 28] The receiving element is a small thallous sulfide button type of cell. The radiation source is a tungsten filament used in conjunction with red and infra-red filters.

An unusual method is employed for modulating the light beam. The transmitter principle used is illustrated in Fig. 3. The modulator consists of an armature driven from a speech amplifier and carrying a small right-angled prism. This prism is mounted so that one side is very close to one side of a larger prism, the distance between them being a fraction of a wave-length of the radiation used. When the armature is set into vibration by tone or voice currents, the thickness of air film

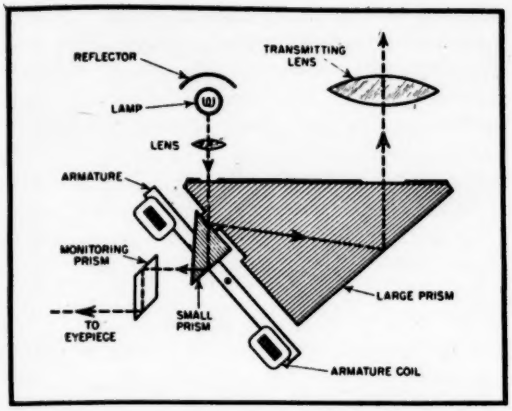

FIG. 3. Modulator system of German Lichtsprecher 80. (Reference 22.)

separating the two prism surfaces changes with displacement of the armature. Light from a tungsten filament is focused by means of a condensing lens onto the point of near contact between the two glass surfaces. The angle which the incident beam inside the large prism makes with the normal to its surface is slightly greater than the critical angle. Total reflection occurs in the large prism except for close approach of the two glass surfaces, at which time a certain fraction of the beam is transmitted into the small prism, the amount depending upon the thickness of the air film. Thus the flux of radiation in the internally reflected beam varies according to the position of the small vibrating prism. The performance of the armature varies with changes of temperature so that the modulation adjustment is very critical. The system has a non-linear characteristic and considerable distortion occurs in transmission of speech.

Lichtsprecher 250/130. Essentially the same modulator optics and receiver elements are employed in Li 60/50 as in Li 250/130. For the purpose of this review it is sufficient to describe only one of these systems. A photograph of the Li 250/130 field equipment as used by the German Army is shown in Fig. 4. The half-width angle of the projected beam is approximately 0.4° and the receiving angle is of the same order of magnitude. An estimate based on "vacuum" range tests (using a virtual image of the source and a short air path) indicates an ACW range of about 6

miles for one unit which was tested.[24] Voice transmission up to 8.5 miles in clear weather was reported for two sets of equipment used in another test.[29] Several reports have been written describing the electrical circuits and giving construction details; one report gives an analysis of the method of modulation used.[30] A brief account of the modulator optics will be given here.

The Lichtsprecher 250/130 employs a tungsten filament source, two sets of grids, and a vibrating galvanometer system with mirror. Instead of the opaque metallic grids of the Japanese photophone, however, the German unit employs a system of long thin glass prisms as grid elements. Figure 5 is a photograph of the modulator showing the vibration galvanometer in the foreground, lamp housing at the left, and the double set of glass prism grids. Figure 6 is a vertical section giving details of the transmitter optics.

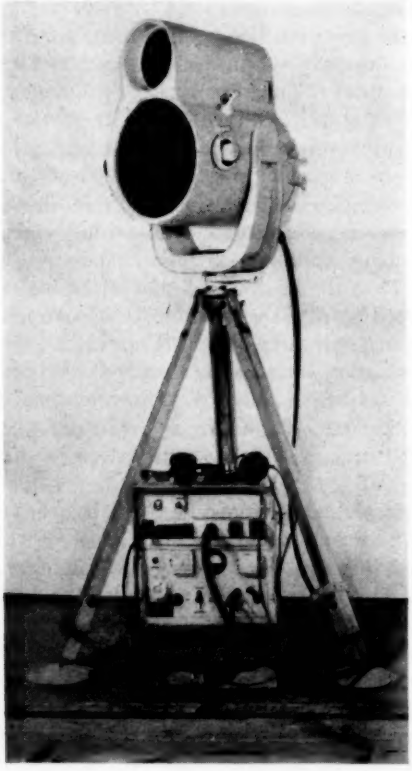

FIG. 4. German Lichtsprecher 250/130.

Light from the source S is condensed on the vibrating mirror C, and in passing through grid G_1 is split into two beams deviating from each other by a small angle. The two sets of glass prism grids, G_1 and G_2, are at conjugate foci of the concave mirror C, so that "images" of the open slits and grids of G_1 are formed in the plane of the grids of G_2.

Modulation of the beam occurs in the following manner. There is one position in the angular swing of mirror C which corresponds to maximum brightness at the center of the projected beam (a, Fig. 7). At this position rays passing between the G_1 prisms fall exactly upon openings of the glass grids in G_2. The prisms in G_2 are so arranged that the rays passing through the prisms in G_1 and falling on the prisms in G_2, for this same position of C, are deviated by the same small angle as that produced in G, but in the *opposite* direction, so that these rays then proceed along with the rays through the openings to form a coherent beam of maximum intensity. The images of the prisms in G_1 then fall exactly upon the prisms in G_2. At the maximum angular excursion of C from the above position, the openings of G_1 are imaged on the grids in G_2, and G_1 grids on the openings in G_2, and at this position of C the two sets of rays upon passing G_2 are deviated in opposite directions away from the axis of the beam (b, Fig. 7). This position corresponds to minimum brightness at the center of the beam. For other intermediate positions of C the deviated and undeviated rays from G_1 overlap the prisms and openings in G_2 by varying amounts resulting in varying brightnesses at the center of the projected beam. The resulting beam patterns are illustrated in Fig. 7. The intensity at the center of the beam varies linearly with the angular displacement of C, and hence is modulated by an amount exactly proportional to the amplitude variations of tone or voice currents passing through the galvanometer coil. An automatic volume control limits the amplitude of swing of mirror C to prevent frequency doubling, and since the galvanometer element has a flat response characteristic over the range of frequencies used, there is a negligible amount of speech distortion.

The receiving element is a lead sulfide photoconductive cell having a sensitive area of about 1 mm² which responds in the IIR out to 3.4

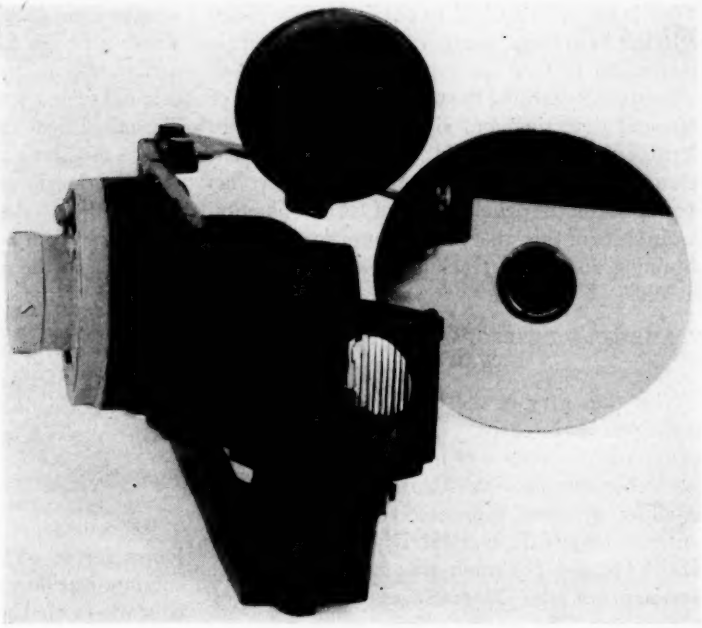

FIG. 5. Modulator optics projector Li 250/130.

microns. Sharp cut-off filters permit operation with minimum danger of detection from visible light which may be present in the beam. For daylight operation there is a sun attachment providing a means of utilizing the high brightness of the sun's surface in place of the tungsten filament. These instruments are equipped with cleverly designed adjusting devices, and are provided with accurate azimuth and horizon positioning scales having slow motion micrometer screws. Receiver and transmitter optics are sealed in air tight chambers provided with rubber gaskets and having a color-indicating drier.

German Ship Identification and Detection. A recent report of the Vacuum Tube Development Committee[31] gives some detail on German IR signaling equipment. Infra-red devices for ship to ship detection were tried on the "Prinz Eugen" in 1942. Both thermal detectors and photo-cells were used by fitting them into the ship searchlight mounts in positions normally occupied by the lamps. Both devices were very sensitive, but the beam angles were so narrow that it was difficult to keep the receiver constantly on the target. However, very accurate bearing information could be obtained using these detectors

Infra-red "Strahlensperren" or barrier systems were used to guard harbor entrances. A 200-watt high pressure d.c. biased mercury arc-modulated at 1000 c.p.s., was used in the transmitter. The lens system gave a $\frac{3}{4}°$ spread to the filtered beam. A PbS photo-conductive cell mounted in a 45-cm mirror provided a working range of 10 km.

Modulated Arcs. It is evident from articles appearing in German physics journals that a considerable amount of research during the war period was spent on arc discharges, their radiation and modulation characteristics. Several new types of mercury lamps were developed, particularly the high pressure, short column, or "gap" lamps. Water-cooled quartz lamps having pressures up to 200 atmospheres were manufactured by Ozram and other companies.

Mention was made above of the use of a 200-watt mercury lamp to provide a detection range of 10 km with a narrow beam of radiation modulated at 1000 c.p.s. Equipment was also developed to produce a beam with a spread of about 8° which was considered adequate to insure continuous contact by hand guiding between ships subject to normal pitch and roll. At this transmitting angle, a 2000-watt high pressure mercury

vapor lamp was required to obtain a voice range of 10 km in average weather.[31] This equipment is referred to in German reports as the "Puma" apparatus. Regarding the state of development of infra-red detecting and signaling equipment in Germany near the close of the war, we quote from reference 31: "An enormous amount of effort has been spent on the development of IR equipments, but in spite of this, there has been little success in obtaining automatic tracking, search or homing devices."

IV. AMERICAN DEVELOPMENTS DURING WORLD WAR II

With the entry of the United States into the recent war an intensive program of research was organized on methods of optical communication and detection. The investigations of light-beam signaling systems sponsored by OSRD were centered largely in Optical Division 16 of the NDRC, whose chairman was Dean George R. Harrison, of the Massachusetts Institute of Technology. The research projects on infra-red were under the direction of Section 16.4, Professor O. S. Duffendack, Chief, and Dr. J. S. Owens, Chief Technical Aide, University of Michigan. Most of what follows is a review of the work on communication systems and components carried out under this section.

The results of the work on communication problems in Section 16.4 are contained in some twenty-four reports and represent activities carried out under about ten contracting universities and industrial laboratories. In many cases where a review has not appeared as a published article, microfilm or photostatic copies of the original report may be obtained from the Office of Technical Services, U. S. Department of Commerce, by the payment of a small fee. The PB (Publication Board) numbers of these reports, as indicated in the abstracts published in the Bibliography of Scientific and Industrial Reports, are given in the appended Bibliography.

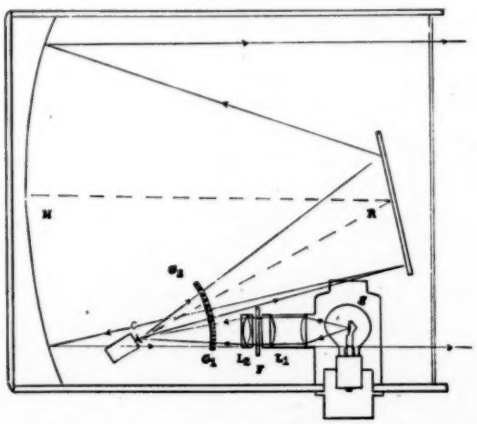

FIG. 6. Sectional view of projector Li 250/130.

Many of the components of the systems developed for the Navy Department and described by Fluke and Porter[6] have since been reported in the open literature in greater detail. In the following accounts, references to the original reports are given wherever possible.

A. Blinker Code Systems

Improvements in the use of tungsten filament lamps for on-off blinker code and carrier-wave communication were made by Black, Geiger, and co-workers on University of Michigan Contract NDCrc-185. Among these were special methods of keying for speeds up to 12 words per minute, and the development of high speed mechanical shutters. These units were employed for all-around coverage, and used in separate reflectors or sealed-beam lamps for directional radiation. The sources are detected and signals read by means of an image tube, such as the phosphor button receivers, or the RCA 1P25 electron telescope.[7]

B. Modulated Code Systems

The Michigan group also developed an efficient low frequency tungsten lamp code system. At first the lamps were modulated by a mechanical chopper. Later, many small 6-watt, 220-volt, fine-filament lamps were mounted in a reflector trough and modulated by a thyratron power supply giving special wave shape. Exceptionally high coding speeds were possible with these lamps.

These systems, developed for use on aircraft and surface ships, were elaborated to provide continuous scanning and rapid identification of craft coming into a ship's field of view as well as to furnish communication channels. Gyroscopically stabilized receivers gave both true and rela-

tive bearings of any source within range. The detecting elements used were photo-conductive cells developed by Cashman under Contract OEMsr-235 with Northwestern University.

C. Modulated Arc Discharge Sources

A new element was brought to optical communication systems with the development of the modulable cesium vapor lamp source in 1944 by Beese at Westinghouse[32] under a contract with the Navy Bureau of Ships. This lamp radiates strongly the cesium resonance lines, 8521 and 8944A, with relatively little visible radiation, so that a weak filter suffices for security. It can be current modulated up to 90 percent with low distortion, and the modulation ratio is about 0.80 up to frequencies of 3000 c.p.s.[33] The arc column is three inches long in a bulb about one inch in diameter. Its use in a transmitter and methods of modulation have been described by Huxford.[21]

In Fluke and Porter's words, the new cesium lamps "provide the desired flux with a fairly wide optical field."[6] This wide-field point of view, expressed here and exemplified in the code systems discussed above, represents an important departure from the design used in the earlier very narrow-beam voice systems. The cesium source is an essential element in the ship-to-ship communication system developed at Northwestern University on Contract OEMsr-990. Its adoption is described by Beese:[32] "Our experimental lamps . . . matched their (Northwestern's) power supply and searchlight reflector, and in a few days an operable field unit demonstrated that this system formed a practical means of communication. Two-way ship-to-shore voice and code communication by invisible infra-red light beam was demonstrated on the Atlantic Ocean October 18 and 19, 1944. . . ."

Beese reports that other styles of cesium lamps have been provided for the Army Air Corps. It seems that these lamps are admirably suited to the problem of optical voice communication in the NIR between moving stations.

Another arc source which appeared early in the war was the concentrated-arc lamp developed at the Western Union Telegraph Company Laboratory by Buckingham and Deibert.[34] In this arc the source of light is the cathode spot which is of small area and has an intensity ten times that of a tungsten filament. The lamps are available in several sizes ranging from 2- to 100-watt ratings, and have been used in many applications requiring a bright "point" source. Some study has been made of their modulation characteristics.[35]

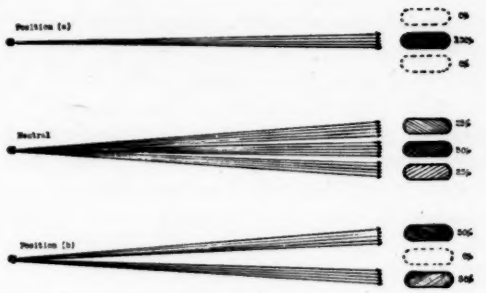

FIG. 7. Pattern of the modulated beam in Li 250/130 at the rest position, and at maximum angular excursions of mirror *C*. (Reference 30.)

D. Ultrasonic Modulation Systems

There are two well-known methods of modulating a beam of light from a steady source at frequencies higher than the audible range. The first method uses the Kerr effect to vary the state of polarization of a beam passing through a liquid in which is established an oscillating electric field of high intensity. This technique has been employed in the laboratory for such purposes as measuring the velocity of light[36] and the frequency response of gas filled photoelectric tubes.[37] It is also used in studying light decay phenomena and in high speed photography. There are several German patents*** on methods of using the Kerr cell for producing modulated light for sound recording and for telephonic communication on a beam of light.

In the second method, the beam is spread into an intensity-modulated pattern by a "grating" of standing ultrasonic waves in a liquid.[38,39] The amplitude of the standing waves is modulated by the voice, and the grating correspondingly throws more or less of the light out of the central beam into the first and second and higher orders. This principle has been employed in the Scophony Television system. Its successful application in an optical communication unit has recently been reported.[61]

*** German Patents 716094 and 727451, available through U. S. Patent Office.

A modification of these methods is one in which the standing waves are set up in a solid block of transparent material and double refraction occurs due to mechanical strains at the antinodes.**** There are several modifications of this scheme in one of which both the ordinary and extraordinary rays are used. Although these methods are very inefficient in converting energy from the source into useful modulated light, they do provide a high degree of message security.

E. New Photo-Cell Receivers

The receivers in most modulated code and voice systems use photo-cells with a.c. amplification. Among the cells which appeared during the war is the Cashman thallous sulfide cell, developed under Contract OEMsr-235 with Northwestern University.[40, 41, 42, 43] This cell is the successor to the Case Thalofide cell, but is very linear in response and stable even when exposed to sunlight. Its long wave-length threshold is about 1.45 microns, and its maximum response occurs at 0.95 micron. Below 5000 c.p.s. its signal-to-noise ratio for interrupted radiation from a tungsten source at 2870°K is considerably higher than the values obtained with average Cs-Ag-O type vacuum or gas filled photo-tubes and photo-tube multipliers under comparable test conditions.

This cell was successfully brought to the stage of manufacture on a production basis by General Electric Company, Contract OEMsr-1322,[44] and by Radio Corporation of America, Contract OEMsr-1486.[45] Some theoretical studies of its characteristics have been made.[46–50]

Cashman has also reported the successful production of lead sulfide cells sensitive to 3.6 microns.[40, 51] Their signal response is almost constant up to 5000 c.p.s. They appear to be equal or superior to the Zeiss lead sulfide cells used in the Lichtsprechers. The existence of the latter was not known in this country until several months after the NDRC development in late 1944. Selenium and silicon cells have also been studied.[53, 54]

V. RÉSUMÉ

During a span of nearly seventy years, optical telephonic and carrier-wave communication systems have evolved from laboratory toys to reliable and highly secret military systems of great sensitivity and range. They have been successfully designed to meet the rigid specifications required of all field equipments used in modern warfare. During World War II systems were developed having wide angle beams and scanning devices suitable for use on mobile stations. Detailed analyses have been made of the characteristics of components used in these systems so that the contribution of each to the attaining of maximum range may be evaluated for a given atmospheric attenuation and specified beam width.[58–60] As a result of these wartime developments new techniques have been evolved for detecting and measuring infra-red radiation and for increasing the sensitivity of methods previously employed.[55] A large number of new sources, cells, amplifiers, light filters, and optical materials have become available for the investigation of spectra and radiation phenomena in the short wave infra-red region.

The authors wish to express their thanks to former personnel of Division 16, NDRC and various individuals in the service branches concerned, for valued help in compiling this survey.

**** German Patents 710404 and 717747, available through U. S. Patent Office.

BIBLIOGRAPHY

1. General

(1) E. O. Hulbert, "Optics of atmospheric haze," J. Opt. Soc. Am. **31**, 472 (1941).

(2) H. G. Houghton, "On the relation between visibility and the constitution of clouds and fog," J. Ae. Sci. **6**, 408 (1939).

(3) T'ing Sui Kê, "Spectroscopic light sources for invisible ultraviolet," J. Opt. Soc. Am. **36**, 719 (1946).

(4) Donald R. Griffin, Ruth Hubbard, and George Wald, "The sensitivity of human rod and cone vision to infra-red radiation," J. Opt. Soc. Am. **36**, 360A (1946).

(5) D. E. Mitchell and R. Tousey, "Photometer for visual transmission of extremely dense filters," J. Opt. Soc. Am. **36**, 362A (1946).

(6) Commander John M. Fluke and Lieutenant Noel E. Porter, Sec. 660E, Navy Bureau of Ships, "Some technical developments in light wave communication," Proc. I.R.E. **34**, 876 (1945). (P.B. 5305.)

(7) G. A. Morton and L. E. Flory, "Infrared image tube," Electronics **19**, No. 9, 112 (1946). Also Electronics **19**, No. 6, 192 (1946).

2. Early Systems and Components

(8) Alexander Graham Bell, "On the production and reproduction of sound by light," Am. Assn. Adv. Science **29**, 115 (1881).
(9) Catherine C. Mackenzie, *Alexander Graham Bell* (Houghton Mifflin Company, Boston, 1928), p. 226.
(10) George B. Prescott, *The Electric Telephone* (D. Appleton-Century Company, Inc., New York, 1890), second edition, pp. 320.
(11) A. G. Bell, "The spectrophone," Bull. Phil. Soc. **4**, 142 (1881).
(12) H. A. Zahl and M. J. E. Golay, "Pneumatic heat detector," Rev. Sci. Inst. **17**, 511 (1946); **18**, 347, 357 (1947).
(13) H. Thirring, "Neue Apparate für Lichttelephonie," Physik. Zeits. **21**, 67 (1920).
(14) E. Beckmann and P. Knipping, "Suggested methods of secret signaling," Sitz. Preuss. Akad. Wiss. **25**, 443 (1920); Sci. Abs. **24A**, No. 858 (1921).
(15) A. O. Rankine, "On the transmission of speech by light," Proc. Phys. Soc. London **31**, 242 (1919).
(16) W. W. Coblentz, "Infra-red signaling," Phys. Rev. **15**, 340 (1920); S.P. No. 398, Bureau of Standards 636 (1920). U. S. Patent 1,345,586.
(17) I. Bernard Cohen, "American physicists at war," Am. J. Phys. **13**, 333 (1945). (Includes bibliography.)
(18) T. W. Case, "Infra-red telegraphy and telephony," J. Opt. Soc. Am. **6**, 398 (1922).
(19) T. W. Case, "Thalofide cell—a new photoelectric substance," Phys. Rev. **15**, 289 (1920).

3. Foreign Equipment in World War II

(20) "Signal Corps Italian photophone," ISR No. 26, 14 pp., 1944 (P.B. 20316).
(21) W. S. Huxford, "Modulation of infrared sources for signaling purposes," Proc. Nat. Elec. Conference **2**, 158 (1946).
(22) D. Gifford, "German 'speech-on-light' signal system," Radio 32 (Nov. 1943).
(23) A. H. Nethercot, Jr. and W. S. Huxford, "Japanese light-beam telephone," OSRD 5763, Northwestern University Contract OEMsr-990, Aug. 1, 1945. See also "Light beam receiver" (P.B. 43889).
(24) A. H. Nethercot, Jr. and W. S. Huxford, "German Lichtsprecher 250/130," OSRD 6200, Northwestern University Contract OEMsr-990, Oct. 20, 1945. (P.B. 2612 and P.B. 16445.)
(25) C. V. Kent and W. L. Hole, "Report on German I-R speech communication apparatus, Li-80," Report 16.4 Special No. 1, University of Michigan Contract NDCrc-185, Sept. 11, 1943.
(26) "German optiphone Li.Spr. 80" (captured enemy equipment report No. 26, Camp Coles Signal Laboratory), 54 pp. (P.B. 1531).
(27) "Operation of Lichtsprecher-80 photo-phone equipment" (P.B. 1623).
(28) "German photophone Li.Spr. 80," Feb. 1943 (P.B. 19746).
(29) "German modulated light beam apparatus Li.Spr. 250/130," U. S. Army Signal Corps (P.B. 2336).
(30) Harvey E. White, "German Lichtsprecher 250 (made by Zeiss 1942)," NDRC Report 16.4—46 (P.B. 32711).
(31) Vacuum Tube Development Committee, "Infra-red research and development in Germany" (P.B. 52344).

4. American Developments in World War II

(32) N. C. Beese, "Cesium vapor lamps," J. Opt. Soc. Am. **36**, 555, 720A (1946).
(33) J. M. Frank, W. S. Huxford, and W. R. Wilson, "Modulation of the resonance lines in a cesium arc," Phys. Rev. **72**, 156 (1947); J. Opt. Soc. Am. **37**, 718 (1947).
(34) W. D. Buckingham and C. R. Deibert, "The concentrated-arc lamp," J. Opt. Soc. Am. **36**, 361A, 245 (1946).
(35) W. S. Huxford and John R. Platt, "Spectral and modulation characteristics of the concentrated-arc," J. Opt. Soc. Am. **36**, 361A (1946); **37**, 10 (1947).
(36) O. Mittelstaedt, "Die Bestimmung der Lichtgeschwinddigheit unter Verwendung des Elektrooptischen Kerreffektes," Physik. Zeits. **29**, 698 (1928); Ann. d. Physik **2**, 303 (1929).
(37) A. Roggendorf, "Investigation of the frequency dependence of gas-filled photo-cells in the region from 20 to 300 kilo-hertz," Physik. Zeits. **36**, 660 (1935).
(38) P. Debye and F. Sears, "Scattering of light by supersonic waves," Proc. Nat. Acad. Sci. **18**, 409 (1932).
(39) Alva W. Smith and Lewis M. Ewing, "Diffraction of light by supersonic waves in liquids . . .," Am. J. Phys. **8**, 57 (1940).
(40) R. J. Cashman, "New photo-conductive cells," J. Opt. Soc. Am. **36**, 356A (1946).
(41) R. J. Cashman, "Development of sensitive thallous sulfide photoconductive cells for detection of near infrared radiation," OSRD 1325, Northwestern University Contract OEMsr-235, March, 1943. Contains bibliography of over 170 references of which 25 relate to thallous sulfide and related cells (P.B. 27332).
(42) W. L. Hole and R. J. Cashman, "Thallous sulfide photoconductive cells, a summary of service characteristics," OSRD 1474, University of Michigan Contract NDCrc-185 and Northwestern University Contract OEMsr-235, March 10, 1943.
(43) R. J. Cashman, "Development of stable thallous sulfide photoconductive cells for detection of near infrared radiation," OSRD 5997, Northwestern University Contract OEMsr-235, October 31, 1945. Selected bibliography (P.B. 27354).
(44) C. W. Hewlett, J. J. Fitz Patrick, and H. T. Wrobel, "Thallous sulfide photoconductive cell," OSRD 5099, February 28, 1945. C. W. Hewlett, Gen. Elec. Rev. **50**, No. 4, 22 (1947).

(45) Ralph W. Engstrom and Alan M. Glover, "Development of methods for manufacturing the thalofide cell," OSRD 6003, Radio Corp. of Am. Contract OEMsr-1486, Oct. 31, 1945.

(46) A. von Hippel and others, "Research on thallous sulfide photoconductive cells," OSRD 4933, Massachusetts Institute of Technology Contract OEMsr-1036, April 1945.

(47) A. von Hippel, F. G. Chesley, H. S. Denmark, P. B. Ulin, and E. S. Rittner, "Photoelectric mechanism of the thallous sulfide photo-conductive cell," Phys. Rev. **69**, 685A (1946).

(48) von Hippel, Chesley, Denmark, Ulin, and Rittner, "Thallous sulfide photo-conductive cells. I. Experimental investigation," J. Chem. Phys. **14**, 355 (1946).

(49) A. von Hippel and E. S. Rittner, "Thallous sulfide photo-conductive cells. II. Theoretical discussion," J. Chem. Phys. **14**, 370 (1946).

(50) A. W. Ewald, W. L. Hole, and G. E. Uhlenbeck, "A theoretical approach to some fundamental properties of thallous sulfide photoconductive cells," OSRD 1474, University of Michigan Contract NDCrc-185, March 15, 1945.

(51) R. J. Cashman, "Development of sensitive lead sulfide photo-conductive cells," OSRD 5998, Northwestern University Contract OEMsr-235, Oct. 31, 1945.

(52) Charles L. Oxley, "Characteristics of cooled lead sulfide photo-conductive cells," J. Opt. Soc. Am. **36**, 356A (1946).

(53) A. von Hippel, J. H. Schulman, and E. S. Rittner, "A new electrolytic selenium photo-cell," J. App. Phys. **17**, 215 (1946).

(54) G. K. Teal, J. R. Fisher, and A. W. Treptow, "A new bridge photo-cell employing a photo-conductive effect in silicon," J. App. Phys. **17**, 879 (1946).

(55) O. S. Duffendack, "Wartime developments in the detection and measurement of thermal radiation," The Engineers' Digest **3**, 483 (1946).

(56) Blout, Amon, Shepherd, Thomas, West, and Land, "Near infra-red transmitting filters," J. Opt. Soc. Am. **36**, 361A, 460 (1946).

(57) Shenk, Hodge, Morris, Pickett, and Brode, "Filters for the visible and near infra-red regions," J. Opt. Soc. Am. **36**, 361A, 569 (1946).

(58) W. L. Hole, "A method for the computation of threshold range as affected by instrumental thresholds and atmospheric attenuation," OSRD 3345, University of Michigan Contract NDCrc-185, Feb. 5, 1944.

(59) Hartland S. Snyder and John R. Platt, "Theoretical aspects of optical communication systems," OSRD 6289, Northwestern University Contract OEMsr-990, Oct. 31, 1945.

(60) H. S. Snyder and J. R. Platt, "Principles of optical communication systems," J. Opt. Soc. Am. **38**, 269 (1947).

(61) R. F. Humphreys, W. W. Watson, and D. L. Woernley, "Ultrasonic modulation of a light beam," J. App. Phys. **18**, 845L (1947).

JOURNAL OF THE OPTICAL SOCIETY OF AMERICA VOLUME 38, NUMBER 3 MARCH, 1948

Principles of Optical Communication Systems*
General Properties of Non-Image Forming Projectors and Receivers

HARTLAND S. SNYDER** AND JOHN R. PLATT***
Northwestern University, Evanston, Illinois

(Received September 22, 1947)

The factors are discussed which determine the range of an optical communication system, such as: atmospheric transmission; source area, flux, brightness, modulation, and audio pass band; transmitter and receiver focal lengths, areas, and beam widths; and detector cell noise and area. Detector cell signal-to-noise ratio varies inversely as the square root of cell area in the ideal case. For non-image-forming systems, the Abbé sine condition is replaced by a useful rule of constancy of area times solid angle. A wide-angle system is a short-range system.

A general equation is given relating the range to these factors; it leads to a simple nomograph for estimating performance of a system. From laboratory measurements on components, the field range of a system may be predicted to an accuracy of $\pm\frac{1}{4}$ mile if the atmospheric transmission is known.

THE near infra-red optical voice and code communication systems surveyed in the preceding paper are now so numerous that it seems worth while to assemble in one place a list of the basic optical principles and limitations to which all such systems must necessarily conform.

Thus, the range of a system of this kind depends on the power and efficiency of the source, the responsivity of the detector, the beam angles, and the optical areas; and it depends most of all on the weather as it affects atmospheric attenuation. Knowledge of the relations between these variables is helpful in evaluating the components of a system or in predicting the over-all performance of an untested system.

First the simple range equation will be given, and then it will be shown how it can be re-expressed inserting various modulation factors and loss factors. Relations will be introduced between receiver cell noise, area, and angles of view. These will be accomodated in a revised range equation.

The relations are formally independent of wave-length, and therefore the usual photometric (visible light) symbols may be used.

THE RANGE EQUATION

The fundamental range equation is

$$R_v^2 = I(A/F), \qquad (1)$$

where R_v is the *vacuum range* of a system, or the maximum distance that the receiver could be separated from the transmitter and still obtain intelligible communication if *no* atmospheric attenuation were present (at night, unless otherwise noted); I is the maximum effective beam intensity (candlepower); A is the gathering area, or entrance pupil, of the receiver optical system; F is the effective "threshold flux" falling on the receiver which is required for just-intelligible communication. Both I and F must properly refer to root mean square a.c. measurements.

Equation (1) can be derived from the primary definition of intensity, I, as the flux, F, per unit solid angle, since A/R^2 is the solid angle subtended at the transmitter by the receiver. This equation must be modified to take account of losses, and it can be rewritten to express I and F in terms of other variables.

ATMOSPHERIC ATTENUATION

Transmission

In the visible and very near infra-red (NIR) out to about 1.3 microns, the most serious loss is the result of absorption and scattering by fog, smoke, and dust in the atmosphere. The absorption of two or three small bands of water vapor may be neglected. In this wave-length region, the transmission obeys Lambert's law to a good approximation; so that if T is the fraction of light transmitted through unit distance of atmosphere ($T<1.0$), then the fraction transmitted through

* Work performed in part under NDRC Section 16.4, Contract OEMsr-990 with Northwestern University.
** Now at the Brookhaven National Laboratory, Upton, New York.
*** Now at the University of Chicago, Chicago, Illinois.

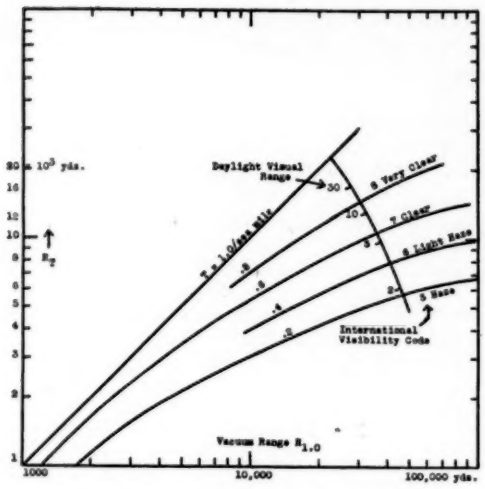

FIG. 1. Atmospheric transmission and range.
$R_{1.0}=R_v$ of text.
$R_T=R$ of text.
Daylight visual range in sea miles.

R units is T^R. The values of T for the visible and the N1R may be taken to be almost the same at any given time.

Operational Range

The measured limiting operational range, R, of communication in weather with transmission T may be much less than the vacuum range, R_v. The illumination, E, in an attenuated beam falls off as[1]

$$E=(I/R^2)T^R. \tag{2}$$

The threshold illumination on a receiver must be the same at R for transmission T as at R_v for transmission unity, or

$$(I/R^2)T^R=I/R_v^2$$

and

$$R^2T^{-R}=R_v^2. \tag{3}$$

The value of R as a function of R_v is plotted for several values of T in Fig. 1. In practice, R_v can either be computed from observed values of R and T, or it can be determined from measurements in the laboratory.

[1] W. L. Hole, "A method for the computation of threshold range as affected by instrumental thresholds and atmospheric attenuation," OSRD 3345, University of Michigan Contract NDCrc-185, Feb. 5, 1944.

Average Clear Weather

As R_v may be several times larger than actual ranges, it is convenient in comparing the performance of systems to specify another standard range, the range in average clear weather (ACW). Usually ACW is taken to refer to a transmission of 0.6 per sea mile. The phrase "0.6 per sea mile" is the accepted substitute for the awkward exact expression, "$0.6^{1/mi}$," which is necessary if T^R is to be dimensionless.

This value of T corresponds to a loss in signal power of 4.5 db per mile, in addition to the reduction by the inverse square law. For convenience, the sum of these two losses in ACW at distances of about 5 miles may be taken as roughly 6 db per mile. These are losses in signal output power in a receiver circuit. The output power is proportional to the square of the radiant power (flux) in the optical beam. The latter therefore decreases by 3 db per mile. Thus, a change by a factor of two in any of the variables determining range—beam intensity, detector responsivity, or receiver gathering area—changes the ACW range by about one mile.

In ACW the daylight visible range (defined below) is about seven sea miles, and the code number is 7, or "clear," in the International Visibility Code.[2]

While the ACW range is an easily interpreted index of the military performance of a system, it is not so satisfactory for laboratory or theoretical comparison of systems as the vacuum range. The ACW range involves arbitrary and not easily verified assumptions about attenuation at the wave-lengths used, and computing it requires troublesome logarithmic conversions and reconversions.[1] The vacuum range should be more widely adopted as a measure of communication system performance.

In order to compute R_v or the ACW range from measured operational ranges, the value of T during the operation must be known. This may be found either from estimates of daylight visible range or from instrumental determinations.

Daylight Visible Range

The daylight visible range, or limiting range at which large black objects can just be seen against

a white sky, is proportional to[2,3]

$$1/\log(1/T),$$

and varies more rapidly with T than does R. The visible range in good weather is greater than the range of a communication system—the visible range becoming infinite for transmission unity, when the communication range only becomes R_v. But in murky weather it may be less than the communication range. Similarly, the photographic penetration of haze is much better in the NIR than in the visible, while the increase in T in the NIR, to which this effect is due, is almost negligible from the point of view of optical communication ranges.

The relation of T to the visible range and to the index numbers used in the International Visibility Code is shown in Fig. 1.

From visibility estimates, values of T may be determined to an accuracy of about 0.1 per mile. Obviously, the daylight visible range can be used to determine T for a night operation only if the weather appears to remain almost unchanged in the interim. The visible range must not be confused with the night visual range (NVR) or range at which a filtered NIR transmitter can be detected by the dark-adapted eye.

Instrumental Determination of T

Several different instrumental methods, none of them very satisfactory, have been used to determine T. The transmission may be found from absolute measurement of the flux received on a photo-cell from a fixed radiation source at a fixed distance of several miles. Or the signal level of communication between a shore station and a moving ship may be plotted against the distance, and the transmission computed from Eq. (2). A variation of the latter method is to use, not the signal level, but the brightness of the distant source compared to a weak calibrated local source, as observed in an optical telescope or electron telescope.

Besides the obvious experimental problems in such determinations, a fundamental difficulty is that the transmission over any path is continually changing. Sometimes "twinkle effects," apparently of refractive origin, are observed. Therefore, a consistent set of values is rare. The spread of instrumental determinations of T in the course of an hour's operations may be less than 0.1 per mile only under exceptionally favorable conditions.

[2] E. O. Hulburt, J. Opt. Soc. Am. **31**, 472 (1941); **36**, 484 (1946).
[3] H. G. Houghton, J. Ae. Sci. **6**, 408 (1939).

TRANSMITTER FACTORS

Modulation

The root mean square variation of flux obtainable from the light source is one of the main parameters determining the usefulness of the source for communication work. This variation is some fraction, z, of the mean flux from the unmodulated source. (In order to make this definition applicable fairly to all kinds of modulation schemes, the "unmodulated source" flux should be measured with the modulating device removed, in cases where the latter is external to the source and obstructs part of the beam.)

Attainable values of z differ considerably for various modulation methods and for various types of sources. In an ideal source permitting modulation from a trough of zero light to a crest of twice the d.c. flux, z would be 0.7 for a sine wave tone of maximum modulation. For a voice signal, because of the variations of intensity in speech, the r.m.s. a.c. signal may be only half of this value, or less, depending on the transmitter circuits.

Pass Band

Maximum voice communication range demands not only maximum modulation of the source light, but also a suitable choice of modulation frequencies. If the strong low frequencies of the human voice are allowed to pass through the transmitter amplifier, they reach amplitudes of overmodulation and distortion while the high frequencies important for intelligibility are still very weak. By cutting out the low frequencies in the amplifier, more energy can be put into the intelligibility frequencies. If the cut-off, for example, is at 1000 c.p.s., 86 percent of the energy is removed, permitting an increase of 17 db in the modulation of high frequencies with a loss of only 7 percent in intelligibility.

Removal of the low frequencies of speech causes much of the naturalness and identifying

characteristics of the individual voice to be lost. For military applications, this is of little consequence.

The conclusions reached from research on optimum pass bands for voice intelligibility in military radio and sound-powered phones can be taken over almost unchanged to optical transmitters and receivers.

TRANSMITTER OPTICS

Narrow Beam Systems

Consider first a collimating transmitter with precision optical elements, focusing an image of the source at infinity. On looking back into such a system from the center of the beam at a great distance away, the exit pupil, A_t, is seen to be completely filled and of brightness about equal to the surface brightness, B, of the source. Then the effective r.m.s. a.c. intensity is

$$I=(e_t'tz)BA_t, \tag{4}$$

where e_t' takes account of the transmission and reflection losses in the optical elements, and t is the effective transmission of any filter in the beam.

The solid angle, Ω_t, into which the beam goes is given by

$$\Omega_t=a_s'/f^2, \tag{5}$$

where a_s' is the effective projected area of the source and f is the effective focal length of the lens or mirror projector.

High Efficiency

The "transmitter efficiency," e_t, may be defined as the fraction of the total flux, ϕ, from the source which goes into the transmitter beam. Then we can also write

$$I=(e_ttz)(\phi/\Omega_t), \tag{6}$$

which follows simply from the definition of intensity.

The efficiency can be increased by increasing the acceptance angle of the projection mirror or lens. Values of e_t in the vicinity of 0.5 and over may be obtained with suitably deep mirrors (focal length short compared to diameter).

In some communication systems the highest efficiency is desired. For these, e_t may be treated as almost constant, say about 0.5. The obtainable source flux and the desired transmitter beam angles then determine the intensity according to Eq. (6). This equation is of particular value with non-collimating systems, or with wide-angle systems, with or without beam-spreading devices.

For such systems, where Ω_t is not sharply defined, it is usually a good approximation to use in Eq. (6) an "effective solid angle" which is bounded by the directions in which the intensity falls to half the peak intensity (hpi).[4]

In other communication systems, it is high intensity which is desired, even at the sacrifice of efficiency. Equations 4 and 5 are more convenient for dealing with this case. For high efficiency systems, it is the modulable total flux, for high intensity systems the modulable surface brightness, which is important in choosing the source.

We see from Eq. (6) that, to obtain maximum intensity and communication range with minimum source power, the beam must be as narrow as possible for the desired purpose. For a given type of source, power, and optical efficiency, wide-angle systems are short-range systems.

Minimum Mirror Area

With high values of e_t, perfect collimation and the formation of a sharp image of a finite source at infinity are no longer possible. There is still a limitation on the beam solid angle, somewhat like Eq. (5), but in the more general case it is connected with the area of the projector mirror (exit pupil). This relation may be derived as follows.

Assume the source is sharply bounded by a convex surface of minimum area a_0 which can be shrunk around it, and that it emits from each element of this area according to the cosine law, with brightness B and total flux πBa_0. A fraction e_t of this flux appears in the projected beam, whose total flux is $\Omega_tB'A_t$, (assuming $\Omega_t \ll \pi$) but the emergent brightness B' cannot be greater than B, so that

$$A_t\Omega_t \geqslant e_ta_0\pi.$$

So, for a given mirror area and efficiency, the beam solid angle is necessarily greater than a

[4] Frank Benford, J. Opt. Soc. Am. **35**, 149 (1945) takes $\frac{1}{10}$ peak intensity as the boundary of the beam for theoretical purposes, but he is dealing with searchlights, which are more effective collimators than the wide-angle systems included in this discussion.

certain minimum. Conversely, for a specified solid angle to be produced, with a given efficiency, the mirror must be larger than a certain minimum,

$$A_t \geq e_t a_0(\pi/\Omega_t). \tag{7}$$

Since all the terms in this inequality except e_t have a wholly geometrical significance, the non-geometrical contributions to e_t, such as reflection and refraction losses, do not contribute to the inequality and should be ignored. In fact, if we replace e_t by a constant, the inequality sign may be replaced by an equality, to give a relation which will be approximately valid for comparing systems with similar aberrations. Such relations are most useful in dealing with gaseous discharge or volume sources of comparatively large surface area.

Inequality (7) indicates that if an attempt is made to put the flux from a large source into a small solid angle with good efficiency, the mirror size may become prohibitive. From this inequality, the rule for choosing the source for a given communication problem is: large source, wide angle; narrow angle, small source.

Laboratory Methods

Candlepower distributions may be measured by placing a source or a transmitter optical system, as the case may be, on a rotating table and determining the response of a fixed detector at some distance away as a function of angle. The distance away must be great enough that the angle subtended by the source at the detector is small compared to the hpi width.

The ratio between the maximum candlepowers, I from a transmitter system, and I_0 from its bare source alone (both a.c. or both d.c. measurements), is the transmitter optics factor, O_t.

$$I = I_0 O_t. \tag{6a}$$

The vacuum range R_v from a given transmitter to a given receiver may be determined in the laboratory by finding the maximum communication range from the bare source to this receiver and multiplying this value by $(O_t)^{\frac{1}{2}}$.

If the source is too intense to measure the bare source-receiver range directly in the laboratory space, it may be measured indirectly by reducing the source intensity by a known amount as follows.[5] A lens or mirror is set up so as to form a reduced image of the source, and so that the receiver can "see" only this image. The intensity from this image is less than the intensity of the source by a factor p^2/q^2, where p and q are the object and image distances from the lens or mirror. The communication range from the image to the receiver is thus less by a factor p/q than the range from the bare source itself.

TABLE I. Mirror area, beam width, and optics factor.

Source area	Mirror	Experimental values θ_t	Ω_t	O_t	Predicted values θ_t	Ω_t	O_t
3 sq. in.	diam. = 14″ $f = 1\frac{1}{2}$″	13°	0.040	40	—	—	—
1.6 sq. in.	diam. = $7\frac{1}{2}$″ $f = \frac{3}{4}$″	16°	0.061	18	18°	0.080	20

From Eqs. (6) and (6a), O_t is evidently inversely proportional to Ω_t. From Eq. (7), moreover, Ω_t varies with a_0/A_t; for beams of similar cross-sectional distribution, the beam diameter, θ_t, then varies with $(a_0/A_t)^{\frac{1}{2}}$. An approximate verification of these relations experimentally is shown for two transmitters in Table I. The sources are tubular sources, mounted axially in the mirrors. The angles indicated are hpi values. On the basis of the rules just noted, the properties of the second system are predicted from those of the first. The agreement with experiment is fair.

Choice of Filter

Commonly, a maximum permissible night visual range (NVR) is specified in the requirements for a military optical communication system. The NVR is defined as the visual range limit of a transmitter to the dark-adapted standard eye in total darkness. It is determined by the spectral distribution of the source, the transmitter candlepower, and the spectral transmission of any filter placed in the beam.

The specified NVR should be made as great as is militarily feasible, because the larger the NVR is allowed to be, the greater the operational range can be for a given transmitter system. This results from the fact that for any filter the percentage absorptions at different wave-lengths all increase or decrease together as the filter thickness or dye concentration is changed.

[5] A. H. Nethercot, Jr. and W. S. Huxford, "Japanese light-beam telephone," OSRD 5763, Northwestern University Contract OEMsr-990, August 1, 1945.

TABLE II. Variation of N and S/N with area in Cashman TF cells.

Projected grid size	Grid area	Noise		S/N	
		Exp.	Theor.	Exp.	Theor.
$\frac{1}{4}\times\frac{1}{4}$ in.	0.062 in.^{2}	21 db	24 db	68 db	68 db
$\frac{3}{4}\times\frac{3}{4}$ in.	0.620	14	—	58	—
$1\frac{1}{2}\times 2\frac{1}{8}$	3.950	8.5	6	56	50

The filter type chosen should then be one which will make as great a differential as practicable—that is, subject to considerations of its weathering properties and thermal and mechanical stability—between the transmission of the communication wave-lengths and the visible wave-lengths. This means it must have a high "index of merit," giving large communication range, R_v, but relatively small visual range, NVR.

Once the NVR has been specified and the filter type chosen, the optical density of the filter used must be chosen so as to bring the NVR right up to the limit specified, so as to make the communication range as great as possible.

The NVR for a given transmitter may be determined by computations from the spectral curves of the source and filter and standard eye; or it may be determined for actual observers in the laboratory, reducing the transmitter intensity by a known amount as described above under *Laboratory Methods* so that the test may be accomodated in a limited laboratory space.

RECEIVER FACTORS

The contribution of the receiver to the range is represented by the term A/F in Eq. (1).

Cell Noise as a Function of Area

To arrive at conclusions about F in this term, we must first examine the inherent noise from photo-detectors and its dependence on other variables.

If two detector cells, one large and one small, are made by identical processes, the larger one will have a smaller signal-to-noise ratio S/N, for the same incident light flux. To prove this, we shall consider photo-emissive tubes and photo-conductive cells separately.

For a photo-emissive tube, the signal output voltage, S, is proportional to the photo-current, which is proportional to the incident flux. The signal is independent of the cell area except as different manufacturing processes are used for cells of different area.

The irreducible minimum noise voltage, N, which comes from the tube itself and is not generated in the load resistor or elsewhere in the amplifier, is shot noise. This varies as the square root of the dark current,[6] which in turn is proportional to the cell area, if the manufacturing process is constant. The basic noise then is proportional to the square root of cell area; and the signal-to-noise ratio S/N, for a given flux, varies inversely with the square root of cell area.

It is convenient to refer to the luminous equivalent of noise, which is the flux required to make $S/N=1$; this evidently varies directly as the square root of cell area.

The end result is the same for photo-conductive cells, but the actual variation of signal and noise is different. The derivation is simple if we consider two photo-conductive cells in parallel having the same sensitivity, the same noise, N_1, and the same resistance, R_1. When they are in parallel, each cell is shunted by an equal resistance, and its noise output is therefore halved, to $N_1/2$. The two noise outputs add at random, so we must take the square root of the sum of the squares, giving a total noise for the pair of $N/(2)^{\frac{1}{2}}$. Evidently the noise varies inversely as the square root of the area.

Similarly, the signal output S, for flux falling on one cell alone, will be cut in half when the two are in parallel because of the shunt, and the output signal will be $S/2$. So the signal varies inversely as the area.

The S/N ratio for constant flux therefore again varies inversely, and the luminous equivalent of noise directly, as the square root of the area.

The validity of this law for photo-conductive cells is illustrated in Table II which gives average values of S/N for constant modulated flux, and N for a group of Cashman TF cells of different

[6] For vacuum photo-tubes, gas-filled photo-tubes, and multiplier photo-tubes, the exact expression for the mean square of the output noise current, n, is given by: $n^2=2kei\mu\Delta f$, where μ is the multiplication or gas amplification factor of the tube, e is the charge on an electron, i is the cathode current, Δf is the frequency pass band, and k is a numerical constant. For a vacuum photo-tube $k=1$. For gas-filled photo-tubes and photo-multipliers, k is greater than 1 (and about equal to 2), because of randomness in the multiplication processes in these tubes.

sizes.[7] The theoretical values are computed for the extreme sizes from the above laws, with the data on the middle group used as a base line. The discrepancies are probably due to variations in the methods of the manufacturing of the different cell types.

The noise in both photo-conductive and photo-emissive cells is proportional to the square root of the pass-band width, Δf, provided the pass band is not too wide.

Threshold Flux

We may now return to the question of the threshold flux F in the voice communication system. Its value depends on the spectral distribution of the radiation and on the spectral response of the detector cell, among other things. Thus, if all other factors are equal, the type of cell chosen must be that giving a maximum S/N ratio for the given spectral distribution and for the given audio or radiofrequency distribution of the modulated radiation from the filtered source. What the best source or filter is also depends on the cell; actually, no one of them should be chosen independently, but all combinations should be studied to find the best for a particular problem.

In addition, the value of F depends on what fraction, e_r, of the flux falling on the receiver entrance pupil actually reaches the photo-detector cell. We may call this fraction the receiver optical efficiency.

However, the big factor in determining threshold flux is the limitation of intelligibility by the noise in the cell and circuit, as just discussed. With NIR photo-detectors, the circuit noise can be reduced so that the inherent cell noise predominates; this is then a function of cell type, cell area, and receiver band width, as explained above. The r.m.s. threshold voice signal is usually larger than the r.m.s. sine-wave luminous equivalent of noise. The exact ratio is a question of the intelligibility of the signal in the presence of the noise and depends on whether the communication is code or voice, on the frequency behavior of the source and detector cell, and the circuits. In laboratory practice, it is usually convenient to determine this ratio once on the system being studied and, thereafter, to make all comparative measurements with some standard code tone for which the luminous equivalent of noise can be reproducibly determined.

This ratio of the threshold to the luminous equivalent may be combined with other constants into a constant, k. Then we finally have

$$F = (k/e_r)[(a\Delta f)^{\frac{1}{2}}]. \tag{8}$$

This flux must be made as small as possible in order to obtain maximum range.

Band Width

One way to make F small is to decrease Δf. For carrier-wave code reception, it may be decreased until the tuned receiver circuit is almost set into self-oscillation.

For voice, when Δf decreases, the S/N ratio required for intelligibility increases, causing an increase in the constant k. The rate of increase of k depends on the shape of the frequency-response curve. Studies on various telephone systems have indicated a minimum of $k[(\Delta f)^{\frac{1}{2}}]$ for a peak response near 1500 c.p.s. with a band width (6 db down) of about 700 c.p.s.

RECEIVER OPTICS

Cell Area and Solid Angle of View

Another way to make F small is to decrease the effective cell area a. With a given optical system this involves a proportional decrease in the solid angle of view, Ω_r. The angle Ω_r will be taken as bounded by the directions in which the receiver response falls to half the peak response (hpr).

If a given hpr receiver solid angle is specified, it may be obtained with a smaller and smaller cell area (and consequently higher and higher sensitivity) by decreasing the focal length of the receiver lens or reflector, up to a certain point. The limiting cell area is given by the relation

$$a \geq e_r(\Omega_r/\pi)A. \tag{9}$$

This inequality is proved by an argument the inverse of that which led to Eq. (7). Again, since all the terms except e_r are geometrical, the non-geometrical parts of e_r, such as reflection and refraction losses, do not contribute to the inequality and should be ignored. With a good

[7] R. J. Cashman, J. Opt. Soc. Am. **36**, 356A (1946); from data cleared for oral presentation in that paper and reprinted here by courtesy of Dr. Cashman.

TABLE III. Proportionality of effective cell area to field of view.

Cell	Effective area	Mirror	Mounting of cell	Field of view	Ratio of fields	Ratio of areas
TF $1\frac{1}{4}\times2\frac{1}{4}$	6 in.²	diam. 14" $f=1\frac{1}{4}$"	axial	circular 18° wide $\Omega=.078$	5.6	7
photo-tube $\frac{5}{8}\times1\frac{1}{4}$"	0.9in.²	diam. 14" $f=6$"	transverse facing mirror	rectang. 5°×9° $\Omega=.014$		

mirror, the geometrical part of e_r can be made almost unity. Off-axis aberrations then may lead to a minimum value of a some 50 percent or more larger than the right-hand side of (9), for a field of view a few degrees wide.

Again, we may insert a correction factor to convert (9) to an equality which will be useful for comparing systems with similar aberrations. Also (9) may be restated: for a given cell size and mirror size, the solid angle of view must be less than some upper limit; or, for a given cell size and solid angle of view, the mirror size must be less than some upper limit. Both these statements are true only if the efficiency is near unity. It is, of course, easy to design crude mirrors which are absurdly large because most of the light misses the cell at all times, or for which the solid angle of view is large for the same reason.

If light is concentrated on both sides of a cell which is photosensitive on both sides, inequality (9) holds for each side. To include this case, (9) can be left unchanged if for area a we use an effective area which includes both surfaces. This effective area is approximately the area of the closed surface of smallest area through which light can reach the photosensitive surface, if such a minimal surface can be defined. From (9) then, a detector of this type can have approximately twice the solid angle of view of the same size one-surface cell, for the same effective mirror area.

The proportionality between total effective cell area and solid angle of view indicated by (9) for constant mirror area is borne out in Table III, which is a tabulation of data on two radically different receiver arrangements. The Cashman TF cell used is a two-surface cell. It is seen that the ratio of fields compares astonishingly well with the ratio of cell areas, considering the great differences in the image-forming properties of the two arrangements.

We may obtain another useful inequality by combining Eq. (9) with Eq. (5), which is also valid for an image-forming receiver system if the subscripts are suitably changed. Remembering that $A=\pi d^2/4$, we obtain a minimum ratio f/d of 0.5; that is to say, no *image-forming* receiver system (or transmitter system, for that matter) can have an f/number smaller than this value. This rule is derived for the condition that the mirror forms its own entrance pupil.

Again, if the mirror forms a poor image, e_r is less than unity, and a larger area of mirror than indicated by $f/0.5$ may contribute light to the cell within the desired solid angle.

The minimum cell area of (9) is indeed reached with an f/number of about $f/0.5$ for a one-surface detector. F/numbers down to about $f/0.1$ may be used with two-surface detectors if they are mounted with their sensitive surfaces parallel to the axis of a reflector. Mirrors are required in order to attain either of these f/numbers.

Summing up the relations between sensitivity, cell area, and angle of view, we may say: the smaller the angle of view specified for the receiver, the higher the sensitivity of the detector cell which may be used. This parallels the relation for transmitters between beam angle and intensity, and leads again to the conclusion that a wide-angle system is a short-range system.

However, it is less important to have a small solid angle at the receiver than at the transmitter, since the best receiver sensitivity is inversely proportional only to the square root of the solid angle of view (Eqs. (8) and (9)), while the transmitter intensity is inversely proportional to the beam solid angle itself.

Laboratory Methods

The "directivity pattern" of receiver response as a function of direction may be determined in the laboratory by placing the receiver on a rotating table to detect a weak source some distance away. The hpr angle of view may be found from this pattern.

If the photo-detector and associated circuits are linear, the ratio of the maximum response of the cell in the optical system in a uniformly

illuminated field to the maximum response of the cell alone (or "bare") is called the receiver optics factor, O_r. In cells uniformly sensitive over their surface, O_r is equal to $e_r A/a'$, where a' is the projected area of the cell. A bare cell may be used for laboratory range measurements, and the range so obtained multiplied by $(O_r)^{\frac{1}{4}}$ to give the range for the assembled receiver optical system.

Backscatter

One practical limitation on receiver sensitivity in a two-way communication system is commonly the noise produced by radiation from the adjacent transmitter beam, scattered back into the receiver by nearby objects or just by atmospheric haze. The backscatter from nearby objects may be avoided by proper location of the system.

As would be expected, the noise from atmospheric scatter is large when the hpi and hpr angles are large, and also when the transmitter and receiver are close together, as they usually are.

Backscatter in wide-angle systems having the transmitter and receiver in one transceiver head may make "duplex operation" impossible. In duplex, transmitter and receiver are continuously ready to operate, permitting great naturalness of conversation. But if the transmitter feeds back optically into the receiver, it may drown out the distant station. "Send-receive operation" must then be used, with the transmitter and receiver energized alternately, as with a press-to-talk button. The transmitter line must be filtered from any modulation or ripple when the system is in the receive condition. If photo-current noise from the remaining steady backscattered radiation is still serious, the transmitter intensity must be reduced or turned off altogether—either electrically or by a mechanical shutter—during reception, in order to achieve threshold sensitivity.

Daylight Operation

The noise produced by steady backscatter is trivial compared with that produced in most photo-detectors by daylight. The operational ranges of NIR systems in daylight may consequently be much decreased from night ranges. Ultraviolet systems are not so much affected, as they can be filtered to receive only below 2900A, where almost no sunlight comes through the ozone layer in the atmosphere.

In vacuum and gas-filled photo-tubes and photo-multipliers, the noise increases as the square root of the d.c. current. With vacuum photo-tubes, this current is proportional to the total steady flux received, which is proportional to the product of Ω_r and A, for a uniformly bright field of view. For photo-conductive cells, the expression for the change produced by background light is less simple. (It seems that the lead sulfide photo-conductive cells used in the Zeiss Lichtsprechers[8] are very little affected by steady background light.)

With detectors sensitive to background radiation, very narrow-angle receivers are evidently better to use in daylight than wide-angle re-

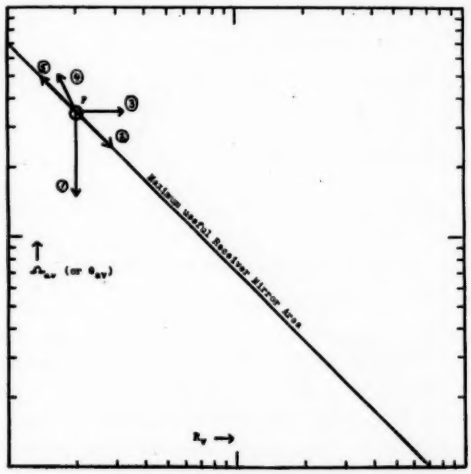

FIG. 2. Range-angle nomograph example. Arrows through point P show effect of increasing single factors by a factor of 2:

1. Receiver focal length: (area constant)	$\Omega_{sv} \div 2$
2. Receiver mirror area: (shape constant)	$\Omega_{sv} \div \sqrt{2}$ $R_v \times \sqrt{2}$
3. Receiver mirror area: (f constant) Sensitivity: Modulated source flux:	$R_v \times \sqrt{2}$
4. Cell area:	$\Omega_{sv} \times \sqrt{2}$ $R_v \div \sqrt[4]{2}$
5. Transmitter solid angle:	$\Omega_{sv} \times \sqrt{2}$ $R_v \div \sqrt{2}$

[8] A. H. Nethercot, Jr. and W. S. Huxford, "German Lichtsprecher 250/130," OSRD 6200, Northwestern University Contract OEMsr-990, Oct. 20, 1945 [PB 2612 and 16,445, *Bibliography of Scientific and Industrial Reports*, U. S. Dept. of Commerce]; R. J. Cashman, J. Opt. Soc. Am. **36**, 356A (1946); Charles L. Oxley, *ibid.*

ceivers. The Lichtsprechers, which have hpr angles of $\frac{1}{4}$ degree *and* lead sulfide cells, seem to have *no* loss of range in daylight. The Japanese light beam telephone[5] has an iris diaphragm over the receiver cell to give a large angle at night and a small angle in the daytime.

This Japanese system showed changes of about 20 percent between the night and day vacuum ranges with the narrow angle opening, but the cells used had very high inherent noise, which would reduce the apparent size of the background effect.

The effect of direct sunlight falling on receivers is not known. An NIR filter and a sunshade over the receiver may be used to reduce background light and improve daylight communication; the filter produces very little additional loss in the already filtered transmitter beam.

REVISED RANGE EQUATION

Combining Eqs. (1), (6), (8), and (9), we have for the limiting vacuum range of a system,

$$R_v^2 = (e_t e_r / k\Delta f) hz(\phi A / \Omega_t (a)^{\frac{1}{2}}), \quad (10a)$$

or

$$R_v^2 = (e_t e_r \sqrt{\pi} / k'\Delta f) hz(\phi \sqrt{A} / \Omega_t \Omega_r), \quad (10b)$$

or

$$R_v^2 = (e_t e_r \pi / k''\Delta f) hz(\phi \sqrt{a} / \Omega_t \Omega_r). \quad (10c)$$

The change from k to k' and k'' in Eqs. (10b) and (10c) respectively, is introduced to take account of the deviation of actual systems from the ideal limit case given by Eq. (9). These constants also include certain geometry factors involving changes from minimal cell surface area to projected area, which depend on the shape of the detector cell. The values of a, A, and Ω_r to be inserted in Eq. (10) are the limiting high efficiency values as discussed for Eq. (9).

Equations (10b) and (10c) are generally the most useful in designing a communication system, since they involve the solid angles explicitly. The last equation has the further advantage that it involves the detector cell area explicitly, and this quantity may be fixed by commercial availability for cells of a given type.

Equation (10b) shows that the vacuum range, R_v, varies as $\sqrt[4]{A}$ if the angles of view are kept constant. This contradicts assertions made in the early literature that R_v is independent of A_r with constant angles; such a conclusion is the result of the neglect of cell noise-area relationships.

All systems having a given type and power of sources and a given type and size of detector cell may be represented by points on a single straight line such as that on the nomograph shown in Fig. 2. The diagram is based on Eq. (10c). When the quantities just mentioned are fixed, this equation becomes

$$R_v \Omega_{av} = \text{constant}, \quad (11)$$

where Ω_{av} is the geometric mean of Ω_t and Ω_r. A log-log plot of R_v against Ω_{av} is then a straight line of slope -1. For convenience, Figs. 1 and 2 can be combined, so that the operational range R for any value of T can be read off at the same time. A scale parallel to Ω_{av} can be affixed to read θ_{av}, a sort of mean beam diameter. If $\Omega_{av} = \Omega_r$ the line of the plot can be marked at intervals to indicate maximum useful receiver mirror area (or diameter) based on Eq. (9), since this quantity is a function of Ω_r.

Several arrows are drawn through a point, P, which represents a system on the straight line in Fig. 2. These arrows show the amount and direction of change of range and Ω_{av} when only one component of the system is changed at a time. The change corresponding to each arrow is indicated in the legend. Thus, to illustrate, an increase in cell area by a factor of 2 causes the point representing a given system to move parallel to the arrow (4): the vacuum range of the system decreases by a factor $\sqrt[4]{2}$, and the average solid angle, Ω_{av}, of the whole system increases by a factor $\sqrt{2}$.

From laboratory measurements on the components of a system and from measurements on the atmospheric transmission at the time of a field operation, it has been found possible to compute, from the equations given here, the limit operational range of a communication system consistently to an accuracy of about $\pm\frac{1}{4}$ mile.

JOURNAL OF THE OPTICAL SOCIETY OF AMERICA VOLUME 38, NUMBER 3 MARCH, 1948

Some Spectral Characteristics of Mercury Arcs for Use in Study of the Raman Effect*

D. H. RANK AND J. S. MCCARTNEY
Physics Department, Pennsylvania State College, State College, Pennsylvania

(Received September 29, 1947)

Several types of commercial Hg arcs and low pressure arcs were investigated with regard to the continuous background in the λ4358 region. The background intensity measurements were made relative to the λ4358 line making use of the Rowland grating ghosts, using a photoelectric spectrograph.

It was found that the relative intensity of the λ4358 group of lines in the Hg spectrum varies almost an order of magnitude with the different vapor pressures used in the various sources.

An intense photograph of the Raman spectrum of CS_2 has been obtained in which ν_3, $\Delta\nu \sim 1520$ cm^{-1} appears. This line is forbidden for a linear molecule and is only about 1/1000 the intensity of the strongest line in the spectrum.

IT has long been recognized that the ideal source of excitation for the production of Raman spectra would be an intense, monochromatic radiation associated with a background of zero intensity. With the above-mentioned type of source, very weak Raman lines could be observed without introducing any doubt concerning their frequency assignement.

The purpose of this investigation was to examine the relative merits of various sources of Hg radiation in use in this laboratory. The region of the spectrum in the neighborhood of λ4358 was the region studied with regard to suitability for the Raman effect. In addition, the fine structure of λ4047, λ4078 and λ4358 was examined to ascertain the suitability of some of these sources for use in investigation of the Brillouin effect. The sources studied were:

(*a*) Westinghouse H-1 lamp operated under normal voltage conditions from a Westinghouse vapor lamp transformer, style 888803. Lamp was operated at 400 watts.

(*b*) Westinghouse H-1 lamp operated at 530 watts.

(*c*) Westinghouse H-11 lamp operated at 75 watts from a standard transformer.

(*d*) Low pressure Hg arc of 20 cm length and 4 cm diameter operated in a vertical position. These arcs have two mercury pool electrodes. They are operated on the vacuum system with air blast cooling of the cathode end. The operating conditions were: (1) 5.0 amperes, 110 watts, (2) 7.2 amperes, 150 watts, (3) 11.1 amperes, 260 watts.

(*e*) Low pressure Hg arc of 70 cm length and 4 cm diameter operating at a current of ten amperes in a horizontal position with air cooling of both anode and cathode sections.

The intensity measurements for this investigation were made with the photoelectric spectrograph described by Rank and Wiegand.[1] Direct light from the arc under investigation was introduced into the optical system of the spectrograph by scattering from white paper. The spectral region to be studied was scanned at the low speed of the instrument. This spectrograph produces a record of intensities on a linear scale by means of a photographic trace of the galva-

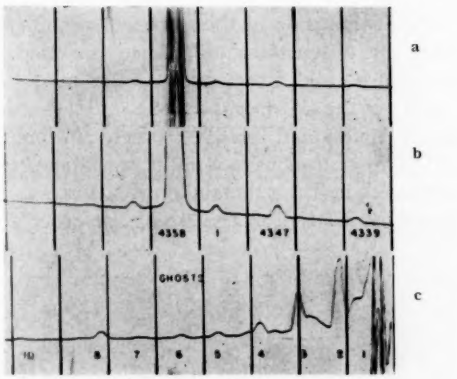

FIG. 1. Photoelectric recordings of the λ4358 triplet of the Hg arc spectrum with different amplifications. The bottom recording shows the Rowland ghosts of the grating. The numbers 1, 2, 3, etc., refer to the order of the Rowland ghost.

* This research was carried out on Contract N6Onr-269, Task V of the Office of Naval Research.

[1] D. H. Rank and R. V. Wiegand, J. Opt. Soc. Am. **36**, 325 (1946).

TABLE I.

Order of ghost	Relative intensity
1st	1/200
2nd	1/1000
3rd	1/1700
4th	1/5700
5th	1/16000
6th	1/20000
7th	1/50000
8th	1/8000

TABLE II. The measurements for background have been reduced to the basis of using an entrance and exit slit width of 1 angstrom unit effective width. λ4358 is considered to have an intensity of 1.

Source	Background $\times 10^5$ λ4420	λ4392	λ4369
(*a*) H-1 400 watts	53	94	640
(*b*) H-1 530 watts	78	150	1000
(*c*) H-11 75 watts	6.3	11.7	34
(*d*) Low pressure lamp 110 watts	4.8	9.6	31
Low pressure lamp 150 watts	5.8	10.0	30
Low pressure lamp 260 watts	6.1	11.1	33

nometer deflections obtained from the amplified photoelectric tube currents.

In order to measure the relative intensity of the background radiation and the variation of the "4358 triplet" in the various sources, use was made of the Rowland ghosts of the grating. This procedure was necessitated by inability to maintain constant intensity on the slit when shifting from one source to the other. It also avoids calibration of the electrical circuits when radically different amplifications are used. The procedure used in measuring the relative intensity of the ghosts was as follows. The strongest ghost is measured relative to the main line (Fig. 1a). The gain of the amplifier was then greatly increased, and the remainder of the ghosts were measured relative to the strong 1st order ghost,

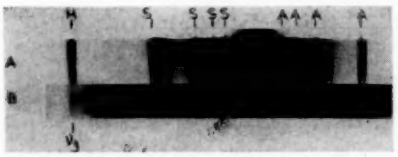

FIG. 2. *A* is a reproduction of the Raman spectrum of CCl_4 obtained by means of excitation with a low pressure arc. *S* and *A* refer respectively to Stokes and anti-Stokes lines. *H* is the harmonic of the 760–790 frequency. *B*, is a reproduction of the Raman spectrum of CS_2 showing ν_3. The remainder of the spectrum is almost completely blotted out by overexposure.

TABLE III.

Source	Intensity λ4358	λ4349	λ4339
(*a*) H-1 400 watts	1	1/22	1/62
(*b*) H-1 530 watts	1	1/17	1/49
(*c*) H-11 Normal	1	1/54	1/136
(*d*) Low pressure lamp 110 watts	1	1/123	1/340
Low pressure lamp 150 watts	1	1/90	1/240
Low pressure lamp 260 watts	1	1/44	1/125
(*e*) 70 cm low pressure arc	1	1/130	1/350

(Fig. 1c). Relative intensities of the ghosts compared to the main line are given in Table I.

The method employed to make background measurements was to adjust the electrical gain of the photoelectric spectrograph so that selected ghosts produced the same deflection with the different sources tested. Thus the measurements of the intensity of the continuum could be directly intercompared. The results of these comparative measurements are given in Table II.

The results of measurement of the relative intensity of the Hg triplet 4358, 4347 and 4339 are given in Table III.

DISCUSSION OF SOURCES

The choice of source will not depend solely on the characteristics given in Table I and Table III. Although the H-11 lamps compare very favorably with arcs under (*d*) operated at high current, they have several disadvantages for certain types of work. The H-11 lamps, because of their smaller size, have a much smaller total flux output than (*d*). The H-11 lamps are not vacuum arcs in that a carrier gas is present in them primarily for starting purposes. These "impurities" would be very obnoxious when it is hoped to photograph very weak lines. The spectral characteristics of these lamps will vary widely with the amount of Hg which is introduced in them in manufacture since all the Hg is vaporized in the lamp and the pressure will be proportional to the amount of Hg present.

H-1 lamps are very bad with regard to their spectral characteristics since they have a high background and a particularly high background associated with the λ4358 line itself. In addition, the lines are very broad. The use of these lamps must be limited to work in which large amounts of flux are needed in conjunction with a high degree of intensity stability for long periods of

time. Arcs under (*c*), (*d*) and (*e*) all show beautiful hyperfine structure patterns for the Hg lines.

The results of the above work show that the continuous background in the Hg arcs investigated is dependent on the gross Hg vapor pressure. The intensity ratio of the λ4358 triplet seems to depend on the temperature and pressure conditions at both electrodes since an arc with both electrode sections cooled gives a much higher triplet ratio than when only one is cooled at approximately the same currents.

B, in Fig. 2, is a reproduction of the Raman spectrum of CS_2 showing ν_3 which is less than 1/1000 the intensity of the strong lines in this spectrum. ν_3 was found to measure 1520 cm^{-1} shift from the exciting line.

JOURNAL OF THE OPTICAL SOCIETY OF AMERICA VOLUME 38, NUMBER 3 MARCH, 1948

Determination of the Depolarization Factors of Highly Polarized Raman Lines*

A. E. Douglas and D. H. Rank
Physics Department of the Pennsylvania State College, State College, Pa.

(Received September 29, 1947)

The errors arising in the measurement of the depolarization factor of highly polarized Raman lines are discussed. Particular attention is given to the error introduced by the convergence of the incident light. It is shown that the ratio of the intensity of the parallel component of the scattered light when incident light is polarized along the direction of observation of the sample to the intensity of the parallel component when the incident light is polarized perpendicular to this, gives a value of the depolarization factor ρ_s that is very nearly free from convergence errors. ρ_s is related to the depolarization factor in unpolarized light ρ_n by $\rho_n = 2\rho_s/(1+\rho_s)$. Using this method, the depolarization factors of some highly polarized lines have been measured with a photoelectric spectrograph. They were found to be considerably below previously accepted values. The depolarization factor ρ_n for the most highly polarized lines of carbon tetrachloride and benzene were found to be 0.013 and 0.038, respectively. It is shown that the depolarization factor is not constant across the width of the line for many Raman lines.

IT is well recognized that great difficulties are encountered in precisely measuring the depolarization factors of Raman lines.[1] Many observers have measured the depolarization factors for the Raman lines of most of the common liquids. The results of the depolarization measurements made by different observers are summarized for several of the most common liquids by Kohlrausch in his book *Ramanspektren*.[2] Agreement between results obtained by different investigators for highly depolarized lines is, in general, quite satisfactory. However, in the case of highly polarized lines, the agreement leaves much to be desired.

The errors involved in the measurement fall into two categories. First, there are those errors produced by non-ideal excitation and observation of the Raman line and, secondly, there are the errors in actually measuring the light intensity. By the use of a photoelectric recording spectrograph, the latter error may be reduced to a very low value. The first type of error is a combination of many factors but of these non-parallelism of the exciting light is by far the most serious. This convergence error is difficult to eliminate since parallelism of the exciting light can be achieved only by reducing the incident flux on the sample. Since Raman spectra are weak at best, it is not possible to sacrifice much of the incident light. It seems desirable, therefore, to consider how accurate measurements of the depolarization factor can be made, using incident light with some degree of convergence.

The convergence errors arising in the measurement of the depolarization factor of Rayleigh scattering have been discussed by many authors.

* This research was carried out on contract N60nr-269 Task V of the office of Naval Research.

[1] J. Cabannes, Ann. d. Physik. **19**, 233 (1933).

[2] K. W. F. Kohlrausch, *Ramanspektren* (Leipzig, 1943) pp. 153, 359.

TABLE I.

Type of excitation	Intensity of S_0 light	Intensity of P_0 light	Observed depolarization	
I_s	$C+Af(\theta)$	A	$\rho_{s_0}=\rho_s+f(\theta)$	(9)
I_p	$C+Af'(\alpha)$	B	$\rho_{p_0}=1+(f'(\alpha)/\rho_p)$	(10)
unpolarized	$2C+Af(\theta)+Af'(\alpha)$	$A+B$	$\rho_{n_0}=\rho_n+f(\theta)+f'(\alpha)$	(11)

The results have been summarized in Bhagavantam's book.[3] Since there can be no question regarding the random nature of Raman scattering, the problem here is somewhat less complex. In the following section, the problem of depolarization measurement will be reconsidered from a simple point of view. Though the results obtained by us are essentially the same as those arrived at by Gans[4] and others, it is believed that this discussion will illustrate more clearly the nature of the errors and a method of eliminating them.

In this discussion, the following notation will be used. The plane of polarization is defined as the plane of the electric vector. The scattering sample will be considered as being in a tube which has its axis along the Z axis of a rectangular coordinate system. The incident light will be considered as approaching the sample along the X axis. The sample is observed along the Z axis. The intensity of the incident light polarized in the XY plane will be denoted by I_s and that polarized in the XZ plane by I_p. The intensity of the scattered light polarized in the XZ plane will be denoted by S and that in the YZ plane by P. The depolarization factors are by definition:

$$\rho_n = S/P \text{ with unpolarized incident light} \quad (1)$$

$$\rho_s = S/P \text{ with polarized incident light } I_s \quad (2)$$

$$\rho_p = S/P \text{ with polarized incident light } I_p. \quad (3)$$

It will be assumed that the only effect of the incident light is that its electric vector E produces three mutually perpendicular oscillating dipoles a, b, and c in each element of volume of the liquid. These hypothetical dipoles oscillate at the frequency of the Raman line under consideration. They represent the integrated effect of the actual radiating molecules, integrated over a large number of molecules with random orientation. The nature of the molecules and the integration need not be considered here. a, b, and c represent the squares of the dipole strength. Therefore, the light intensities emitted by each element of the liquid are directly proportional to the magnitude of a, b and c. The integrated effect of the dipoles a, b, and c over the whole sample can be represented by three equivalent dipoles A, B, and C.

These dipoles are oriented so that a is in the direction of E; b is at right angles to E and to the direction of propagation of the incident light, and c is at right angles to E but along the direction of propagation of the incident light. It will be assumed that b is equal to c as should be expected if the molecules have a random orientation and the scattering is purely electric dipole scattering. For a highly polarized line $a \gg b$.

Each of the dipoles will radiate light with the usual directional pattern for a radiating dipole. That is

$$I_\gamma = I_0 \sin^2\gamma, \quad (4)$$

where I_0 is the light intensity radiated perpendicular to the axis of the dipole; I_γ is the light intensity radiated at an angle γ and γ is the angle between the axis of the dipole and the direction of observation. This light will be polarized in a plane determined by the axis of the dipole and the direction of observation.

In the ideal case with light approaching the sample along the X axis and being observed along the Z axis, we have

$$\rho_s = \Sigma c/\Sigma a = C/A \quad (5)$$

$$\rho_p = C/B = 1 \quad (6)$$

$$\rho_n = (C+C)/(A+B) = 2C/(A+C) = 2\rho_s/(1+\rho_s). \quad (7)$$

In any actual case, the light does not approach the sample along the X axis but converges into the sample. Therefore, the dipoles are not oriented along the coordinate axis. It is necessary

TABLE II.

Type of incident light	Intensity of S_0 light	Intensity of P_0 light	Observed depolarization
I_s	$C+vA$	A	$\rho_{s_0}=\rho_s+v$
I_p	C	$B+wA$	$\rho_{p_0}=\rho_s/(\rho_s+w)$
unpolarized	$2C+vA$	$A+B$	$\rho_{n_0}=\rho_n+v$

[3] S. Bhagavantam, *Scattering of Light and the Raman Effect* (Chemical Publishing Company, Brooklyn, New York, 1942).

[4] R. Gans, Physik. Zeits. **28**, 661 (1927).

to consider the intensity of the scattered light polarized in the XZ and YZ plane under these conditions. In the following discussion, we shall use a number of approximations which apply only to highly polarized lines and, therefore, all the conclusions resulting from this analysis can be applied only to such lines.

First consider the case in which the incident light is polarized in the XY plane and approaches the sample at an angle θ with the X axis in the XY plane. This will cause some of the light emitted by the dipoles a to be observed as scattered light polarized in the XZ plane. As in the ideal case, $A=\Sigma a$ and $B=\Sigma b$. If we let S_0 and P_0 be the observed intensities of scattered light polarized in the XZ and YZ planes, respectively, then, from Eq. (4):

$$S_0=A\sin^2\theta+C\cos^2\theta\doteq A\theta^2+C,$$
$$P_0=A\cos^2\theta+C\sin^2\theta\doteq A.$$

The approximate equation assumes that $A\gg C$ and that θ is small. The observed depolarization factor ρ_{s0} is, therefore,

$$\rho_{s0}=(A\theta^2+C)/A=\rho_s+\theta^2. \qquad (8)$$

In any actual apparatus, the light converges into the sample, and it is necessary to integrate the above expression over a range of values of θ (here we are considering all the incident light parallel to the XY plane). In the general case, the light intensity is not uniform over the range of values of θ, and the relationship giving the intensity as a function of θ is not known. However, for any highly polarized line, as long as θ does not become too great we can write the intensities of the scattered light,

$$S_0=C+Af(\theta),\quad P_0=A.$$

$f(\theta)$ is a function that depends on the geometry of the apparatus and to some extent on the index of refraction of the sample. So long as ρ_s is small, $f(\theta)$ can be considered independent of ρ_s.

TABLE III.

Molecule	$\Delta\nu$ cm^{-1}	ρ_n (authors)	ρ_n (literature)
Carbon tetrachloride	459	0.013	0.045*
Benzene	992	0.038	0.060*
Mesitylene	570	0.057	
Cyclohexane	802	0.063	
Chloroform	366	0.13	0.18**
Chloroform	668	0.026	0.06**

* See reference 2.
** See reference 3.

TABLE IV.

Raman line	ν cm^{-1}	ρ_s	ρ_{s0}	ρ_{p0}	$f(\theta)$	$f'(\alpha)$	ρ_{n0} calc.	ρ_{n0} obs.
CCl_4	459	0.0074	0.030	4.90	0.023	0.029	0.066	0.061
C_6H_6	992	0.020	0.042	2.38	0.022	0.028	0.088	0.090

In a similar manner we can consider the case where the light approaches the sample at an angle α with the X axis in the XZ plane. Under these conditions,

$$S_0=C\cos^2\alpha+B\sin^2\alpha=C,\quad \text{(since } B=C\text{)}$$
$$P_0=A.$$

Thus, no error is introduced into the measurement of ρ_s by convergence in the XY plane of polarized incident light I_s.

Similarly, it is possible to find the effect of convergence when the sample is illuminated by light polarized in the XZ plane. In the real apparatus, the light will converge into the sample from all angles. To a good approximation, as long as the convergence error is small, we can consider the total error simply as the sum of the error resulting from convergence in the XZ plane and that resulting from convergence in the XY plane. On this assumption, Table I has been made. This table shows the observed intensities of the scattered light when either type of polarized light or unpolarized light is used to excite the Raman line. In this table, the function $f'(\alpha)$ is entirely analogous to the function $f(\theta)$ already introduced except that it refers to the XZ plane.

From Table I it can be seen that ρ_s, ρ_p and ρ_n, measured in the usual way, are subject to error because of the convergence of the incident light. These errors are always such as to give a value of ρ which is too large. Means of eliminating these errors will now be considered.

First, the incident light may be made sufficiently parallel that the quantities $f(\theta)$ and $f'(\alpha)$ become negligibly small. This type of correction can be carried out only to a certain extent since it entails a loss of exciting light. A rough calculation shows that, in order to reduce the convergence error in ρ_n to 0.001 in the apparatus used by us, the light intensity would have to be reduced to one-fiftieth.

Secondly, one may try to calculate $f(\theta)$ and

FIG. 1. Showing the weak and the strong component of the $\Delta\nu 459$ cm^{-1} line of CCl_4. The amplifier was adjusted to make the traces of comparable height. The rise in the background of the weak component is due to a contribution from the depolarized $\Delta\nu 314$ cm^{-1} line.

$f'(\alpha)$ from the geometry of the apparatus. Because of the finite size of the light source and the sample and the large aberration in the condensing lens, such a calculation is subject to many uncertainties.

Thirdly, from the measured values of ρ_{s0}, ρ_{p0} and ρ_{u0}, Eqs. (7), (9), (10) and (11) may be used to calculate ρ_s and also the convergence factors $f(\theta)$ and $f(\alpha)$. We have used this method of determining ρ_s with some degree of success.

Finally, it can be seen from Table I that the ratio of the intensity of the P-scattered light when the incident light is polarized in the XZ plane to the intensity of the P-scattered light when the incident light is polarized in the XY plane gives a value of ρ_s *which, to the degree of approximation considered here, is without convergence error. This, we believe, is the most simple and accurate way of measuring the depolarization factors of highly polarized lines.* In the following sections, this method of measuring ρ_s will be referred to as the method of polarized incident light.

Consideration will now be given to various types of errors that remain when the method of polarized incident light is used to measure ρ_s. In this work, the following factors have been taken into consideration:

1. incomplete polarization by the incident and analysing polaroid;
2. depolarization of the incident light by reflection at the surface of the sample tube;
3. terms that have been omitted from Table I (these additional terms arise from the fact that convergence in the two planes cannot strictly be considered independently);
4. the fact that the sample is not observed exactly along the Z axis.

Of these errors, the first is significant but its magnitude can be measured. Suppose that the light transmitted by the incident polaroid contains a fraction $1-w$ polarized in the plane of the polaroid and a fraction w polarized perpendicular to this plane. w will be called the light leak of the polaroid. Similarly, let the light leak of the analysing polaroid be v.

By a simple analysis, it is possible to construct a table similar to Table I. The errors in Table I and Table II can be considered as acting independently and the total error obtained by adding them.

If ρ_s is determined by the method of polarized incident light, then the observed value will be ρ_s+w. Since w may be determined experimentally, it is possible to correct for this polaroid leak.

The magnitude of the second error cannot readily be calculated. Fortunately, as will be discussed later, it is possible to eliminate this effect by a suitable experimental arrangement.

The order of magnitude of the third error may be calculated. If the geometry of a skew ray passing through the sample is considered, it can be seen that the error is of the order of the product of $f(\theta)$ and $f'(\alpha)$. Unless the convergence factors are large, this term will be very small.

The fourth error could represent a difficult one to correct. Suppose that the effective part of the condensing lens that focuses the scattered beam from the sample onto the slit of the spectrograph makes an angle 2φ at the sample. The P component of the light entering the spectrograph when the sample is illuminated with I_p polarized light must now be represented by $B+Af''(\phi)$. The function $f''(\phi)$ like $f(\theta)$ and $f'(\alpha)$ can not readily be calculated. However, we do know that $f''(\phi)$ like $f(\theta)$ is certainly less than ϕ^2 and will probably be closer to $\phi^2/4$. Fortunately, in the apparatus used by us, ϕ had a value of 1/33 radians and therefore a term of the order of $\phi^2/4$ is negligible.[4**]

[4] The derivation of convergence error given by Gans is for a spherical condensing system and a point source of illumination. Any practical case used for the Raman effect would not be strictly in accord with Gans' theory even if a spherical condensing system is used. It would always be necessary to make use of an extended source in

EXPERIMENTAL

The apparatus used in this work was a photoelectric spectrograph which has been described previously.[5] In a paper by one of us, it has been shown that it is relatively easy to measure depolarization factors with this instrument.[6] It was shown at that time that without any correction for the convergence errors, results approximately the same as the best values given in the literature could be obtained.

It is not immediately obvious why only a small convergence error should appear since the f number of the cylindrical condensing lenses is small. The reason for the smallness of the convergence error in the XY plane can be seen immediately upon a close inspection of the geometric optics of the condensing system. The component parts of this system are disposed in such a way as to concentrate the greatest amount of light in a line image across the diameter of the scattering tube. When one obtains the sharpest line image in the scattering tube, the centre of the tube is approximately at the paraxial focus of the total thick lens system. A trace of the rim and zonal rays through the system shows that the spherical aberrations of the condensing lenses are so large that the effect of the rays striking the lenses above the half aperture is nil. Therefore, the value of $f(\theta)$ is not large and is actually nearly equal to $f'(\alpha)$. This allows Eq. (7) to be fulfilled for the observed values of ρ_s and ρ_n in spite of the convergence error.

Our experimental work consisted essentially of the measurement by the method of incident polarized light of a relatively few highly polarized lines of well known substances. We have endeavoured to correct for all known errors. Finally, we have shown that in numerous cases the depolarization factor of a Raman "line" is not constant across the width of the "line."

RESULTS

The leaks of both the analysing and the incident polaroid were measured. This was done by examining the transmitted light at 4358A with a Nicol prism. The intensities were recorded by means of a photo-cell.

It was found that the leak of the incident polaroid was 0.002 and that of the analysing polaroid 0.003. Using the corrections given in Table II, all data were corrected for the leaks. All the figures quoted below have been corrected in this manner.

Table III shows the depolarization factors for a number of lines as measured by the method of polarized incident light. Actually, ρ_s is measured but since ρ_n is usually quoted, it has been calculated from ρ_s by Eq. (7). Also shown in the table are some commonly quoted values for the depolarization factors.

Each of these lines was measured under conditions such that the weak component gave a galvanometer deflection of from three to ten centimeters. The slit width of the spectrograph was 2.1A. The height of the peaks was considered a measure of the light intensity. The background fluctuations varied from trace to trace but, in

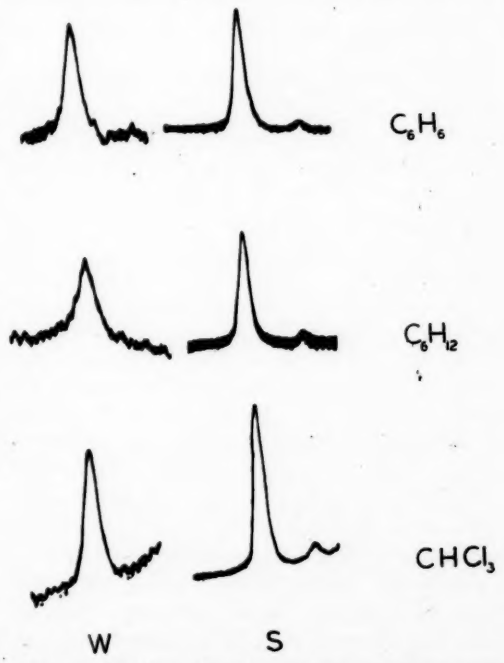

FIG. 2. Showing the shape of the weak and strong components of a number of highly polarized Raman lines. The two components are brought to comparable heights by a suitable adjustment of the amplifier.

order to obtain sufficient illumination. In the case of an extended source, rays of greater obliquity than that indicated by the relative aperture of the condensing system must inevitably become operative.

[5] D. H. Rank and R. V. Weigand, J. Opt. Soc. Am. **36**, 325 (1946).

[6] D. H. Rank, J. Opt. Soc. Am. **37**, 798 (1947).

TABLE V.

Raman line	ν cm^{-1}	ρ_s from height	ρ_s from area	Ratio
Cyclohexane	802	0.031	0.065	2.09
Benzene	992	0.020	0.028	1.40
Chloroform	366	0.072	0.092	1.29
Carbon tetrachloride	459	0.0065	0.0065	1.00

general, did not exceed ten percent of the line height for the weak component. Thus, it is believed that the error in the measurement of the true height of the peak does not exceed ten percent and is considerably less in most cases.

The depolarization factors obtained are very considerably below those quoted by other observers. It should be remembered that all errors in the measurement of the depolarization factors of highly polarized lines, save those errors in actually measuring the light intensity, are positive quantities. Since our error in the measurement of intensities is small, we believe that these new depolarization measurements are either above or equal to the true value. Therefore it is believed that the new values represent a considerable improvement over results obtained previously.

Under the same conditions as those used to obtain the data in Table III, measurements were made of ρ_{s0}, ρ_{p0}, and ρ_{n0} for the carbon tetrachloride and benzene lines. This allows the convergence errors to be calculated. Also, if we assume that the method of incident polarized light gives the correct value of ρ_s then from the relationships (9), (10) and (11), we can calculate ρ_{n0}. A comparison of the calculated and measured values of ρ_{n0} will give some indication of the accuracy of the work. Table IV shows the results of these measurements. It should be noted, however, that agreement between the calculated and measured values of ρ_{n0} is not a definite proof of accurate results, since this agreement is insensitive to certain types of errors.

The point of greatest interest in Table III is that it shows that it is possible to measure a depolarization factor as low as 0.015 even though the sum of the convergence errors is 0.051. The values of ρ_s given in Table IV do not quite agree with those quoted in Table III because the reflection error discussed below has not been taken into account in Table IV.

It is difficult to estimate the extent of the experimental errors. Two sets of experiments were conducted to show the effect, first, of convergence and, secondly, of reflected and stray light on the measured value of ρ_s.

By means of a system of slits and by reducing the aperture of the condensing lens, the incident light was made more nearly parallel. Under these conditions the sum of $f(\theta)$ and $f'(\alpha)$ was reduced to 0.018. Since the total light intensity was considerable reduced by this arrangement, the accuracy of our measurement was somewhat reduced. Within our estimated experimental error however, the measured values of the depolarization factor ρ_s was the same as that obtained with the more convergent light.

In order to determine if stray light and incident light reflected from the walls of the sample tube had any effect, the type of tube and holder was changed. A sample tube 4.5 cm in diameter was placed along the axis of a three-liter beaker which had a window of optical quality in the bottom. The walls of the beaker were painted black except for two slits through which the incident light passed. The beaker was filled with water.

In this experimental arrangement, the cell was large enough so that no light from the wall could enter the spectrograph. The water surrounding the cell greatly reduced the reflections from the wall. The black wall of the beaker also prevented stray light from entering the cell. The carbon tetrachloride line which has the highest polarization and is therefore most sensitive to errors, was run under these conditions. The depolarization factor ρ_s was found to be 0.0065 as compared with 0.0074 when run in the usual way. Thus the sum of the errors caused by reflections, stray light, and scattered light is about 0.001. This value is assumed to exist for all of the samples, and it has been taken into account in the figures in Table III. Figure 1 shows two traces taken under these conditions. The height of the peak on the weak trace is 6 cm while the gain of the amplifier was reduced 125 times for the strong peak so as to make it of comparable size.

In the course of this work it was found that the value of the depolarization factor for some lines depends on the slit width of the spectrograph. The reason for this can be seen from

Fig. 2. Here the weak and the strong components of some highly polarized lines taken with a relatively narrow slit (0.6A) are shown. The amplifier gain was reduced for the strong component so that the two traces are of comparable size. It can be seen that the weak components are considerably broader than the strong. From these traces Table V was constructed. This table shows the depolarization factor, first as determined by the height of the two peaks and secondly as determined by the area under the curve. The values for CCl_4 shown in this table were taken from the traces shown in Fig. 1 where a wide slit was used.

Our measurements here show that these lines (except CCl_4; 459 cm^{-1}) must consist of a highly polarized central component with less highly polarized wings on either side. Therefore, care must be taken if one is to get a significant number for the depolarization factor. The most desirable measurement would be a curve representing the depolarization factor as a function of wave number within a single line. Since only in exceptional cases are the Raman spectra measurements taken with sufficient resolving power to do this, one must decide if he wishes to measure the mean depolarization across the line or if he wishes to get as close as possible to the depolarization factor of the central components. In any case, for many Raman lines any statement of a measured value of the depolarization factor must be accompanied by a statement of the method of measurement, if the quoted value is to be significant.

JOURNAL OF THE OPTICAL SOCIETY OF AMERICA VOLUME 38, NUMBER 3 MARCH, 1948

Intensity and Polarization of Brillouin Spectra*

D. H. RANK, J. S. MCCARTNEY, AND G. J. SZASZ
Physics Department, Pennsylvania State College, State College, Pennsylvania

(Received September 29, 1947)

Apparatus is described for the production of intense Brillouin spectra. The fine structure of the transverse scattered light (Rayleigh scattering) has been analyzed by means of a large Fabry and Perot etalon placed in the parallel beam of a high aperture glass spectrograph. Interferograms have been obtained of the Brillouin spectrum of acetone, ethyl alcohol, and water using λ4078 of Hg as the exciting line. Intensity measurements of these interference patterns show that the theory of Landau and Placzek is a very close approximation to the truth in the spectra investigated.

Polarization measurements have been made on these spectra excited by λ4358 Hg by means of the method of Douglas and Rank. These polarization measurements show that ρ_s is small but not zero for the modified Brillouin components. The polarization of the unmodified Brillouin components seems to be somewhat less complete than that of the modified components. However the polarization measurements on the unmodified lines are vitiated by parasitic light and are not nearly as reliable as measurements on the modified lines.

THE remarkable phenomenon predicted by L. Brillouin[1] deserves further attention because of the complexities introduced by the scattering molecules themselves.

The prediction of L. Brillouin that Rayleigh scattering should exhibit a fine structure has been amply verified experimentally. The Brillouin theory predicts that, in addition to the incident frequency, the scattered light should contain a pair of "Doppler" components whose frequency shift from the parent line is given by the following equation:

$$\Delta\nu = \pm 2\nu(v/c)\mu \sin(\varphi/2), \qquad (1)$$

TABLE I. Intensity and polarization of Brillouin spectra.

Liquid	$Ic/2I_b$	$\gamma-1$	$\rho_s \sim B$	$\rho_s \sim C$	$\rho_n \sim B$ calc.	$\rho_n \sim C$ calc.
Water	.14	.01	.02	<.30	.04	.46
C_2H_5OH	.15	.18	.013	<.08	.026	.15
Acetone	.42	.39	.079	<.14	.15	.25

* This research was carried out on contract N60nr-269, Task V of the Office of Naval Research.

[1] L. Brillouin, Ann. de physique **17**, 88 (1922).

where ν is the frequency of the exciting light, v the velocity of sound in the liquid, c the velocity of light, μ the refractive index, and φ the angle of scattering. The validity of the above equation has been verified by Gross[2] who first experimentally discovered the Brillouin effect. Since the work of Gross a number of investigators in Europe and India have verified the above relationship. Particularly extensive work on this phase of the problem of the Brillouin effect has been accomplished by Venkateswaren.[3]

Landau and Placzek[4] have calculated the ratio of intensity of the unmodified to modified Rayleigh scattering on the basis of fluctuation density theory. This theory would predict complete polarization of both modified and unmodified lines for transverse scattering.

Let us examine the experimental facts concerning the Brillouin effect which are apparently incontrovertible.

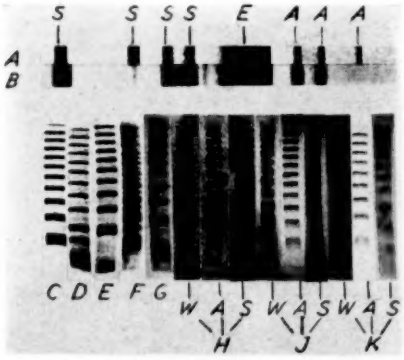

FIG. 1. Reproductions of the interference spectra *C*, *D*, *E*, *F*, *G*, *H*, *J*, and *K* have the following significance. *C* and *E* are interferograms of λ4078 of Hg. *D*, *F*, and *G* are the Brillouin spectra of water, acetone, and ethyl alcohol, respectively. The spectra are lined up so that the unmodified components are in juxtaposition to the arc fringes. *H*, *J*, and *K* are polarization interferograms of water, acetone, and ethyl alcohol, respectively, obtained with λ4358 of Hg. *W* and *S* of *H*, *J*, and *K* refer to the weak and strong components, respectively. *A* of *H*, *J*, and *K* refers to an interferogram of λ4358 of Hg. Parts *A* and *B* of Fig. 1 are enlargements of the Raman spectrum of CCl_4 excited by λ4358 Hg. *A* was obtained with unpolarized exciting light. The *S*'s and *A*'s refer to stokes and anti-stokes Raman lines respectively. *B* was obtained using *P* polarized exciting light and is the weak *P* polarized component of the transversely scattered light. All spectra were obtained with the liquids at a temperature of 28°C. *Note: D*, the bottom unmodified fringe shown in the reproduction, is much too strong by virtue of the fact that parasitic light from an imperfect window enters the interference pattern. It must be remembered that the interference patterns are not integrated by the etalon as is ordinarily the case when light from the source is focussed on the etalon. A stigmatic image of the source is focused on the slit of the spectrograph with the present disposition of the apparatus. A fringe will appear in the interference pattern wherever the wave-length is such that the etalon is capable of transmitting light at the angle in question.

(a) Equation (1) accurately expresses the frequency dependence of the Brillouin satellites.
(b) Both the Brillouin components and the central component are polarized to a more or less complete extent.
(c) There is a continuum of more or less intensity covering the Brillouin pattern.
(d) The continuum mentioned in (c) above is practically completely depolarized.

The theory of Placzek and Landau is completely classical since it does not take into account the contributions to the intensity due to the existence of the rotational Raman effect. It is well known that highly depolarized "rotational wings" accompany the Rayleigh scattering from liquids. The intensity of these wings varies through a wide range from liquid to liquid. A fair test of the theory of Placzek and Landau must involve cases where the non-classical part of the Rayleigh scattering is a minimum so as to avoid complications arising from non-classical reasons.

The state of polarization of Brillouin spectra has been studied by a number of investigators. Rao[5] and Birus[6] conclude that both the modified and unmodified lines are completely polarized. Venkateswaren[7] and Sunanda Bai[8] have made a rather extensive investigation of the state of polarization of the Brillouin spectra of a number of liquids. Apparently Rao[5] and Birus[6] were plagued by the low intensity of the spectra and were not able to observe the weak polarized component. Venkateswaren[7] and Bai[8] rectified this difficulty of obtaining sufficient intensity by making use of a Lummer plate as the interference spectrograph. However, even with the Lummer plate long exposures were necessary. The latter authors were able to show that the Brillouin spectra are not completely polarized.

Unfortunately, the Lummer plate used by both Venkateswaren[7] and Bai[8] was incapable of resolving the Brillouin components even moderately clearly from the unmodified line. Thus, only a general over-all picture of the state of polarization of modified and unmodified compo-

[2] E. Gross, Naturwiss. **1**, 718 (1930).
[3] C. S. Venkateswaren, Proc. Ind. Acad. Sci. **15**, 371 (1942).
[4] L. Landau and G. Placzek, Physik. Zeits. Sowjetunion **5**, 172 (1934).
[5] B. V. R. Rao, Proc. Ind. Acad. Sci. **2**, 236 (1935).
[6] K. Birus, Physik. Zeits. **39**, 80 (1938).
[7] C. S. Venkateswaren, Proc. Ind. Acad. Sci. **15**, 322 (1942).
[8] K. Sunanda Bai, Proc. Ind. Acad. Sci. **15**, 357 (1942).

nents could be obtained. These results showed the polarization to be incomplete.

It is well known that measurement of the depolarization of Rayleigh scattering is not easy. Extreme care must be taken to purify the materials so that the scattering is purely a function of the material investigated and free of dust which would completely vitiate the results obtained. The method used must be free of "convergence error" which seriously affects measurement when the polarization is strong. In addition, if the polarization of the individual Brillouin components is desired, a suitable interference spectroscope reduces the intensity by at least two orders of magnitude over that ordinarily available for study of Rayleigh scattering.

Recently in this laboratory, low pressure Hg arcs of very high intensity and very pure spectral characteristics have been developed for the study of Raman spectra.[9] Simultaneously, one of us[10] has demonstrated the utility of using plane polarized light for the measurement of depolarization factors in Raman spectra. Of more importance, however, is the method recently developed by Douglas and Rank[11] for obtaining precise depolarization factors making use of polarized exciting light. This method eliminates convergence errors of lower order than the third and also eliminates the transmission of the spectrograph, since it is only necessary to use the P component of the scattered light to obtain ρ_s.

EXPERIMENTAL

The general arrangement of arcs, cylindrical lenses, and scattering tube has been described previously.[11] The spectrograph was a three-prism instrument with an $f=3.5$ objective lens for the camera. The free aperture of the spectrograph is somewhat greater than two inches. A Fabry and Perot etalon with plates 10 cm in diameter was placed in the parallel beam of the spectrograph. The spacing ring for the plates used had Invar plugs for separators. Since the collimator of the spectrograph had a focal length of about 30 inches, the etalon was slightly tilted so that only half of the ring system would appear in the photograph. This procedure was desirable so as to obtain a convenient number of fringes for microphotometry.

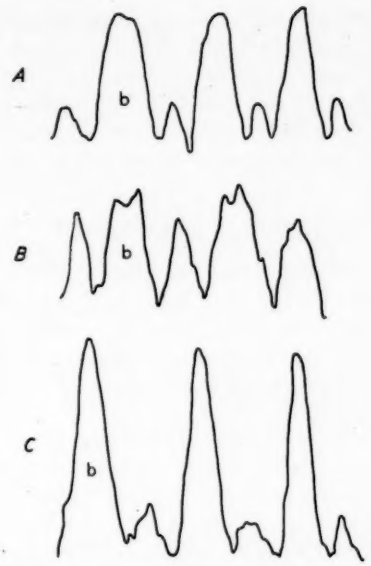

FIG. 2. Reproductions of microphotometer traces of Brillouin spectra obtained with natural unpolarized exciting light using λ4078 of Hg. *A*, ethyl alcohol; *B*, acetone; and *C*, water. The small *b*'s refer to the modified component of the Brillouin pattern. *Note:* The overlapping of the modified Brillouin components is not perfect with the 10.5-mm spacer in the case of ethyl alcohol and acetone. In *A* and *B*, it can be seen that the two modified Brillouin components are just resolved from each other. The resolving power of the etalon with the spacer employed is in excess of 500,000.

Liquids used were freed from dust by repeated distillation in vacuum directly into the scattering tube. The separation chosen for the plates of the etalon was 10.5 mm. With this separation the + and − Brillouin components of benzene, water, and carbon bisulfide are thrown on top of each other thus doubling their intensity. In addition to increasing the intensity of the modified components this procedure has the advantage of almost doubling the resolving power over that which would be available when the modified components are separated from each other. The situation with the hyperfine structure satellites with λ4047 and λ4078 is that with a 10.5-mm spacer the strongest satellites fall nearly on top of the main line.

With the arrangement described above, it was possible to photograph the Brillouin spectrum of benzene with an exposure time of only 30 sec., using λ4047 of Hg as the exciting line.

Brillouin spectra of benzene, water, acetone,

[9] D. H. Rank and J. S. McCartney, J. Opt. Soc. Am. (in press).
[10] D. H. Rank, J. Opt. Soc. Am. **37**, 798 (1947).
[11] A. E. Douglas and D. H. Rank, J. Opt. Soc. Am. (in press).

and ethyl alcohol were obtained, excited with natural unpolarized light. The intensities of the modified and unmodified lines were measured with a Leeds and Northrup microphotometer. The ratio of the intensity of the central component to the Brillouin components is given in Table I.

POLARIZATION MEASUREMENTS

The method employed for depolarization measurements was the polarized light method for obtaining ρ_s, described by Douglas and Rank.[11] As a test of the apparatus the Raman spectrum of CCl_4 was photographed using P polarized exciting light and the analyzer set so as to pass only the P component. A reproduction of this photograph shown in Fig. 1 clearly shows that the value of ρ_s obtained with this apparatus is less than 0.01, which is in agreement with Douglas and Rank's[11] results obtained with the photoelectric spectrograph.

Using the polarized light method it is necessary to take two separate exposures, first using S polarized exciting light and secondly with P polarized light. The intensity of the light source probably did not vary by more than five percent in making any set of exposures so that any errors from this cause would be considerably smaller than those occasioned from the microphotometry of the fringes. For polarization measurements λ4358 was made use of in spite of its rather poor fine structure pattern due to considerable breadth of the central component. Use was made of this line because of its large intensity. It was also known that the polaroids used were rather perfect polarizers at this wave-length.

In order to avoid any correction for failure of the reciprocity law, exposures of weak and strong components were made on the same plate and of equal duration. The exposure for the strong component was made through a neutral screen which had a transmission of 7.9 percent. In the cases investigated this procedure produced comparable photographic densities for strong and weak components. A photograph of the fringes obtained directly from the arc was also made on the same plate for identification purposes.

The results of this investigation are summarized in Table I. It can be seen that $I_c/2I_b$ closely approaches $\gamma-1$ as demanded by the Landau Placzek theory. I_c and $2I_b$ are the intensities of the unmodified and modified components, respectively. γ is the ratio of the specific heats of the liquid (C_P/C_v). Reproductions of microphotometer traces of these Brillouin spectra can be seen in Fig. 2. The intensities were obtained by integrating the areas under the microphotometer curves. The failure of water to fulfill the Landau Placzek relationship is probably due to our inability to completely remove parasitic light from the apparatus. The measured values of $\rho_s \sim B$ (see column 4, Table I) should be reliable in that the error probably does not exceed 25 percent. The values of $\rho_s \sim C$ (column 5, Table I) are recognized to be probably very bad values. The errors in $\rho_s \sim C$ are occasioned by the presence of parasitic light and particularly by scattering of unmodified radiation by the analyzing polaroid. The values are given only to represent the upper limit of the depolarization of the unmodified component. The values given in columns 6 and 7 are calculated from the relationship $\rho_n = 2\rho_s/1+\rho_s$.

CONCLUSION

The results of this investigation are that the Landau Placzek formula for the Brillouin effect appears to be quantitatively confirmed for liquids in which the rotational Raman effect is probably negligible. This is in contradiction to the results given by Venkateswaren[7] and by Bai.[8] It is certain that the inability of the above authors to verify the Landau Placzek relationship in the cases investigated by us was due to two causes—(a) insufficient resolving power and (b) failure to exclude the parasitic unmodified light to a sufficient extent. The fluctuation density theory of Landau and Placzek appears to explain adequately the intensities in Brillouin spectra when non-classical effects are small or negligible.

POLARIZATION

Moderately accurate measurements of the polarization of the modified Brillouin components have been obtained. ρ_s is definitely not zero for the molecules investigated. The values obtained for ρ_s for the unmodified component, although grossly inaccurate due to unavoidable presence of parasitic light, seem to be somewhat larger than ρ_s for the modified component.

A Table of Planckian Radiation

PARRY MOON
Massachusetts Institute of Technology, Cambridge, Massachusetts
(Received October 8, 1947)

A table is presented for the radiation from a Planckian radiator operating between 2000 and 3500°K (100° intervals). Values of $J(\lambda)$ are given for a wave-length range of 0.38 to 0.76μ at 0.01μ intervals. This is part of a more extensive table (10° intervals) that has been published.

INTRODUCTION

PLANCK'S equation for the radiation from a a blackbody has many applications in colorimetry and theoretical photometry. Calculations can, of course, be made directly from the equation, but the formula is sufficiently complex so that there is a definite practical advantage in having tabulated values. Various tables have been published,[1] but none is entirely satisfactory.

Over ten years ago, computation was started on a comprehensive table of Planckian radiation to cover the temperature range of 2000 to 8000°K, at 100-deg. intervals. It was immediately evident that, below about 3500°, the computed values could not be checked by means of differences. Accordingly, the work was split into two parts: one from 3500 to 8000° with 100-deg. intervals, the other from 2000 to 3500° with 10-deg. intervals. The first part[2] was published in 1937. The progress of the second part was interrupted by other work, but was finally completed and published[3] as a 75-page table. The values at 100-deg. intervals, taken from the complete table, are given here.

COMPUTATION

Planck's equation is

$$J(\lambda)=\frac{C_1}{\lambda^5}\frac{1}{\exp(C_2/\lambda T)-1}, \qquad (1)$$

where $J(\lambda)$ is expressed in watts radiated per square cm of blackbody opening, per micron wave-length band, and where λ=wave-length (micron), T=absolute temperature (°K), C_1 =36970, and C_2=14320.

The actual computation made use of the previous[2] Table I. Values were obtained by means of electrically-driven computing machines, results being tabulated to 10 figures. The computed values were then checked by use of fifth

TABLE I. Values of constants in Planck's equation.

	$C_1=2\pi hc^2$	$C_2=hc/k$	$\bar{J}(\lambda)/J(\lambda)$	$\bar{T}/T$
International temperature scale,[a] *1927*		**14320**		1.0000 0000
Birge,[b] 1929 (experimental)		14320±30		1.0000 0000
(indirect)	36972±50	14317.4±6	1.0000 5410	0.9998 1844
Commission Internationale de l'Eclairage.[c] 1931		14350		1.0020 9497
Wensel,[d] 1939	37320±6	14360±10	1.0094 6714	1.0027 9330
Birge,[e] 1941	37403	14384.8±3.4	1.0117 1220	1.0045 2514
O.S.A. Colorimetry Committee,[f] 1944	37400	14385	1.0116 3105	1.0045 3911
This table and previous table[g]	**36970**	**14320**	1.0000 0000	1.0000 0000

[a] See reference 4.
[b] See reference 5.
[c] See reference 7.
[d] See reference 8.
[e] See reference 11.
[f] See reference 10.
[g] See references 2 and 3.

[1] Frehafer and Snow, "Tables and graphs for facilitating computations of spectral energy distributions," Bur. Stand. Misc. Pub. No. 56 (1925); F. E. Fowle, "Radiation from a perfect (blackbody) radiator," *International Critical Tables* (McGraw-Hill Book Company, Inc., New York, 1929), Vol. V, pp. 239–241; C. Fabry, *Introduction générale à la photométrie* (Paris, 1927), p. 121; J. F. Skogland, "Tables of spectral energy distribution," Bur. Stand. Misc. Pub. No. 86 (1929); Yamauti and Okamatu, "Tables of Planck's formula of radiation," Res. El. Lab., Tokyo, No. 395 (1936).

[2] Parry Moon, "A table of Planck's function from 3500 to 8000°K," J. Math. Phys. **16**, 133 (1937); Massachusetts Institute of Technology, Elec. Eng. Dept., Contribution No. 131, 1938.

[3] Parry Moon, *A Table of Planck's Function 2000 to 3500°K* (Massachusetts Institute of Technology, Cambridge, Massachusetts, 1947).

TABLE II.

$J(\lambda)$ in watt cm^{-2} micron^{-1}.

λ (micron)	2000°K	2100	2200
0.38	3061 3228	7508 9094	1697 5410
0.39	4358 3807	1044 7236	2312 9256
0.40	6076 8466	1425 1567	3093 0994
0.41	8311 2351	1909 0664	4065 7832
0.42	1116 6476	2514 6218	5259 9140
0.43	1475 7034	3261 0439	6705 1578
0.44	1920 5713	4168 3263	8431 3917
0.45	2464 2183	5256 9275	1.046 8175
0.46	3120 1275	6547 4450	1.284 4224
0.47	3902 1113	8060 2825	1.558 6910
0.48	4824 1120	9815 3206	1.872 1793
0.49	5899 9987	1.183 1598	2.227 2201
0.50	7143 3628	1.412 7016	2.625 8860
0.51	8567 3205	1.671 8065	3.069 9594
0.52	1.018 4325	1.961 9587	3.560 9079
0.53	1.200 5993	2.284 4571	4.099 8667
0.54	1.404 2948	2.640 3991	4.687 6272
0.55	1.630 4686	3.030 6672	5.324 6318
0.56	1.879 9460	3.455 9208	6.010 9744
0.57	2.153 4186	3.916 5908	6.746 4058
0.58	2.451 4378	4.412 8781	7.530 3443
0.59	2.774 4094	4.944 7554	8.361 8898
0.60	3.122 5919	5.511 9717	9.239 8417
0.61	3.496 0953	6.114 0600	10.16 2719
0.62	3.894 8829	6.750 3468	11.12 8784
0.63	4.318 7741	7.419 9636	12.13 6065
0.64	4.767 4492	8.121 8605	13.18 2383
0.65	5.240 4557	8.854 8199	14.26 5377
0.66	5.737 2148	9.617 4727	15.38 2530
0.67	6.257 0296	10.40 8314	16.53 1195
0.68	6.799 0944	11.22 5718	17.70 8621
0.69	7.362 5034	12.06 7958	18.91 1976
0.70	7.946 2607	12.93 3217	20.13 8371
0.71	8.549 2903	13.81 9610	21.38 4883
0.72	9.170 4461	14.72 5195	22.64 8574
0.73	9.808 5220	15.64 7989	23.92 6510
0.74	10.46 2261	16.58 5981	25.21 5782
0.75	11.13 0368	17.53 7150	26.51 3518
0.76	11.81 1512	18.49 9470	27.81 6900

TABLE II.—*Continued.*

	2300	2400	2500
0.38	3574 8671	7075 3226	1.325 9090
0.39	4778 6804	9293 7745	1.713 8215
0.40	6275 6909	1.200 3934	2.179 9813
0.41	8108 0715	1.526 5459	2.732 2400
0.42	1.031 8452	1.913 6576	3.377 9562
0.43	1.294 9097	2.367 2865	4.123 8361
0.44	1.604 1081	2.892 6124	4.975 7953
0.45	1.963 3510	3.494 3348	5.938 8446
0.46	2.376 2787	4.176 5846	7.017 0015
0.47	2.846 1956	4.942 8524	8.213 2280
0.48	3.376 0141	5.795 9324	9.529 3943
0.49	3.968 2080	6.737 8837	10.96 6267
0.50	4.624 7761	7.770 0080	12.52 3521
0.51	5.347 2166	8.892 8422	14.19 9766
0.52	6.136 5123	10.10 6167	15.99 2602
0.53	6.993 1244	11.40 9025	17.89 8671
0.54	7.916 9966	12.79 9754	19.91 3743
0.55	8.907 5665	14.27 6026	22.03 2786
0.56	9.963 7843	15.83 4898	24.25 0063
0.57	11.08 4138	17.47 2860	26.55 9223
0.58	12.26 6685	19.18 5901	28.95 3389
0.59	13.50 9081	20.96 9562	31.42 5258
0.60	14.80 8624	22.81 9005	33.96 7186
0.61	16.16 2288	24.72 9068	36.57 1281
0.62	17.56 6767	26.69 4333	39.22 9483
0.63	19.01 8510	28.70 9180	41.93 3642
0.64	20.51 3768	30.76 7848	44.67 5592
0.65	22.04 8631	32.86 4485	47.44 7216
0.66	23.61 9064	34.99 3200	50.24 0505
0.67	25.22 0947	37.14 8110	53.04 7613
0.68	26.85 0107	39.32 3381	55.86 0902
0.69	28.50 2352	41.51 3267	58.67 2983
0.70	30.17 3498	43.71 2144	61.47 6751
0.71	31.85 9401	45.91 4537	64.26 5410
0.72	33.55 5977	48.11 5152	67.03 2502
0.73	35.25 9226	50.30 8893	69.77 1917
0.74	36.96 5252	52.49 0881	72.47 7916
0.75	38.67 0279	54.65 6472	75.14 5130
0.76	40.37 0666	56.80 1264	77.76 8572

differences, after which the figures were rounded off to 8 digits. The results are given in Table II. In general, the numbers given in this table are believed to be correct in the last digit.

OTHER VALUES OF C_1 AND C_2

The value $C_2=14320$ was adopted internationally in 1927 and has been used ever since as the basis of the international temperature scale[4] at high temperatures. The other constant ($C_1=36970$) is in accordance with the international temperature scale and established physical constants.[5] As indicated in Table I, these two values were employed in the computation of the present table.[6]

Various other values of the constants have been used in the literature. For instance, colorimetrists[7] have frequently used $C_2=14350$. Wensel[8] has advocated 14360, and a recent colorimetric table[9] by Harding employs the value 14384.8. The O.S.A. Colorimetry Committee[10] recommends 14385. The Harding and O.S.A. values are taken from Birge's study[11] of 1941.

[4] G. K. Burgess, "The international temperature scale," Bur. Stand. J. Research **1**, 635 (1928).

[5] R. T. Birge, "Probable values of the general physical constants," Rev. Mod. Phys. **1**, 1 (1929).

[6] Used also in the previous table (reference 2) and in other works. See, for instance, *Scientific Basis of Illuminating Engineering* (McGraw-Hill Book Company, Inc., New York, 1936); *Lighting Design* (Addison-Wesley Press, Cambridge, Massachusetts, 1938).

[7] Commission Internationale de l'Éclairage, *Compte rendu des séances* (Cambridge University Press, Teddington, England, 1932), p. 19.

[8] H. T. Wensel, "The international temperature scale and some related physical constants," Bur. Stands. J. Research **22**, 375 (1939).

[9] H. G. W. Harding, "Colors of total radiators expressed on the C.I.E. trichromatic system," Phys. Soc. Proc. (London) **58**, 1 (1946).

[10] O.S.A. Colorimetry Committee, "Quantitative data and methods for colorimetry," J. Opt. Soc. Am. **34**, 633 (1944); D. L. MacAdam, "Note concerning the maximum luminous efficiency of radiant energy," J. Opt. Soc. Am. **35**, 615 (1945).

[11] R. T. Birge, "The general physical constants," Reports on Progress in Physics **8**, 90 (1942).

TABLE II.—*Continued.*

	2600		2700		2800	
0.38	2.367	5498	4.049	8022	6.666	7801
0.39	3.015	0533	5.086	8853	8.267	6777
0.40	3.781	3685	6.296	9047	10.11	0801
0.41	4.676	0711	7.690	5505	12.20	6748
0.42	5.707	6866	9.276	6659	14.56	3222
0.43	6.883	5078	11.06	2070	17.18	4908
0.44	8.209	4502	13.05	1441	20.07	3432
0.45	9.689	9487	15.24	7261	23.22	7403
0.46	11.32	7894	17.64	9813	26.64	2520
0.47	13.12	4607	20.25	7226	30.31	1731
0.48	15.07	9849	23.06	5572	34.22	5453
0.49	17.19	1864	26.06	8985	38.37	1808
0.50	19.45	7445	29.25	9821	42.73	6897
0.51	21.87	2028	32.62	8830	47.30	5083
0.52	24 42	9796	36.16	5347	52.05	9281
0.53	27.12	3807	39.85	7491	56.98	1245
0.54	29.94	6119	43.69	2370	62.05	1851
0.55	32.88	7933	47.65	6274	67.25	1364
0.56	35.93	9725	51.73	4875	72.55	9691
0.57	39.09	1388	55.91	3413	77.95	6613
0.58	42.33	2362	60.17	6868	83.42	1997
0.59	45.65	1768	64.51	0125	88.93	5987
0.60	49 03	8521	68.89	8121	94.47	9166
0.61	52.48	1450	73.32	5976	100.0	3271
0.62	55.96	9397	77.77	9116	105.5	7850
0.63	59.49	1313	82.24	3371	111.0	9920
0.64	63.03	6341	86.70	5066	116.5	7848
0.65	66.59	3890	91.15	1094	122 0	0080
0.66	70 15	3699	95.56	8976	127.3	5173
0.67	73 70	5892	99.94	6910	132.6	1787
0.68	77.24	1020	104.2	7381	137.7	8683
0.69	80.75	0104	108.5	3931	142.8	4731
0.70	84.22	4658	112.7	3383	147.7	8906
0.71	87.65	6712	116.8	4853	152.6	0284
0.72	91.03	8828	120.8	7533	157.2	8046
0.73	94.36	4108	124.8	0691	161.8	1471
0.74	97.62	6197	128.6	3670	166.1	9930
0.75	100.8	1928	132.3	5884	170.4	2889
0.76	103.9	3808	135.9	6818	174.4	9900

TABLE II.—*Continued.*

	2900		3000		3100	
0.38	10.60	3977	16.35	2523	24.52	2486
0.39	12.99	4761	19.81	8054	29.41	2282
0.40	15.71	3064	23.71	2182	34.84	5997
0.41	18.76	7456	28.03	8681	40.81	8945
0.42	22.16	2332	32.79	5690	47.31	9275
0.43	25.89	7907	37.97	5921	54.32	8467
0.44	29.97	0323	43.56	6974	61.82	1961
0.45	34.37	1840	49.55	1764	69.76	9879
0.46	39.09	1111	55.90	9010	78.13	7789
0.47	44.11	3510	62.61	3784	86.88	7512
0.48	49.42	1506	69.63	8075	95.97	7920
0.49	54.99	5053	76.95	1372	105.3	6571
0.50	60.81	2009	84.52	1229	115.0	0614
0.51	66.84	7542	92.31	3818	124.8	5372
0.52	73.07	9532	100.2	9445	134.8	6286
0.53	79.47	8958	108.4	2804	144.9	8837
0.54	86.02	0260	116.6	7957	155.1	8604
0.55	92.67	6671	125.0	1445	165.4	1298
0.56	99.42	1524	133.3	9888	175.6	2801
0.57	106.2	2852	141.8	0011	185.7	9198
0.58	113.0	7196	150.1	8674	195.8	6795
0.59	119.9	2697	158.5	2888	205.8	2138
0.60	126.7	6966	166.7	9831	215.6	2027
0.61	133.5	7724	174.9	6863	225.2	3521
0.62	140.3	2818	183.0	1530	234.6	3943
0.63	147.0	0228	190.9	1573	243.8	0881
0.64	153.5	8072	198.6	4931	252.7	2182
0.65	160.0	4609	206.1	9737	261.3	5949
0.66	166.3	8245	213.5	4320	269.7	0533
0.67	172.5	7529	220.6	7198	277.7	4522
0.68	178.6	1155	227.5	7075	285.4	6734
0.69	184.4	7959	234.2	2835	292.8	6200
0.70	190.1	6911	240.6	3530	299.9	2156
0.71	195.6	7119	246.7	8377	306.6	4030
0.72	200.9	7814	252.6	6747	313.0	1424
0.73	206.0	8354	258.2	8154	319.0	4107
0.74	210.9	8210	263.6	2249	324.7	1999
0.75	215.6	6963	268.6	8808	330.0	5158
0.76	220.1	4299	273.4	7723	335.0	3767

As long as the international value of C_2 remains at 14320, this value seems the advisable one to use in computing tables. This is particularly true, since if one departs from the standard value he has no dependable foundation on which to base his work. Each new research on the physical constants will alter the average values of C_1 and C_2. For example, the best value of C_2 in 1929 was 14317.4 ± 6 (See Table I), but new experimental data led in 1941 to the best value of 14384.8 ± 3.4, which differs from the previous value by much more than the "probable error." It is conceivable that further research will give a still higher result, or, conversely, we may eventually find that the international 14320 is approximately correct.

The present tabulated results can be altered rather easily to conform to any other values of C_1 and C_2. In colorimetry, usually only *relative* values of $J(\lambda)$ are employed, so C_1 need not be considered. Let $C_2=14320$, $\bar{C}_2=$new value chosen for Planck's second constant, $T=$true temperature, in accordance with the international temperature scale, and $\bar{T}=$new temperature, corresponding to $\bar{C}_2$. Then, according to Eq. (1), $J(\lambda)$ will remain unchanged if

$$\bar{T}=T(\bar{C}_2/14320). \tag{2}$$

Values of $\bar{T}/T$ are listed in Table I. By altering the temperature in accordance with Eq. (2), one obtains the correct relative spectral distribution curve directly from Table II.

If absolute values of $J(\lambda)$ are necessary, the temperature is changed as before, and the tabulated values are multiplied by the constant ratio of the C_1's:

$$\bar{J}(\lambda)=J(\lambda)(\bar{C}_1/C_1), \tag{3}$$

where $C_1=36970$, $\bar{C}_1=$new value chosen for Planck's first constant, $J(\lambda)=$tabulated value (Table II), and $\bar{J}(\lambda)=$value corresponding to $\bar{C}_1$. The ratios $\bar{J}(\lambda)/J(\lambda)$ are listed in Table I for various recommended values of $\bar{C}_1$.

In conclusion, it is a pleasure to thank the

TABLE II.—*Continued.*

	3200		3300		3400	
0.38	35.85	4679	51.23	0519	71.67	9602
0.39	42.58	7304	60.29	6155	83.64	0553
0.40	49.99	0329	70.16	5048	96.53	7418
0.41	58.04	6052	80.80	1078	110.3	0954
0.42	66.72	8128	92.15	8243	124.8	8556
0.43	76.00	2473	104.1	8207	140.1	8549
0.44	85.82	8280	116.8	1108	156.1	2265
0.45	96.15	9097	129.9	7833	172.6	0566
0.46	106.9	4393	143.6	1282	189.5	4024
0.47	118.1	2834	157.6	4091	206.8	3095
0.48	129.6	5546	171.9	8761	224.3	8263
0.49	141.4	6701	186.5	7775	242.1	0180
0.50	153.5	0417	201.3	3702	259.8	9773
0.51	165.7	0840	216.1	9288	277.6	8344
0.52	178.0	2219	231.0	7531	295.3	7644
0.53	190.3	8961	245.9	1743	312.8	9931
0.54	202.7	5686	260.6	5605	330.1	8017
0.55	215.0	7271	275.2	3203	347.1	5297
0.56	227.2	8884	289.5	9057	363.7	5765
0.57	239.3	6006	303.6	8134	379.9	4022
0.58	251.2	4452	317.4	5869	395.6	5271
0.59	262.9	0382	330.8	8154	410.8	5309
0.60	274.3	0308	343.9	1345	425.5	0509
0.61	285.4	1090	356.5	2247	439.5	7796
0.62	296.1	9939	368.6	8100	453.0	4625
0.63	306.6	4403	380.3	6564	465.8	8947
0.64	316.7	2362	391.5	5700	478.0	9182
0.65	326.4	2009	402.2	3946	489.6	4183
0.66	335.7	1844	412.4	0092	500.5	3207
0.67	344.6	0647	422.0	3260	510.7	5878
0.68	353.0	7471	431.1	2879	520.3	2157
0.69	361.1	1619	439.6	8656	529.2	2308
0.70	368.7	2625	447.7	0558	537.4	6867
0.71	375.9	0239	455.1	8782	545.0	6615
0.72	382.6	4408	462.1	3735	552.0	2547
0.73	388.9	5258	468.5	6016	558.3	5846
0.74	394.8	3078	474.4	6385	564.0	7858
0.75	400.2	8300	479.8	5752	569.2	0070
0.76	405.3	1491	484.7	5155	573.7	4084

TABLE II.—*Continued.*

	3500			3500 (*continued*)	
0.38	98.38	4766	0.60	520.1	0770
0.39	113.8	7371	0.61	535.5	5654
			0.64	550.2	2380
0.40	130.4	2266	0.63	564.0	9429
0.41	147.9	3973	0.64	577.1	5756
0.42	166.3	2224			
0.43	185.4	5940	0.65	589.4	0837
0.44	205.2	3488	0.66	600.8	4580
			0.67	611.4	7291
0.45	225.5	2920	0.68	621.2	9633
0.46	246.2	2192	0.69	630.3	2585
0.47	267.1	9361			
0.48	288.3	2753	0.70	638.5	7405
0.49	309.5	1103	0.71	646.0	5594
			0.72	652.7	8865
0.50	330.6	3672	0.73	658.7	9106
0.51	351.6	0344	0.74	664.0	8358
0.52	372.3	1689			
0.53	392.6	9018	0.75	668.6	8784
0.54	412.6	4413	0.76	672.6	2645
0.55	432.1	0736			
0.56	451.0	1641			
0.57	469.3	1553			
0.58	486.9	5655			
0.59	503.8	9858			

Note—Superscripts refer to the number of zeros after the decimal point. For example,

$$11166476 = {}^{0}11166476 = 0.11166476.$$

National Youth Administration, the trustees of the Kennelly Fund, and the computers, Messrs. J. L. Ahern, H. Azarian, E. D. Benson, J. E. Castanias, L. E. Duval, P. J. deGeorge, J. Margolskee, J. J. Murphy, J. D. Pigott, J. S. Quill, D. L. Shapiro, and L. F. Zorio. I am particularly indebted to Becky Hayes Tuttle and David F. Tuttle, Jr. for their painstaking care in preparing the table for publication. Copies of the complete table (10-deg. temperature intervals) are available and will be supplied gratis as long as the supply lasts. Address the Electrical Engineering Department, Massachusetts Institute of Technology, Cambridge, Massachusetts.